DESIGN AND ANALYSIS OF WATER-ENERGY NEXUS AS INTERCONNECTED NETWORKS FOR SUSTAINABILITY, SURVIVABILITY AND RESILIENCE

A Dissertation

by

SPYRIDON TSOLAS

Submitted to the Graduate and Professional School of
Texas A&M University
in partial fulfillment of the requirements for the degree of

DOCTOR OF PHILOSOPHY

Chair of Committee,	M. M. Faruque Hasan
Committee Members,	Efstratios N. Pistikopoulos
	Mahmoud M. El-Halwagi
	Sergiy Butenko
Head of Department,	Arul Jayaraman

August 2021

Major Subject: Chemical Engineering

ABSTRACT

Satisfaction of global energy and water demands in a sustainable manner is a great challenge, which is often amplified by the high interdependence between energy and water networks. This interdependence is captured in a Water-Energy Nexus (WEN) and can result in redundant or excess resource withdrawal. Sustainability, survivability and resilience are three key concepts in complex interconnected networks such as WENs. These need to be analyzed and quantified for economic WEN design. WEN interdependence has high impact during disruption events, impairing the network operability and profitability. For example, internal connectivity disruptions in a power network affect the performance of a water distribution network, and vice versa. In addition, prolonged demand and generation disruptions can put the long-term survivability of an interconnected supply chain at risk. Recent natural disasters (2021 Texas Freeze, Hurricane Harvey) and COVID-19 pandemic-induced lockdowns revealed such vulnerabilities. In this dissertation, a framework is presented to (i) ensure minimal redundancies and cost-effective regional WEN design, (ii) guarantee network resilience against connectivity disruptions with minimum additional costs, and (iii) ensure economic survivability during demand disruptions.

To address sustainability, a graph-theoretic approach is proposed defining a nexus as a directed bipartite graph with water and energy flows. The network representation allows the decomposition of a complex nexus into its essential and redundant components based on the intensity of the generating technologies. It is shown that for specified external grid demands, the optimal nexus configuration with minimum water and energy generation is the one without any redundant subnetworks. A novel WEN diagram is introduced to represent networks and a graphical pinch method is developed to identify and eliminate redundant subnetworks. This leads to minimum generation/resource utilization, while also taking into account for matching restrictions and water quality specifications. The method can be used as a screening and targeting tool for optimal technology combinations with minimum redundancies. Furthermore, a WEN superstructure optimization-based approach is developed to find optimal WEN infrastructures while considering wastewater

reclaim and reuse, multiple resource types, varying water quality, and facility location-allocation, via a mixed-integer nonlinear programming (MINLP) model.

To address resilience, the operational and economic performances of a WEN during connectivity disruptions are analyzed. To this end, minimum cost of resilience (MCOR) and operation-based resilience metrics are introduced and utilized to identify critical connections in interconnected networks. MCOR corresponds to the minimum additional infrastructure investment that is required to achieve a certain degree of resilience. To guarantee MCOR for grass-root or retrofitting applications, the metrics are incorporated in a multi-scenario mixed-integer linear program (MILP) that accounts for resilience in the design phase of interconnected networks. Increasing immunity to connectivity disruptions leads to increased investments allocated in excess system capacities or higher dependence on external supplies.

To address survivability and predict the economic performance of supply chains against demand disruptions, the concept of economic survivability (ES) is introduced and incorporated in a mixed-integer nonlinear program (MINLP). ES is the ability to maintain a net positive economic worth, or at least keeping it above a certain threshold, in the presence of sudden and prolonged disruptions that drastically reduce the product demands, prices, resource availability or others. It is observed that, maximizing ES leads to systems with higher return-on-investment (ROI) and profitability. However, for multi-regional, distributed and interdependent supply chains, a more balanced distribution of investment portfolio is important to improve the local survivability of each region, but it comes at the expense of overall profitability. The effect of overdesigning for the event of increased demands is also explored. Higher demands satisfied lead to lower economic survivability under demand decreases, so the decision-makers should balance the trade-offs between survivability and excess demand satisfaction by thoroughly assessing the probability of positive and negative demand fluctuations.

DEDICATION

To my mother Eirini and my father Dimitris.

ACKNOWLEDGMENTS

I would like to express my sincerest gratitude to my Ph.D. advisor Professor M. M. Faruque Hasan who welcomed me to his research group and introduced me to the art and science of process systems engineering. Professor Hasan has constantly supported me academically and professionally, guided me with his expertise through my graduate journey, and encouraged me by example to seek excellence and be dependable. Furthermore, I would like to express my appreciation for my late co-advisor, Professor M. Nazmul Karim, whom I had the pleasure of working with until my third year before his sudden passing away. With his support Professor Karim made it possible for me to join Dr. Hasan's research group and would always provide me with a second perspective on my research endeavors.

Next I would like to express my sincere appreciation to the members of my thesis committee, Professor Efstratios Pistikopoulos, Professor Mahmoud El-Halwagi, and Professor Sergiy Butenko, who devoted valuable time to provide me with invaluable feedback through our committee meeting, preliminary exam, and to read my preliminary Ph.D proposal and this Ph.D thesis. In addition, their significant respective research work was crucial, as it inspired me and guided me to contribute my part to the process systems engineering field. I really appreciated Professor Pistikopoulos' and Butenko's graduate course teaching, as they equipped me with the appropriate tools to perform my graduate research.

I would like to sincerely thank the current and former members of Hasan's research group; Dr. Ishan Bajaj, Dr. Shachit Iyer, Dr. Akhil Arora, Mohamhed Monjur Sadaf, Manali Zantye, Ahmed Harhaha, Akhilesh Ghandi, as well as other colleagues in GERB building. I was lucky to spend the past five years with such unique individuals and share fun memories from group hangouts and conferences. I would especially like to recognize my former colleagues Dr. Salih Emre Demirel, Dr. Jianping Li, and Dr. Baris Burnak for the thought-provoking discussions, their senior guidance, and for the joy of their friendship.

Finally, I would like to express my deepest of thanks to my family; my father Dimitris Tsolas,

my mother Eirini Drakatou, my sister Foteini, and my grandparents Spyros and Niki Drakatou. I would not be where I am today without their never-ending support during stressful times and their ever-gazing thought from my home back in Greece. They were and will be always in my heart, as I am truly blessed to share their love and support. I would like to thank my colleague, roommate, and close friend Iosif Pappas, for the joy of his companionship for more than 9 years of undergraduate and graduate studies. I wish to him all the personal and professional happiness. Finally, I would like to thank Dimitra Mastrogianni for her companionship through difficult times and for providing me with an additional motivation to complete this stage in my life.

CONTRIBUTORS AND FUNDING SOURCES

Contributors

This work was supported by a dissertation committee consisting of Professor M. M. Faruque Hasan [advisor], Professor Efstratios Pistikopoulos, and Professor Mahmoud El-Halwagi of the Artie McFerrin Department of Chemical Engineering and Professor Sergiy Butenko of the Department of Industrial and Systems Engineering.

All the work conducted for the dissertation including the algorithmic and program code development was completed by the student independently.

Funding Sources

Graduate study was supported by Texas A&M University, Texas A&M Engineering Experiment Station (TEES), National Science Foundation, and Department of Energy.

TABLE OF CONTENTS

Page

ABSTRACT ii

DEDICATION iv

ACKNOWLEDGMENTS v

CONTRIBUTORS AND FUNDING SOURCES vii

TABLE OF CONTENTS viii

LIST OF FIGURES x

LIST OF TABLES xiii

1. INTRODUCTION 1

    1.1 Water-Energy Nexus (WEN) 2
    1.2 Interconnected Networks undergoing Disruptions 3
    1.3 Previous Works on WEN Design and Optimization 6
    1.4 Previous Works Addressing Resilience and Survivability 8
    1.5 Research Gaps and Challenges 13
    1.6 Key Contributions 15

2. GRAPH-THEORETIC APPROACH 18

    2.1 Water-Energy Nexus Graph 20
    2.2 Water-Energy Diagram 23
    2.3 Graphical Water-Energy Nexus Optimization using Water-Energy Diagram 26
        2.3.1 Minimization of Total Generation 27
        2.3.2 Maximization of Grid Supplies 30
        2.3.3 Nexus Optimization in the Presence of Restricted Matches 32
        2.3.4 Nexus Optimization in the Presence of Quality Requirements 35
    2.4 Results on Regional WEN Optimization 37
    2.5 Summary 39

3. SUPERSTRUCTURE-BASED REGIONAL WEN DESIGN 42

    3.1 Water-Energy Nexus Superstructure 42
    3.2 Model Formulation 45
        3.2.1 Balance Constraints 45

3.2.2 Logical Constraints 50
3.2.3 Problem feasibility in terms of intensity 51
3.2.4 Distance Constraints 52
3.2.5 Non-overlapping Constraints 52
3.2.6 Lower and upper bounds of variables 53
3.2.7 Objective function 53
3.3 Case Study on Jack County (TX) 55

4. RESILIENCE-AWARE DESIGN 58

4.1 Trade-offs between network efficiency and resilience 58
4.1.1 Motivating example 59
4.1.2 Motivating Example under Connectivity Failures 62
4.2 Resilience Metrics for Existing Infrastructures 63
4.2.1 Resilience analysis and reinforcement of motivating example 64
4.2.2 Identification of Critical Connections 65
4.2.3 Minimum Cost of Resilience (MCOR) 66
4.3 Resilience-aware Design 67
4.3.1 Multi-scenario formulation 68
4.4 Results: Revisiting Illustrative Example 75
4.4.1 Grass-root resilient design 75
4.4.2 Zero Nexus Interdependence 78
4.4.3 Resilience-aware Retrofitting 79
4.5 Case Study on Bexar County WEN 81
4.5.1 Initial superstructure 82
4.5.2 Regional WEN resilience analysis 85
4.6 Summary 87

5. SURVIVABILITY-AWARE DESIGN 89

5.1 Economic Survivability 89
5.2 Incorporating Economic Survivability in Supply Chain Design 93
5.3 Case Study on Economic Survivability 101
5.4 Summary 110

6. CONCLUSIONS 112

6.1 Directions for Future Work 113
6.1.1 Resilience Analysis Expansion for Facility Disruptions 113
6.1.2 Holistic framework for all disruption events 115
6.2 List of Publications 118

REFERENCES 119

APPENDIX A. SUPPLEMENTARY DATA FOR CHAPTER 2 RESULTS 137

APPENDIX B. NOMENCLATURE FOR CHAPTER 4 139

LIST OF FIGURES

FIGURE Page

1.1 An example of a regional Water-Energy Nexus. 3

1.2 An example of a generic supply chain network configuration and how it can be affected by systemic shocks. 4

2.1 A motivating example of a water-energy nexus graph. 19

2.2 Classification of graphs in terms of redundancy within a Water-Energy Nexus. 22

2.3 Water-Energy Nexus diagram representing the network and the supplies of the motivating example 24

2.4 Rearrangement of the WEN diagram for the identification of redundant generation and utilization of water and energy resources: (a) revised WEN diagram and (b) corresponding nexus graph. 28

2.5 Isolated redundant system (diagram and graph) that can be omitted without affecting the rest of the WEN. 29

2.6 Isolated essential system (diagram and graph) with minimum generation to satisfy demands. 30

2.7 Graphical energy grid maximization procedure with reconfigured WEN diagram and corresponding graph 31

2.8 Graphical water grid maximization procedure with reconfigured WEN diagram and corresponding graph 32

2.9 Revised WEN diagram to address prohibited match $W_1 - E_2$ for the case where the essential nexus is unaffected. 34

2.10 Revised WEN diagram to address prohibited match $W_1 - E_2$ for the case where the essential nexus is affected. 35

2.11 Revised WEN diagram to satisfy the quality specification of E_3. 37

2.12 Water-energy nexus diagram for electricity and water sources for the case study on Spain. 39

2.13 Water-energy nexus diagram for electricity and water sources of Spain, using biofuels for electricity generation. 40

3.1 The Water-Energy Superstructure depicts regional system as a three-echelon supply chain. 43

3.2 Analysis of incoming and outgoing streams for every node within the WEN superstructure. 46

3.3 Optimal WEN result for regional planning 56

4.1 Water-energy nexus design and operation superstructure. 59

4.2 Illustrative motivating example of a nominal WEN design and operation problem. 61

4.3 Modified WEN of motivating example with user-specified over-design for resilience reinforcement. 65

4.4 Connection criticality identification for the modified motivating example using connection-specific operational resilience. 66

4.5 Grass-root resilient design resulting cost distribution and resilience for motivating example. 76

4.6 Network progression and WEN configurations for parametric values of λ. 77

4.7 Fully resilient network configurations for grass-root case without interdependence and retrofitting cases. 79

4.8 Minimum cost of resilience (MCOR) distribution for parametric penalties for all applications. 80

4.9 Summary of initial WEN superstructure (available resources, potential sources, consumers) for regional Bexar case 83

4.10 Optimization results for minimum cost and resilience-aware design for Bexar WEN. 86

5.1 Types of systemic shocks and their impact on economic survivability. 91

5.2 Geographically interconnected multi-period supply chain network synthesis superstructure. 93

5.3 Resulting supply chain network connectivity and facility allocation for two distinct optimization objectives. 103

5.4 Resulting supply chain network and connectivity with maximized local economic survivability ES^{local} 105

5.5 Effect of over-designing for additional demands ϵ on system profitability and survivability. 107

6.1 Comparison of resilience-aware design between tolerance against connectivity and facility failures. 114

6.2 Holistic Framework for all potential disruption types along with nominal operation. . 116

LIST OF TABLES

TABLE Page

2.1 Quality specifications for the motivating example of WEN base case. 36

4.1 Operational and cost parameters for the illustrative example. 60

4.2 Operational and cost parameters for energy and water sources of regional case study[1, 2, 3, 4]. 84

5.1 Parameters for manufacturing facilities and distribution centers. 102

5.2 Summary of profit and economic survivability results for the three cases. 104

A.1 Energy data and calculated water requirements used in the case study of Spain [5]. .. 137

A.2 Water data used in the Case Study on Spain [6, 7]. 138

1. INTRODUCTION[1]

Every modern commercial activity requires power, water, or a combination of both [11]. As population constantly increases, demands for those goods continue to grow. Global annual water demands are expected to increase by 20-30% by 2050 [12], and energy demands by 30% according to the Annual Energy Outlook of 2020 [13]. In the same time, the natural reserves of energy carriers and freshwater, from which the clean fuel, power and drinkable water are generated, are becoming scarce and most regions deal with seasonal water shortages and power outages. It is essential and a great challenge to design cost-effective but also sustainable regional water and power networks.

Individual power and water planning have been developed and regulated independently for years [11]. However, water is expedited in all stages of fuel and power production, and water requires energy to be extracted, treated, and distributed to consumers. Indicatively, approximately 15% of global water is now used for energy [14], and 8% of global energy is used for water [15]. This poses an additional challenge, because an increase in the power demand will affect the water treatment and strain even more the water resources. Inversely, when severe drought affected more than a third of the United States in 2012, limited water availability limited the operation of power plants and other commercial activity [11]. This has a tremendous impact on economic and political stability, as power outages can lead to commercial losses and water rights can be restrictively expensive for future energy endeavors. This interdependence becomes more evident as we are transitioning from traditional to non-conventional processes, such as seawater desalination or shale gas and biomass processing, which are also more energy and water intensive respectively.

[1]Reproduced in parts with permission from: (i) Tsolas, S. D., Karim, M. N., & Hasan, M. M. F. (2018). Optimization of water-energy nexus: A network representation-based graphical approach. *Applied Energy*, 224, 230-250. [8], (ii) Tsolas, S. D., Karim, M. N., & Hasan, M. M. F. (2019). Systematic Design, Analysis and Optimization of Water-Energy Nexus. In Computer Aided Chemical Engineering, vol. 47, pp. 227-232. Elsevier [9], (iii) Tsolas, S. D. & Hasan, M. M. F. (2021). Resilience-Aware Design of Interconnected Supply Chain Networks with Application to Water-Energy Nexus. *Submitted for Publication*, and (iv) Tsolas, S. D. & Hasan, M. M. F. (2021). Survivability-Aware Design and Optimization of Distributed Supply Chain Networks in the Post COVID-19 Era. *Journal of Advanced Manufacturing and Processing* [10].

1.1 Water-Energy Nexus (WEN)

This interconnection and complex dynamics between and energy and water are captured within the Water-Energy Nexus (WEN). We consider a nexus to be a system of two interconnected water and energy networks. These networks are highly coupled because they are comprised of one or more processing nodes that exchange energy for water and water for energy. The role of the nexus is to receive various water and energy resources as inputs, exchange them via the networks, and deliver them as outputs to external grids or consumers. This formalization is highly scalable, and depending on the system boundary and how we define the entities that comprise the networks, we can define nexus at different scales.

To illustrate, consider a regional (city-, state- or country-level) Water-Energy Nexus example demonstrated in Figure 1.1. The external energy and water inputs are withdrawn by the sources from various natural resources within the region (e.g., fossil fuel reserves, solar energy, wind, rivers, lakes, aquifers, seawater), as well as from other regions (e.g., liquefied natural gas or LNG, electricity, freshwater). In this example, the shale gas formation and the surface water basin constitute the resources of the nexus. Within the nexus, an energy source is a plant or processing facility that collects energy resources and converts them to higher quality, in the expense of water acting also as a water sink. Examples of regional energy sources include fuel processing plants, solar parks, and power generation plants. In this example, a shale gas extraction facility and a natural gas power plant act as the energy sources and water sinks of the Nexus. Similarly, a water source in a regional nexus is a plant or processing facility that collects water resources to obtain treated water, in the expense of energy. In this example, a surface water treatment plant and a wastewater treatment plant are the water sources and energy sinks of the Nexus. Finally, the clean natural gas fuel, the power generated, and the treated water are supplied from the sources to the external grids for consumption.

Our Water-Energy Nexus definition is in line with the notion that a nexus can be considered as a 'system of systems' [16]. Plenty of survey studies and reports demonstrate the need of systematic planning and decision making to optimally handle simultaneous energy and water in different

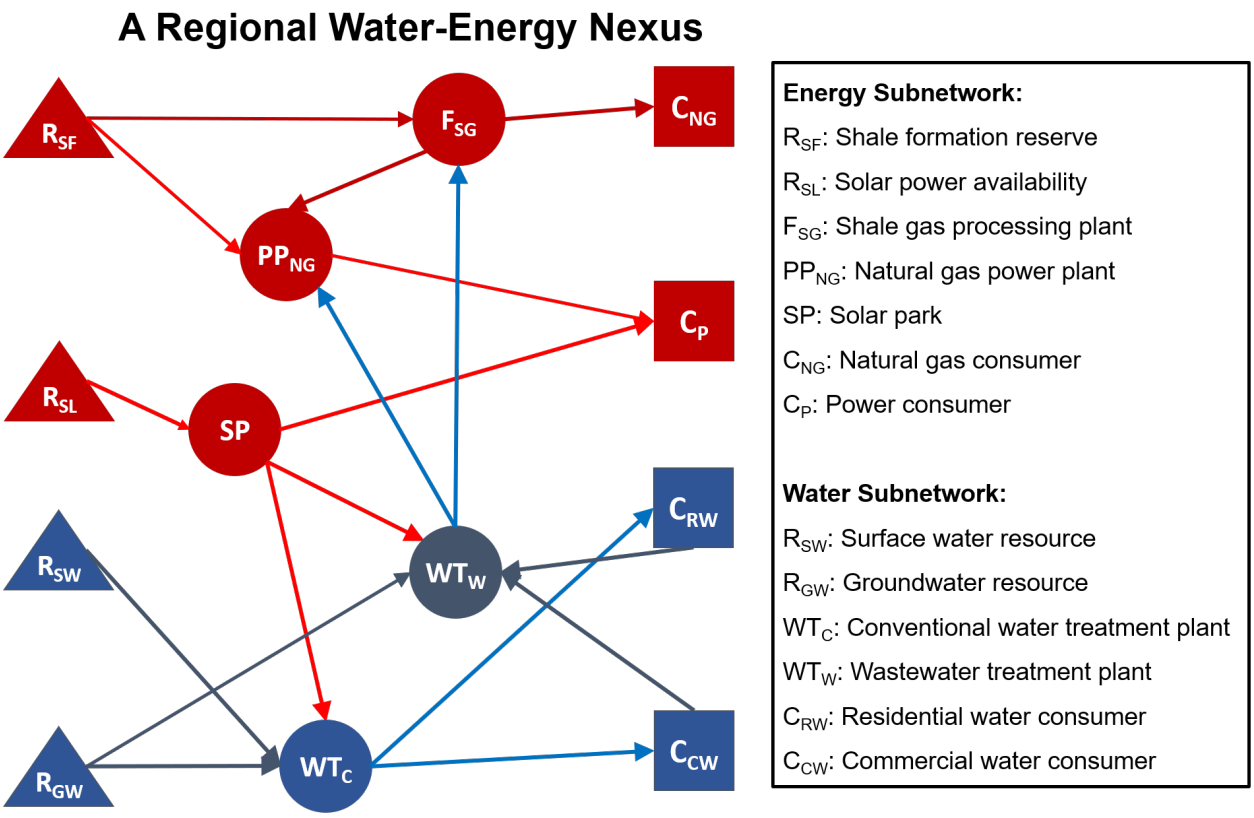

Figure 1.1: An example of a regional Water-Energy Nexus. The red entities belong to the energy subnetwork, while the blue entities to the water subnetwork. The energy resources and water resources are withdrawn from the generating facilities (sources). The sources generate useful fuel, power and treated water, exchange it and distribute it to consumer centers or other distributors.

systems [17, 11, 18]. Plenty of case studies have presented data in challenging nexus regions, like the state of Texas [19], China [20], Middle East and North Africa [21], and Spain [22]. Finally, extensive reviews regarding methods and decision making approaches are present in the literature [23, 24, 25]. The interconnection of water and energy infrastructure does not affect only the nominal operation of regional systems, but also their performance during disruption events.

1.2 Interconnected Networks undergoing Disruptions

Complex supply chain networks such as WEN are the backbone of modern cities, industrial sectors, and commercial activities. Other examples include transportation, telecommunication networks and supply chains of chemicals, commodity products and perishable goods. These networks

should be designed considering unforeseen disruption events that can impair their operability and productivity. Potential causes of such events include pandemic-induced lockdowns (e.g., COVID-19), geo-political conflicts, sanctions and restrictions on commercial activities and sudden natural disasters (e.g., Hurricane Harvey, 2021 Texas freeze). These events can lead to systemic shocks, such as connectivity disruptions, unforeseen demand spikes, resource supply cut-offs, productivity reductions and even shutdowns of whole processing plants (Figure 1.2). If disruptions continue for prolonged time periods, it may eventually lead to partially or completely shutting down a supply chain, major financial losses and impairment of social welfare.

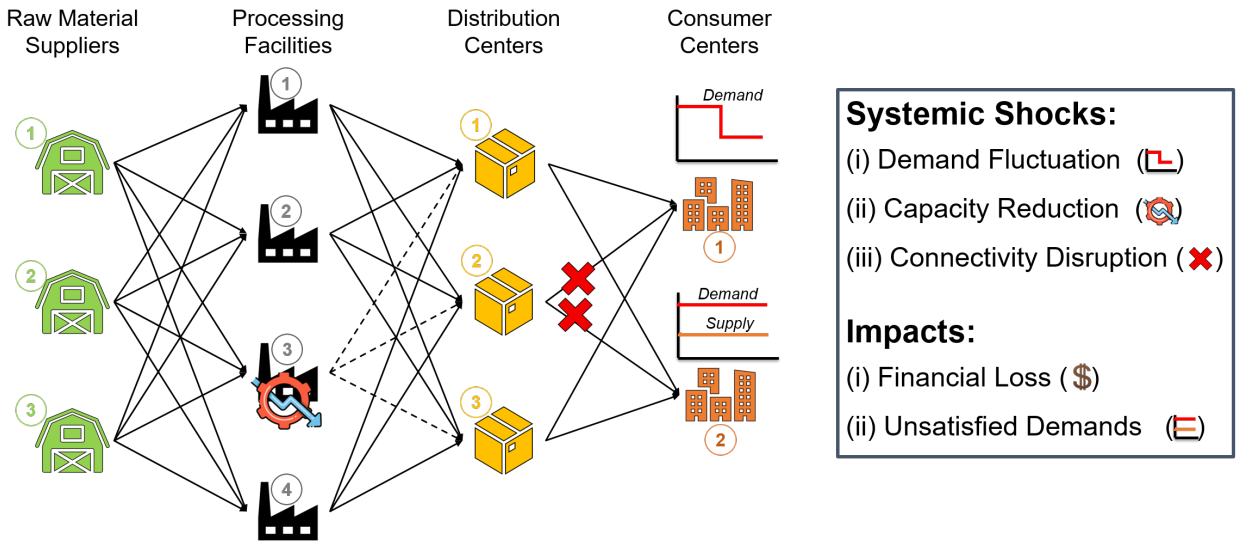

Figure 1.2: An example of a generic supply chain network configuration and how it can be affected by systemic shocks. The network consists of three raw material suppliers, four processing facilities, three distribution centers, and two consumer centers. Due to forced capacity reduction in Processing Facility 3, the flow of products from this facility to all three distribution centers are disrupted, as shown by the dotted lines. Due to a forced lockdown, no products are transported from Distribution Center 2 to the consumer center. This can result in demand violations and associated penalties. Finally, Consumer Center 1 faces a sudden reduction of product demands, which in turn affects the material flows and processing in the upstream. All these can lead to financial losses.

Network interdependence, like in the case of WEN, amplifies the catastrophic effects of systemic shocks and disruption events, as they can propagate across the interconnected networks.

Even in a power distribution network, a local power outage can cascade from adjacent nodes and create whole country black-outs [26]. If we consider now the interdependence, additional challenges arise. A cascading effect can be induced if a power plant reduces its output due to cooling water shortage, and nearby power stations overload, and then cascading outages are spread. So, it is very important to explore the effect of nexus interdependence on the resilience of the system under disruption events.

The disruptions and prolonged lockdowns that followed the COVID-19 pandemic have brought to light the vulnerabilities of many supply chains in the food, manufacturing, chemicals, health, energy and other sectors. Although a global-scale pandemic, such as COVID-19, occurs with low frequency, its impact was huge and multidimensional. A major impact of pandemic-induced lockdown has been a sudden change in demands due to purchase changes and mandatory capacity reductions. For example, the restaurants were asked to reduce to 50% occupancy as a measure to curb the spread of COVID-19 [27]. Social distancing, self-isolation, and travel restrictions resulted in reduced workforce in the energy and chemical industries which led to reduced production [28]. There was a sudden and sharp shortfall of demand in the hospitality industry (hotels, restaurants, bars), resulting in 47% less sales between March 1 and March 22 of 2020 [29]. Furthermore, the mandatory remote employment led to productivity reductions and loss of jobs in the manufacturing industry. The reduced demand of cars in the automotive industry led to reduced demands of associated chemicals for the chemical and petrochemical industry. Transport restrictions and lockdowns led to supply cut-offs. For example, many materials that are often sourced from China and other Asian developing countries were cut-off during COVID-19, and companies had to change their production lines [30]. Automobile firms could not produce everything in-house, since they depended heavily on microelectronics from external suppliers [31, 32]. In the health sector, the chemicals used for creating DNA- and mRNA-based COVID-19 vaccines and drug therapies depend on precursors, some of which are mainly produced overseas. It is very important to identify the vulnerabilities of interconnected systems and prepare contigencies in the light of sudden systemic shocks and disruptions.

1.3 Previous Works on WEN Design and Optimization

Plenty of isolated energy or water systems applications exist in the literature from a synthesis and optimization perspective. Non-conventional technologies, like shale gas production and hydrofracturing processes are challenging intensive application that have been dealt with [33, 34, 35, 36, 37, 38, 39, 40]. Desalination is an indicative energy-intensive technology that has received attention in terms of energy requirements, optimal performance and configuration [41, 42, 43, 44, 45, 46]. Except from isolated cases, hybrid or co-production systems have also been searched. Pressure-retarded osmosis for power generation [47, 48], energy and water dependence in algae cultivation [49] are indicative examples. Intensification applications are also present in literature, like membrane distillation receiving residual brine input from desalination plants [50] and intensified solar systems [51]. A review from Zak et al. has been also performed of methods regarding co-production of power and water using hybrid desalination [52]. González-Bravo examined the optimal design of a regional water and power distribution network, including dual-purpose solar power and desalination plants. The same case study was examined for uncertain parameters for demand and resources, where the distributions were obtained by individual scenarios solutions, leading to the final stochastic MINLP model [53].

From a modeling perspective, plentiful of researchers have done profound work with heat and mass integration. Lihnhoff and Hindmarsh introduced the pinch design method for optimal heat source and sink matching in heat exchanger networks [54]. El-Halwagi and Manousiouthakis developed a similar pinch analysis for mass integration in mass exchange networks for plant-level systems [55]. These are graphical methods that identify the thermodynamic limits of heat and mass exchange and have been revisited to include more extensive objectives and applications [56, 57].

Mathematical programming approaches are very important for source-sink heat or mass integration. Papoulias and Grossmann proposed a linear program (LP) and mixed-integer nonlinear program (MINLP)-based transshipment models for maximum heat integration and minimum cost heat exchanger networks [58]. More recently, Chen et al. revised the transshipment model to reduce solving times for large-scale heat exchanger networks [59].

On the water side, the mathematical programming approach to mass integration has given rise to rigorous design of water networks. Chew et al. applied synthesis approaches for the direct and indirect inter-plant water integration [60]. Lovelady et al. applied water integration for the optimal design of eco-industrial parks [61]. Napoles-Rivera et al. developed a multi-period model to minimize the cost of macroscopic energy-water systems, by employing alternative water sources [62]. Bishnu et al. also developed a multi-period optimization model for the synthesis of industrial city reuse networks [63]. Alnouri et al. studied central and distributed water treatment systems for an industrial city [64, 65].

At the plant level, Baliban et al. proposed an MINLP model for simultaneous heat, power, and water integration in thermochemical facilities that also utilize wastewater treatment [66]. Gabriel et al. analyzed the water management for different routes of gas-to-liquid processes with energy and water management [67]. Indicatively, Tovar Facio et al. designed a minimum-cost water network incorporating electroagulation technology for refinery power networks [68]. Nunez et al. followed a superstructure-based optimization approach for the simultaneous water-energy and waste management within residential complexes [69, 70].

Beyond the plant and the residential levels, plethora of works have dealt with simultaneous power and water management in regional systems.Segurado et al. investigated the effect of wind, hydropower and desalination units in a case study of an African Island, and showed the effect on the fuel sources deployment, the relief on freshwater resources and the trade-offs with the total network costs [71]. Zhang and Vesselinov approached decision making in a water-energy nexus with a two-level programming scheme in order to balance maximum power generation with minimum total cost [72]. Gabriel et al. also attempted to maximize the efficiency of a highly coupled power production GTL facility which utilizes desalination in the pool of the water sources in the complex interaction case of Qatar [73]. Chen and Chen captured the complex interactions of entangled water and energy networks in an inter-plant level for an urban nexus [74]. Saif and Almansoori dealt with the power and water management in gas-fired plants, which included renewable energy sources coupled with thermal desalination, and addition of carbon capture [75].

Pereira-Cardenal et al. studied the broader interdependencies of water and energy, using stochastic dynamic modeling with economic objectives and testing their model on the Iberian Peninsula [76]. Gonzalez-Bravo et al. considered the regional design of water and power distribution network, which included dual-purpose solar power and desalination plants [77]. Tai et al. also examined the integrated operation of hydropower, desalination, wind and solar energy, taking into consideration the intermittency of the renewables. Specifically, they proposed utilizing seawater desalination along with wind and solar processes during cold seasons, so that the existing water reservoirs would be reserve to operate during hot peak seasons [78, 79]. Chen et al. utilized multi-regional input-output analysis to demonstrate the energy-water nexus interdependence and management of Hong Kong and its hinterlands [80]. Payet-Burin et al. also demonstrated the spatial and temporal management of water and power infrastructure of the Iberian Peninsula, and especially the effect of power plants cooling in different future climate change scenarios [81].

WEN is a specific instance of a more generic problem in the area of Water-Energy-Food Nexus (WEF). Food needs both energy and water to be produced, and from food waste products water and energy can be reclaimed. Hang et al. designed optimal integrated production systems for a designated eco-town in the UK [82]. Zhang et al. proposed a water-energy-food for multi-period socioeconomic planning [83]. Bieber et al. developed a platform for scenario-based decision making in contemporary systems, with sustainability, carbon emission and seasonal constraints [84]. Gao et al. [85] in the Water-Energy Food (WEF) nexus context, illustrated the effect of land and water availability constraints in coal and agricultural production in provinces of China [85]. Mroue et al. introduced a novel Energy Portfolio Assessment Tool (EPAT) for the trade-off analysis of policies within the WEF Nexus [86]. Nie et al. developed models for the food-energy-water nexus framework for crop-livestock systems and land use optimization [87, 88].

1.4 Previous Works Addressing Resilience and Survivability

The concept of resilience has a broad scope and definition. It has been described as the ability of a system to efficiently withstand, contain and quickly respond to and recover from disruptions that impair its nominal operation. A more concrete definition relies in the four Rs, which are also

known as the pillars of resilience [89]. These fours Rs are as follows:

1. Robustness: the ability of a system to withstand a given level of stress without suffering degradation or loss of function,

2. Redundancy: the extent to which elements and systems are substitutable, providing alternative resources in the event of degradation or loss of functionality,

3. Resourcefulness: the capacity to identify problems, establish priorities, and employ resources to achieve goals, and

4. Rapidity: the capacity to meet such priorities in a timely manner in order to contain losses and avoid future disruptions.

Defining and analyzing different aspects of resilience has been a well studied field. El-Halwagi et al. [90] have compiled an extensive review of process engineering-based methods to tackle different aspects of resilience.

In light of the frequency of major disruption events, such as COVID-19 or the hurricane Harvey, resilience of distribution and manufacturing networks has gained rekindled interest as an attempt to prepare supply chains to absorb and recover from systemic shocks. Hynes et al. [91] explored the impact of the pandemic and highlighted the importance of resilience of the whole system, over the individual efficiency and cost. Golan et al. [92] provided a thorough review of past resilience analysis and emphasized on the importance of a system's capability to absorb, adapt, and recover from shocks in the context of interconnected supply chains. Ivanov and Das [93] modeled the ripple effect of an outbreak considering rate of propagation, duration of disruptions, and demand declines. El-Halwagi et al. [90] also provided a thorough literature review on different aspect of resilience and future directions for disaster-resilient static and dynamic manufacturing processes.

While 'survivability' is not entirely new to both small and large businesses, it has re-emerged as a critical concept in the context of COVID-19. In the 1960s, the U.S. Department of Defense formally defined survivability as "the capacity of a system to resist a hostile environment so that it

can fulfill its mission" [94, 95, 96]. For engineering systems, survivability is an emergent property of system architecture, depending on the context to which it relates [94]. Venkatsubramanian et al. [97] investigated the evolutionary topological adaptation of natural and artificial networks and what affects their survivability. They showed that a network's robustness, efficiency and cost affect its short-term and long-term survivability and also dictate its evolutionary adaptability. Thadakamaila et al. [98] also used network topology and graph properties to improve the robustness, responsiveness, flexibility, and adaptivity of supply chain networks. Ivanov and Dolgui [99] applied dynamic game-theoretic modeling to illustrate that the survivability of interwined supply networks within an ecosystem can be achieved by enhancing the resilience of the individual networks as well as the ability to meet the changing demands. Sharma et al. [100] also stressed on increasing the viability of a supply network to enhance its survivability.

Prior research has analyzed and quantified network robustness using a graph-theoretic approach [101, 102]. Power and water distribution networks can be represented as graphs with nodes and arcs. These works investigate different graphs using connectivity metrics, such as characteristic path length, clustering coefficient [101], and local and global efficiency [102]. One can then analyze the performance of these graphs under different kinds of attacks. The attacks refer to node removals, which can be random or targeted to critical nodes. The graph-theoretical approach compares and obtains graph topologies that increase overall resilience. Works exist that explore different topological properties to obtain a critical capacity factor to maximize resilience [103, 104, 105]. For example, Kinney et al. followed a similar approach to analyze the North American power grid [105]. Others dealt with mitigation strategies against different types of attacks for various ideal and real networks [106, 107]. On the water side, Yazdani and coworkers have defined various connectivity properties and explored their effect on resilience performance [108, 109, 110, 111]. Meng et al. recently provided a comprehensive list of different complex network topology measures affecting resilience [112]. These studies have been successful in analyzing fixed networks and identifying desirable connectivity for ideal resilient networks, providing insights for resilient design.

Tackling resilience has been a key issue in the design phase of processes and plants in the chemical industry. Ade et al. [113] considered inherent safety, process reliability, and risk analysis in processing plant design. Jain et al. [114] developed a process resilience analysis framework (PRAF) in order to account for risk and safety management in discrete phases of plant design. Ye et al. [115] considered the trade-offs between process reliability, expressed as availability of parallel equipment and total cost. Moreno-Sader et al. [116] introduced a return on investment (ROI) metric for optimal process design. The modified weighted objective considers reliability, resilience, safety and sustainability at the expense of plant profitability. Al-Douri et al. [117] explored the trade-offs between the system reliability and the total cost. They utilized a markov procedure in the early stages of process design to identify and avoid potential failure events before finalizing conceptual design.

While the design and optimization of supply chains under uncertainty have been extensively studied in the literature (readers can refer to many excellent reviews including [118, 119, 120, 121, 122, 123, 124], and an exhaustive survey on the topic is beyond the scope of this work), few considered survivability as a central issue. In most cases, minimizing the cost and investment risks, or maximizing the profit was considered as the primary objective. Fisher et al. [125] utilized multiple levers, such as shorter lead times, increased reactive production capacity and improved market intelligence, to reduce the cost of demand uncertainty. Tsiakis and Pantelides [126] considered the design of multi-product multi-echelon supply chains under demand uncertainty using a scenario-based approach. Gupta and Maranas [127] employed stochastic programming with probabilistic demands for the midterm planning of multi-site supply chains. Jung et al. [128] developed deterministic planning and scheduling models incorporating safety stock levels to counteract demand uncertainties. Chen and Lee [129] addressed demand and price uncertainty using scenarios and fuzzy sets in a multi-product multi-stage multi-period setting. You and Grossmann [130] tackled demand uncertainty balancing the trade-offs between economical and responsiveness criteria. They optimized net present value and expected lead times using a multi-period mixed-integer nonlinear programming (MINLP) formulation. He and Zhao [131] performed a Nash bargaining analysis

and obtained optimal contracts to coordinate supply chains under supply and demand uncertainties. Zeballos et al. [132] utilized stochastic programming with discrete known scenarios and fuzzy variables to address a multi-period multi-product closed-loop supply chain problem with uncertainties in demand and resource availability. Significant research also exists dealing with disruptions in supply chains. Snyder et al. [133] argued that planning for disruptions should be considered in the design phase of supply chains. Tomlin et al. [134] sought for optimal ordering policies to balance the economic and risk trade-offs between cheap/unreliable and expensive/reliable suppliers. Wu et al. [135] developed a network-based modeling methodology to determine how disruptions propagate in supply chains. They considered policies resulting in quicker response times, lower costs, lower inventories, increased flexibility, and reduced bullwhip effect. Rickey et al. [136] investigated the contingency strategies based on system flexibility to minimize risk exposure to supply chain disruptions. Paul and Chowdhury developed a production recovery plan to counter the sudden demand increase, the supply cut-offs and the production capacity constraints [137]. They proposed increase in production capacity, emergency sourcing and collaboration as recovery strategies. Nikolopoulos et al. developed models to simulate the outbreak and forecast the demand and supply chain disruptions [138]. Their policy recommendation was to secure high volumes of inventory before the lockdown.

From a supply chain point of view, resilience and performance enhancement of systems have been investigated. Terrazas-Moreno et al. [139] considered the trade-offs between the network cost and the robustness. They developed a mixed-integer linear programming (MILP) model to consider parallel units and intermediate storage to equip a network against markov-based disruptions. Turnquist et al. highlighted the use of a combination of three resilience enhancement strategies: (i) Absorptive capacity - augmenting existing capacities, (ii) expansion capacity - installing new connections, and (iii) restorative capacity - investing on back-up resources. They utilized stochastic programming to obtain the most economical solution for these pre-planned system reinforcement strategies [140]. Zhang et al. used a multi-disaster-scenario robust planning model for the optimal pre-planned line hardening and back-up resources planning, to enhance power grid resilience

against random power line outages [141].

Significant work has also dealt with the time-dependent aspect of resilience. Xu et al. [142] utilized stochastic integer programming to optimize the post-earthquake restoration of electric power systems. Ivanov et al. analyzed dynamic recovery policies of multi-stage supply chains [143, 144]. You and coworkers proposed a multi-objective two-stage adaptive robust optimization approach to enhance the dynamic resilience of supply chains against disruption events [145, 146]. Matthews et al. used two-stage robust optimization to improve supply chain resilience against edge failures, which were modeled as random binary variables [147]. Jiaxin and Pingfeng considered the post-disruption performance recovery of power grids and determined optimal restoration strategies [148].

There are notable works that define and utilize resilience metrics as objectives of their supply chain design. For example, Ahmadian et al. defined resilience metrics to analyze the performance of given systems, and developed an optimization model to maximize these metrics towards resilience enhancement under budget limitations [149]. More recently, Yu and Baroud proposed stochastic block models to quantify the uncertain interconnection between interwined networks and studied the effect of the single components to the static and dynamic resilience [150]. Behzadi et al. provided a comprehensive review of supply chain resilience metrics focusing on post disaster system performance. They also proposed new metrics and incorporated them in a stochastic programming-based restoration scheduling framework [151]. Bachman et al. presented a comprehensive review on frameworks towards the robustness analysis and the resilience improvement of interconnected networks [152].

1.5 Research Gaps and Challenges

In previous works, water and energy integration were addressed separately in the aspects of methods and applications. In order to obtain truly optimal network configurations, it is needed to consider energy and water integration simultaneously on a regional level. For example, what are the implications on the power network (fuel withdrawal, satisfaction of power demands, power generation) for a regional wastewater reclaim and reuse optimization application? On the other

hand, plenty of researchers have followed mathematical programming approaches with deterministic or stochastic simultaneous design of energy and water networks for different applications and scales. However, there is a missing background providing theoretical targets to describe the effect of interdependence on the designed networks. Furthermore, network topology and its effect on nexus interdependence has not been formally addressed.

As far as the nexus resilience is concerned, it is essential to be addressed in the design phase of a supply chain, and not only use it for post-design analysis. While previous theoretical works considered network topology properties, such as the number of shortest paths from a node representing the power load [103], it is nontrivial to include them in supply chain design. Previously used properties and metrics also typically refer to undirected, uncapacitated graphs, whereas a nexus is comprised of directed and weighted graphs, where every node has its own operational and economical properties. The topological properties are very complex to be utilized in a mathematical-programming formulation in order to predict a network's resilience. Finally, most works listed in the above indicative review deal with the robustness and resilience of single commodity networks. Ivanov and Dolqui highlighted the importance of interwined supply networks in view of the COVID-19 outbreak [99].

Recent works [98, 100] have explored survivability as a combination of resilience, robustness, and system viability. The literature is already rich and mature on how to manage uncertainties in supply chains and improving their resilience. Survivability can be thought of as an extreme case of a system's resilience beyond which the existence of the system itself is threatened. The state-of-the-art on survivability mainly focuses on the operational aspect of systems in the events of disruptions. However, the economic implications of systemic shocks need to be considered systematically when designing and analyzing supply chain networks. In this context, survivability is a critical property that needs further exploration.

Key challenges and questions that arise from literature can be summarized as follows:

- how to systematically quantify the nexus interdependence and trade-offs between energy and water generating technologies,

- how to identify and eliminate eliminate excess use of water and energy for sustainability,
- how to design cost-effective regional complex WEN in grass-root and retrofit cases,
- how to analyze the economic and operational performance of interconnected networks against connectivity disruptions,
- how to analyze the survivability of supply chain networks during demand disruption events, and
- how to incorporate resilience and economic survivability in the design phase of complex networks.

1.6 Key Contributions

In this dissertation, a framework is presented towards improving the sustainability, resilience, and survivability of interconnected networks with an emphasis on water-energy nexus. The framework can analyze given WENs and optimally design new systems with the aforementioned targets embedded. To address the aforementioned questions the key objectives of this work can be summarized as follows:

Objective 1: Develop a systematic method for the identification and quantification of Water-Energy Nexus interdependence. The original contributions of this dissertation are (Chapter 2):

- Introduced a novel graph representation for water and energy interconnected networks.
- Introduced a novel water-energy diagram for redundancy identification and isolation.
- Developed graphical pinch-based analyses for optimal source-sink matching and utilization of detected redundancies.
- Expanded graphical approach for matching restrictions and quality specifications.

Objective 2: Establish a framework for optimal design and operation of regional Water-Energy Nexus. The original contributions of this dissertation are (Chapter 3):

- Introduced a superstructure representation for interwined regional water and energy supply chains.
- Constructed a mixed-integer nonlinear programming (MINLP) model to capture complex trade-offs in regional water-energy nexus.
- Obtained a grass-root and retrofit design framework for regional energy-water planning and resource management.

Objective 3: Establish a framework for resilience-aware analysis of interdependent networks. The original contributions of this dissertation are (Chapter 3):

- Introduced resilience metrics and quantified performance of interconnected networks under connectivity disruptions.
- Identified critical network components for the operation under disruption events.
- Incorporated resilience in the design phase of supply chains to ensure minimum over-design.
- Explored the trade-offs between capacity reinforcements for resilience and external emergency supplies.
- Established a procedure for grass-root and retrofit resilient designs, which is applicable to any type of (non-)interconnected supply chains.

Objective 4: Establish a method for the survivability-aware analysis of interconnected supply chains under prolonged disruptions. The original contributions of this dissertation are (Chapter 5):

- Introduced economic survivability as an economic metric for the analysis of given supply chains' break-even limits.
- Incorporated economic survivability as an alternative economic objective in new supply chain design.
- Explored the effect of geographical interdependence across multi-regional supply chains.

- Explored the trade-offs between economic survivability and over-designing for demand increases.

With these, the outline of this thesis is as follows. In Chapter 2, a graphical approach is presented to quantify nexus interdependence and identify redundancies. In Chapter 3, a superstructure-based optimization approach is proposed to address the sustainability and cost-optimal regional WEN design. Chapter 4 addresses the resilience analysis of interconnected networks, along with a resilience-aware design mathematical programming formulation. In Chapter 5, the effect of demand-related disruption events is analyzed and incorporated in supply chain network designs. Chapter 6 concludes the dissertation by highlighting major contributions and identifying directions for future research.

2. GRAPH-THEORETIC APPROACH[1]

In the introduction a water-energy nexus (WEN) definition and example were discussed. In this chapter, nexus interdependence between energy and water generation is analyzed. Let us consider an example of a simple nexus with three energy sources (E_1, E_2 and E_3) and two water sources (W_1 and W_2). A network representation of the nexus is shown in Figure 2.1, where the red and blue circles represent the sources of energy and water, respectively. We assume that all the flows are of the same quality. Therefore, the sources are determined solely based on the net positive quantities. E1 is an energy source because it produces 4 units of energy. It is also a water sink because it consumes 5 units of water. The energy produced by E_1 is used in W_1 that produces a total of 18 units of water. The produced water from W_1 is delivered to three different water sinks. These are E_1 (5 units), E_2 (4 units), E_3 (3 units), and the external water grid (6 units). In this particular example, all energy sources act as water sinks, and all water sources act as energy sinks. E_1, E_2 and E_3 generate 4, 6 and 9 units of energy, and require 5, 4 and 3 units of water, respectively. W_1 and W_2 provide 18 and 6 units of water, and consume 5 and 7 units of energy, respectively. The total energy generated (19 units) is greater than the total energy needed to produce water (12 units). Therefore, the nexus is able to provide an excess amount of 7 units to the external energy grid. Similarly, the total water generated or taken from external inputs (24 units) is greater than the total water usage (12 units). Therefore, there is a positive flow of water to the external water grid (12 units). Note that the total inputs that are processed by the nexus to produce all the energy and water are considered to be taken from natural resources. However, for simplicity, we do not show them explicitly in the network. We further assume that there is no loss of water or energy due to processing or transportation.

The water network consists of W_1 and W_2 as sources, and E_1, E_2, E_3 and the water-grid as sinks. The energy network, on the other hand, consists of E_1, E_2 and E_3 as sources, and W_1 and W_2

[1]Reproduced in part with permission from [8] Tsolas, S. D., Karim, M. N., & Hasan, M. M. F. (2018). Optimization of water-energy nexus: A network representation-based graphical approach. *Applied Energy*, 224, 230-250.

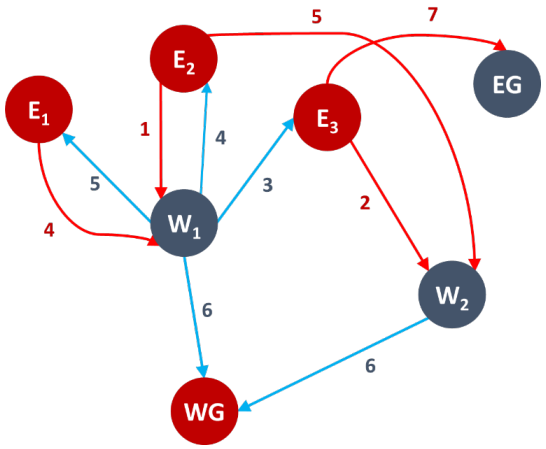

Figure 2.1: A motivating example of a water-energy nexus graph (base case). With solid line the energy supplies are represented, and with the blue dotted line the water supplies are displayed. With red circles the energy sources/sinks are depicted, and with blue circles the water sources/energy sinks are shown.

and the energy-grid as sinks. Because these networks have shared nodes, we consider them together as a nexus. Even though this appears to be a simple example, the analysis and optimization of this nexus is nontrivial because of the complex and cascading interactions. Considering the water and energy networks separately may result in suboptimal decisions.

Intensity Factor: Different sources of energy have different water requirement or intensity. This intensity is a measure of how much water is needed to produce one unit of energy for an energy source, and how much energy is needed to produce one unit of water for a water source. The intensity factor ϕ of a source is defined as follows:

$$\phi_e = \frac{water\,required}{energy\,generated} \tag{2.1}$$

$$\phi_w = \frac{energy\,required}{water\,generated} \tag{2.2}$$

Here, ϕ_w and ϕ_e are the intensity factors for sources of water and energy, respectively. For instance, the water intensity of E_1 and E_2 are 5/4 and 4/6, respectively. Intensity is inversely proportional to efficiency. The more efficient a process is, the less intensive it is in terms of water

or energy consumption. A low energy-intensive water source such as surface water pumping is also a cheap source compared to a more energy-intensive source such as seawater desalination. In many cases, there exist redundant subnetworks because of this two-way communication between the sources and sinks.

Consequently, we need to identify and eliminate redundant parts of the networks for optimal design and operation of a nexus. It is possible to reconfigure a nexus to numerous other equivalent configurations that use the same sources and sinks, take the same amount of total external inputs (total generation), and provide the same external outputs to the grids. Here, we assume that the effects of the changes in distances between the nodes are negligible. Interestingly, the configuration shown in Figure 2.1 is sub-optimal because (i) there exist other configurations that supply the same energy and water to the grids but use less external inputs (in other words, generate less energy and water from natural resources), and (ii) there exist other configurations that can supply more energy and water to the grids without increasing the total generation. A key benefit of the network representation is that we can consider a nexus as a graph consisting of water and energy sources as nodes and their connectivity as edges. As we discuss in the following section, the various features of a nexus graph can be systematically defined, analyzed and optimized by taking a graph-theoretical approach.

2.1 Water-Energy Nexus Graph

A water-energy nexus can be represented using a directed bipartite graph whose oppositely-directed arcs incident with the same vertex and have two different product flows. It is bipartite because the vertices representing the energy sources are only connected with the vertices representing the water sources. Since we do not allow two sources of the same product to connect with each other, this definition is consistent even in the presence of the energy and water grids that are the external sinks connected to only energy and water sources, respectively. A nexus can be also viewed as a special case of a general multi-product supply chain with product transformation since the alternating arcs correspond to only water and energy flows.

A nexus may or may not contain cycles. Because a nexus graph is bipartite and a cycle can

only have distinct internal vertices, any cycle in a nexus graph will always consist of the same number of water and energy sources. Therefore, no cycle in a nexus graph can have vertices more than $[2 \cdot min(N_W, N_E))]$, where N_W and N_E are the total number of water and energy sources, excluding the grids. Grids do not participate in forming any cycles, since there are no arcs heading out of the grid nodes. Furthermore, if a nexus has all sources and sinks with $\phi_w > 0$ and $\phi_e > 0$ and must supply to the grids, then there must be at least one cycle present allowing mutual exchange of water and energy.

The identification and analysis of cycles are critical because their presence in a nexus graph may indicate excess generation/consumption of water and energy resources within the nexus. As shown in Figure 2.2a, a graph with cycles can be of three major types – redundant, essential, and partially redundant. A redundant graph has one or more cycles connected in such a way that the overall output from the graph is zero (see Figure 2.2a). An essential graph, on the other hand, has non-zero outputs and the cycle is essential to deliver these outputs (as shown in 2.2b). Lastly, a partially redundant graph (or network) is a combination of both redundant and essential sub-graphs. An example of a partially redundant graph is shown in 2.2c. The graph in is partially redundant since it can be further decomposed into two separate subgraphs – where one subgraph is redundant but the other is essential. We can discard the redundant sub-graph and still meet the external grid demands. Note that the decomposition of a graph into multiple subgraphs may require splitting a source into several smaller sources while maintaining the same intensity factor. Based on the above graph-theoretic approach, we can state the following:

Lemma 1: *For specified grid demands, the optimal nexus configuration with minimum generation is the one that has no redundant sub-graphs.*

Lemma 2: *For specified external inputs/generation, the optimal nexus configuration with maximum outputs to external grids is the one that has no redundant sub-graphs.*

The above is valid for both grass-root design and retrofitting of a water-energy nexus. In both cases, all redundant sub-graphs need to be eliminated. However, the identification and isolation of such redundant sub-graphs is not always trivial, because a redundant sub-graph can be hidden in

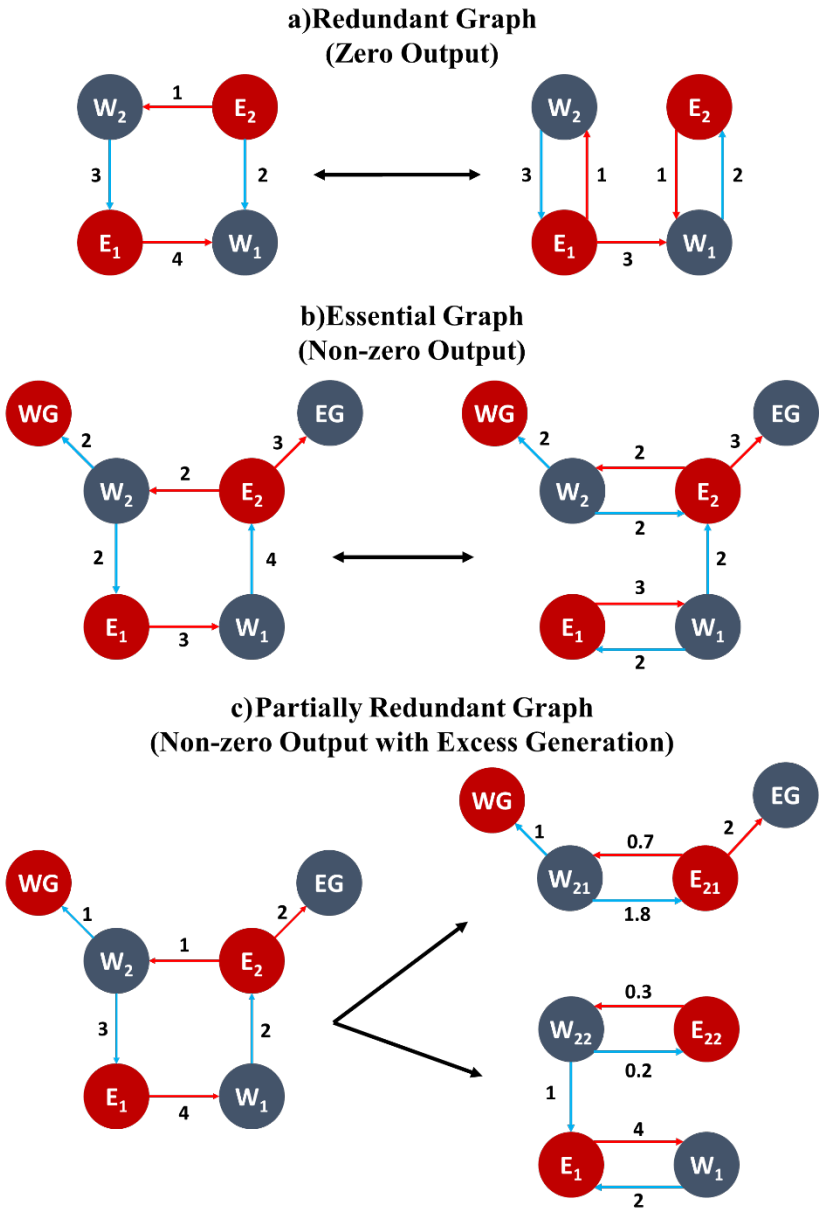

Figure 2.2: Classification of graphs in terms of redundancy within a Water-Energy Nexus. (a) A redundant graph composed of a 4-cycle of 2 water and 2 energy sources and its equivalent containing two 2-cycles. The redundant graph provides no output to the grid supplies. (b) An essential graph provides water and energy outputs to the external grids and every processing node is required for the delivery of the output. (c) A partially redundant graph provides a non-zero output to the grids, but there is excess generation in the nexus. Consequently, a partially redundant can be split into an essential and a redundant subgraph.

a complex nexus graph, and we may need to break/combine sources and/or alter the connectivity among the sources and sinks. A natural question then is how one can systematically identify and eliminate redundant sub-graphs for the design of a new nexus or for the retrofitting an existing nexus. To this end, we now present a water-energy diagram that can be used to systematically identify and isolate both redundant and essential sub-graphs, and obtain the optimal splitting of sources for minimum generation or maximum grid supplies.

2.2 Water-Energy Diagram

We construct a two-dimensional water-energy nexus (WEN) diagram with the cumulative water production in the x-axis and the cumulative energy consumption (not production) in the y-axis. As an example, the diagram for the motivating example 2.1 is shown in 2.3, where the piecewise blue line represents the composite curve for water sources and the piecewise red line represents the composite curve of energy sources. Both composite curves start at the origin. Each composite curve consists of the contributions from individual sources. For instance, the energy composite curve for the example nexus consists of three linear segments, representing the three energy sources (E_1–E_3). The water composite curve has the contributions from W_1 and W_2. Because a water source can be a sink for energy only, the contributions from the sinks are in the opposite directions of the sources. A water source contributes to the positive direction of the x-axis, while a water sink contributes to the negative direction. An energy source, on the other hand, contributes to the negative direction of the y-axis, while an energy sink contributes to the positive direction. This way, all energy and water processing nodes can be represented in one diagram.

The slope of each linear segment of the water composite curve indicates the energy intensity of each water source. Therefore, we take this slope as equal to ϕ_w. The more energy intensive a water source is, the steeper is the corresponding line segment in the water composite curve. The slope of each linear segment of the energy composite curve indicates the water efficiency of each energy source. Therefore, we take this slope to be the inverse of water intensity, i.e., $1/\phi_e$. The energy source segments with higher slope are more water-efficient (or less water-intensive), and the water source segments with the lower slope are more energy-efficient (or less energy-intensive).

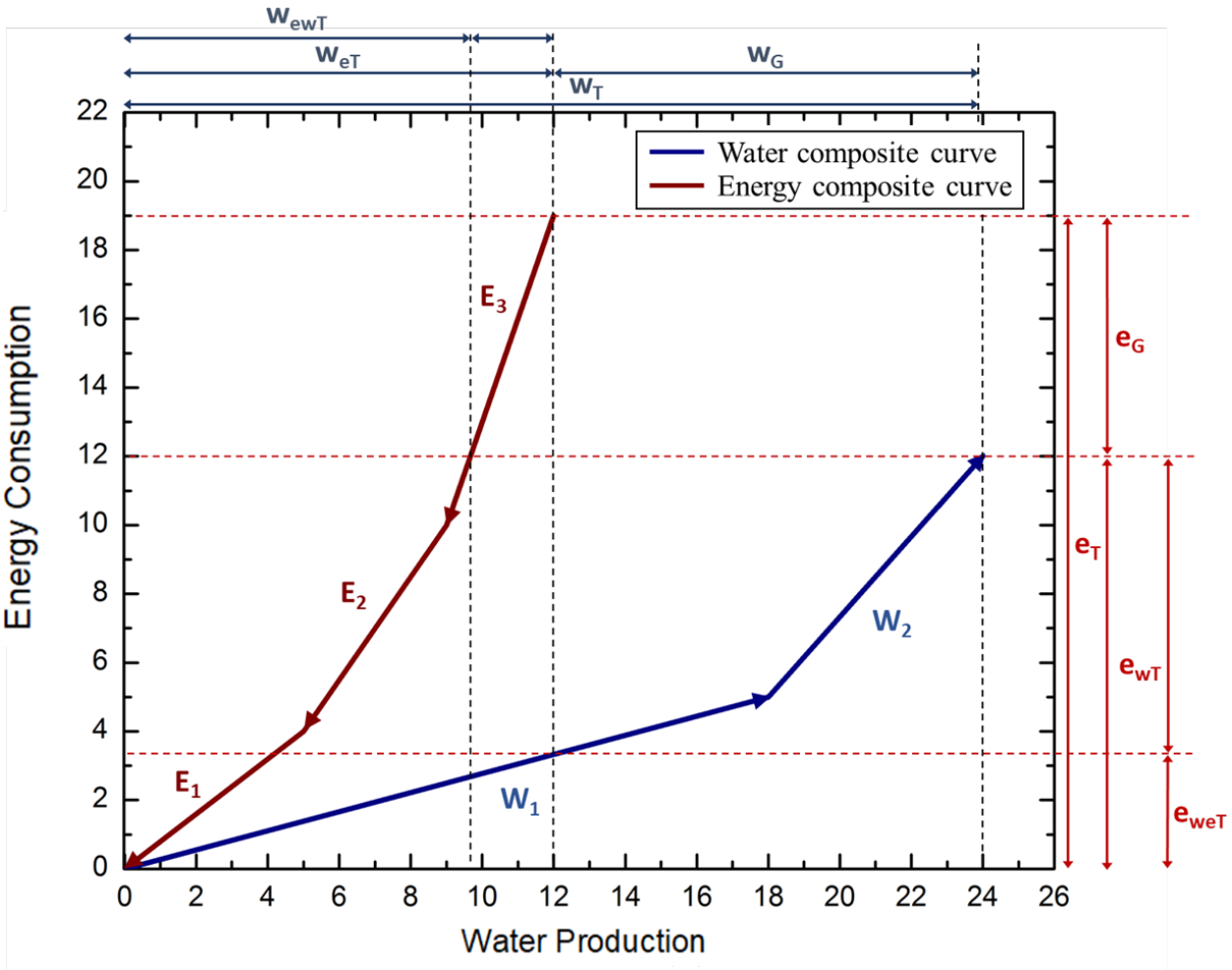

Figure 2.3: Water-Energy Nexus diagram representing the network and the supplies of the motivating example. The red composite curve corresponds to the nexus' energy sources/blue sources, while the blue composite curve the nexus' water sources/energy sinks.

The projection of the water composite curve on the x-axis represents the total water production (denoted by w_T), while its projection on y-axis represents the total energy requirement for all water production (denoted by e_{wT}). For example, the cumulative water production from W_1 and W_2 is 24 water units, while the total energy requirement of W_1 and W_2 is 12 energy units. Therefore, w_T = 24, and $e_{wT} = 12$. In similar fashion, the projection of the energy composite curve on the y-axis represents the total energy production (e_T), while its projection on x-axis represents the total water requirement for the production of all energy production (w_{eT}). For the example case, we have $e_T = 19$, and $w_{eT} = 12$. The amount of water that remains after utilizing for energy generation

goes out of the nexus as external supply to the water grid, which is denoted by w_G. Therefore, $w_G = w_T - w_{eT}$. For the example case, we have $w_G = 12$. Similarly, the difference between e_T and e_{wT} is the amount that is finally supplied to the energy grid, which is denoted by e_G. For the example case, we have $e_G = 7$. We introduce two more indicators, namely w_{ewT} and e_{weT}. w_{ewT} is the amount of water that goes to produce e_{wT}, while e_{weT} is the amount of energy that goes to produce w_{eT}.

We make the following assumptions for the representation of a nexus using our proposed diagram:

1. Water and energy enter the nexus only as external inputs to a source. Similarly, all water and energy leaving the nexus exit only as supplies to the grids.

2. A water source that needs energy only takes energy from energy sources present within the nexus. It does not take energy from external energy resources as inputs. Similarly, an energy source that needs water only takes water from other water sources. It does not take water from external water resources as inputs.

3. A water sink does not supply water to another water sink. Similarly, an energy sink does not supply energy to another energy sink.

4. A source can supply to multiple sinks. A sink can take from multiple sources.

5. A nexus is reconfigurable. We can change the capacity of a source or a sink within the allowable lower and upper limits.

6. Distances between the nodes do not affect the nexus performance.

7. The intensity factor of a source remains constant and does not change with its capacity. This leads to a linear relationship between water and energy usage at any given node or processing facility.

Assumption 1 implies that there is no loss or waste of energy and water from any facility or node. In addition, a water source that needs energy can take the energy from any energy source.

Similarly, an energy source that needs water can take the water from any water source. Assumption 3 implies that a sink completely consumes whatever energy or water is supplied to it. However, if the wastes are significant, then they can be considered as lower-quality resources to the nexus. This way, we can address the secondary treatment of energy and water within the nexus boundary. Note that these wastes can only enter to sources but not to sinks. This is ensured by assumption 1. Assumption 6 implies that there is no additional cost of transportation when we alter any source-sink connectivity. Assumption 7 in conjunction with assumption 6 implies that we can aggregate all sources with the same intensity factor to a single source. Similarly, we can split a source into multiple sources with the same intensity factor. These new sources can receive inputs from different resources and supply outputs to different sinks.

The WEN diagram is constructed such that it allows targeting water and energy simultaneously. This property enables us to reconfigure the composite curves and see how it affects the matching between nodes that can act as both water sources and energy sinks, or energy sources and water sinks. By changing the sequence of these sources and sinks appearing in the diagram, we can design new networks.

2.3 Graphical Water-Energy Nexus Optimization using Water-Energy Diagram

Based on the WEN diagram, we now describe a graphical method to reconfigure a nexus to perform the following:

- identify and eliminate redundant cycles, flows and entities within a nexus for sustainability,
- redesign a nexus with minimum generation/extraction of water and energy resources from the environment, and
- redesign a nexus for maximum yield of water and energy that can be supplied to external demands.

2.3.1 Minimization of Total Generation

To minimize the total generation of water and energy resources within a nexus, we need to identify if there is any redundant cycling of water and energy. This can be done as follows:

- Step 1: Arrange the linear segments of the energy composite curve in ascending order of their slopes ($1/\phi_{e_1} \leq 1/\phi_{e_2} \leq ...$)
- Step 2: Arrange the linear segments of the water composite curve in descending order of their slopes ($\phi_{w_1} \geq \phi_{w_2} \geq ...$)
- Step 3: Eliminate the overlapping section of the WEN diagram since this section represents redundant exchange of water and energy resources without net output. This can be done by eliminating any segment of the water composite curve that falls above the energy composite curve, and eliminating any segment of the energy composite curve that falls below the water composite curve.

Steps 1-2 ensure that the most intensive water and energy sources exchange resources with each other while leaving the most efficient water and energy sources to provide to the external grids. This is observed in the revised WEN diagram (Figure 2.4a) and the corresponding nexus graph (Figure 2.4b) after reordering the original composite curves for the example case. Notice that the energy composite curve has increasing slope, whereas the water composite curve has decreasing slope. Furthermore, there is an overlap between the water and energy composite curves near the origin. The overlapping of the composite curves divides the total diagram in two subsystems. The subsystem below the crossing point (the region encapsulated by the dotted square in the revised WEN diagram) corresponds to a subnetwork of water and energy sources that contributes no net flows to the grids. In other words, this subsystem represents redundant exchanges between water and energy resources without any net output. Therefore, this can be eliminated from the nexus.

Figure 2.5 shows a more detailed version of the redundant subsystem of the WEN diagram with the corresponding redundant nexus subgraph. As we can see from Figure 2.5b, E_1 provides energy

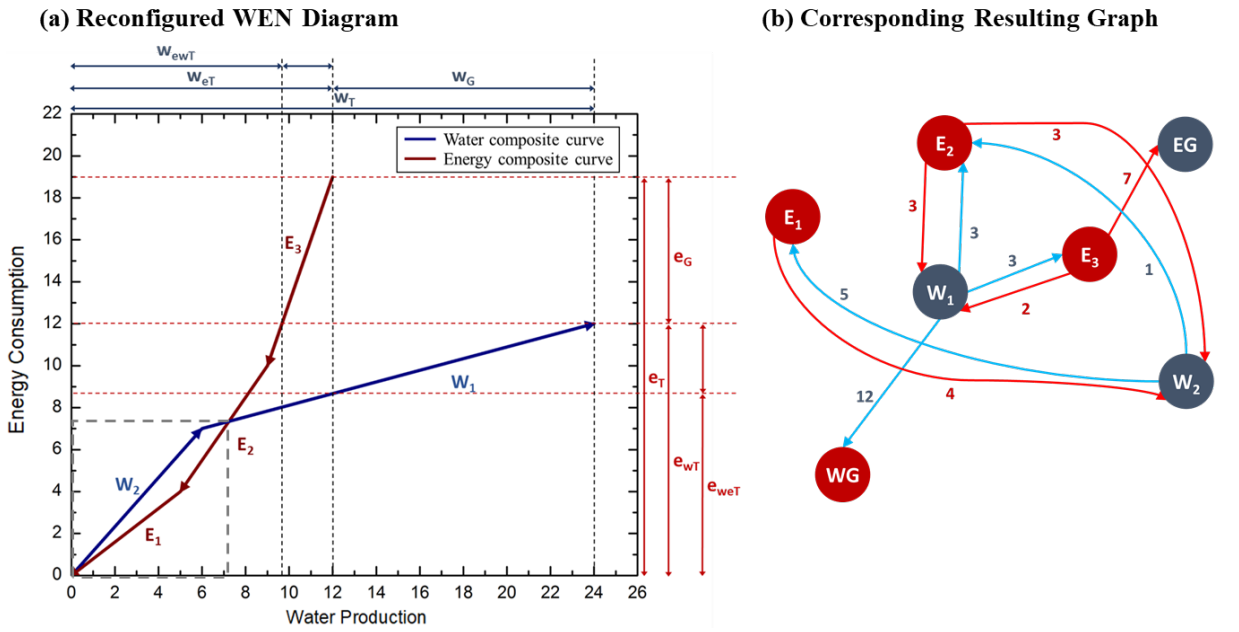

Figure 2.4: Rearrangement of the WEN diagram for the identification of redundant generation and utilization of water and energy resources: (a) revised WEN diagram and (b) corresponding nexus graph. The revised WEN diagram is obtained by structuring the source segments in decreasing intensity (or increasing efficiency). This means that the energy composite curve has increasing slope, whereas the water composite curve has decreasing slope. The region encapsulated by the dotted circle in the revised WEN diagram represents the exchanges between water and energy resources without any net output. Therefore, this region is redundant and can be eliminated from the nexus.

to W_2 which provides water to E_1 and a part of E_2. This part of E_2 provides energy to W_2 and part of W_1. W_1 in return provides water back to E_2. Therefore, there is no net output of water and energy from this subsystem, and hence this can be omitted from the total nexus graph. In contrast, the subsystem over the crossing point (Figure 2.6a) is essential and can solely satisfy the total system's energy and water demands. The corresponding nexus subgraph is shown in Figure 2.6b. Note that this essential component of the nexus does not utilize E_1 and W_2 at all. Furthermore, it utilizes only a part of E_2 and W_1.

In summary, the original nexus configuration shown in Figure 2.1 contains excess sources and excess production and consumption capacities. Therefore, the original nexus configuration was suboptimal in a sense that it was partially redundant. On the other hand, the configuration shown

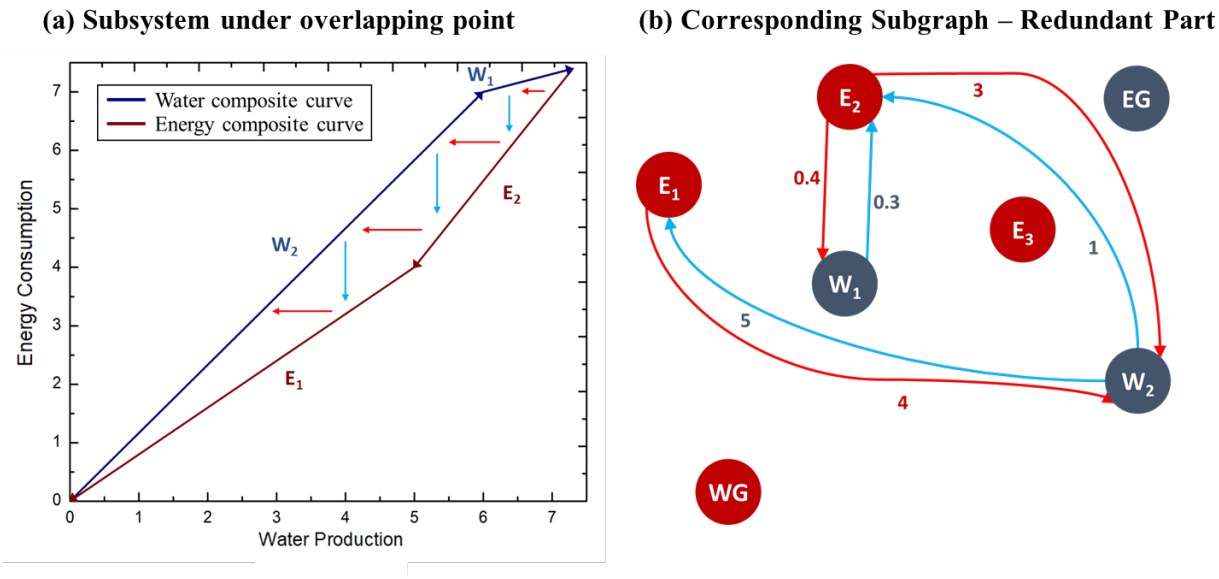

Figure 2.5: Redundancy in the motivating example case. (a) Component of the revised WEN diagram that is redundant with zero net output, and (b) the corresponding redundant subgraph with zero net output showing the redundancy of the original network. This entire subsystem can be isolated and removed without affecting the total outputs from the nexus to external grids.

in Figure 9b achieves the same outputs while using less sources and utilizing only the essential capacities of the remaining sources. The sources that entirely belong to the subsystem below the crossing point are completely discarded. However, the sources that fall in both subsystems are split and only their essential capacities are kept. In the end, the optimal configuration contains only the most efficient sources.

The fact that the arrangement of the energy and water composite curves described above leads to optimal nexus configuration with minimum generation of water and energy resources can be easily demonstrated using geometric arguments. To minimize the overall generation of water and energy, we need to maximize the overlap between the composite curves in the WEN diagram. This occurs when the energy source segments are arranged with increasing slope, and the water source segments with decreasing slope. Interestingly, for any continuous water-energy diagram, there exists a corresponding graph. However, not all graphs can be represented using a continuous water-energy diagram. This is a limitation of the graphical approach.

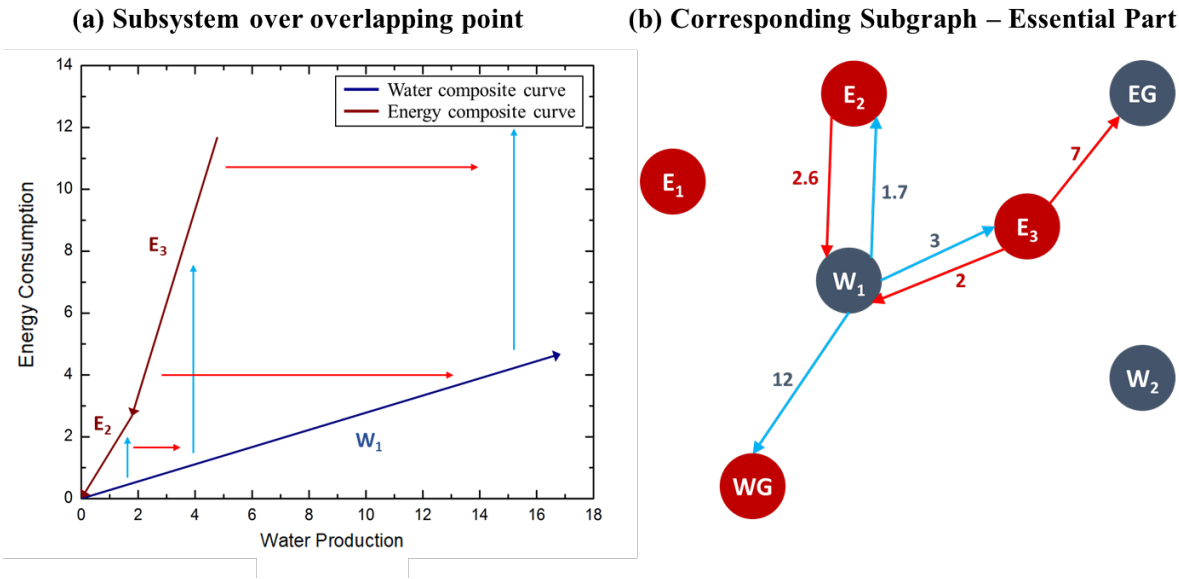

Figure 2.6: Essential component of the nexus in the motivating example case for minimum generation. (a) Essential component of the revised WEN diagram, and (b) the corresponding essential nexus subgraph that is needed to satisfy existing energy and water grid demands for the motivating example problem.

2.3.2 Maximization of Grid Supplies

In the case of minimization of the total generation while satisfying the existing grid demands, all redundant subgraphs in a water-energy nexus should be completely eliminated. However, if the goal is to harness highest economic and/or environmental benefits from a nexus, these redundant subgraphs should be further utilized to maximize the energy or water grid supplies.

Maximization of Supply to the Energy Grid: In this case, we rearrange the WEN diagram in the same way as described in Steps 1-2 in the previous section. However, instead of the Step 3, we now shift the energy composite curve vertically upward until we reach the pinch point where the two composite curves just touch each other without overlapping (Figure 2.7a). The portions of the energy and water composite curves that fall below the pinch point are discarded, while the portions of the composite curves above the pinch point now contribute to the final nexus configuration. In this way, we generate excess energy within the nexus system that can be delivered to external energy grid. Note that moving the energy composite curve vertically beyond the pinch point does

not increase the energy supply to the grid any further. There will be no closed network and any additional energy to the energy grid must be supplied from sources that are external to the current nexus system.

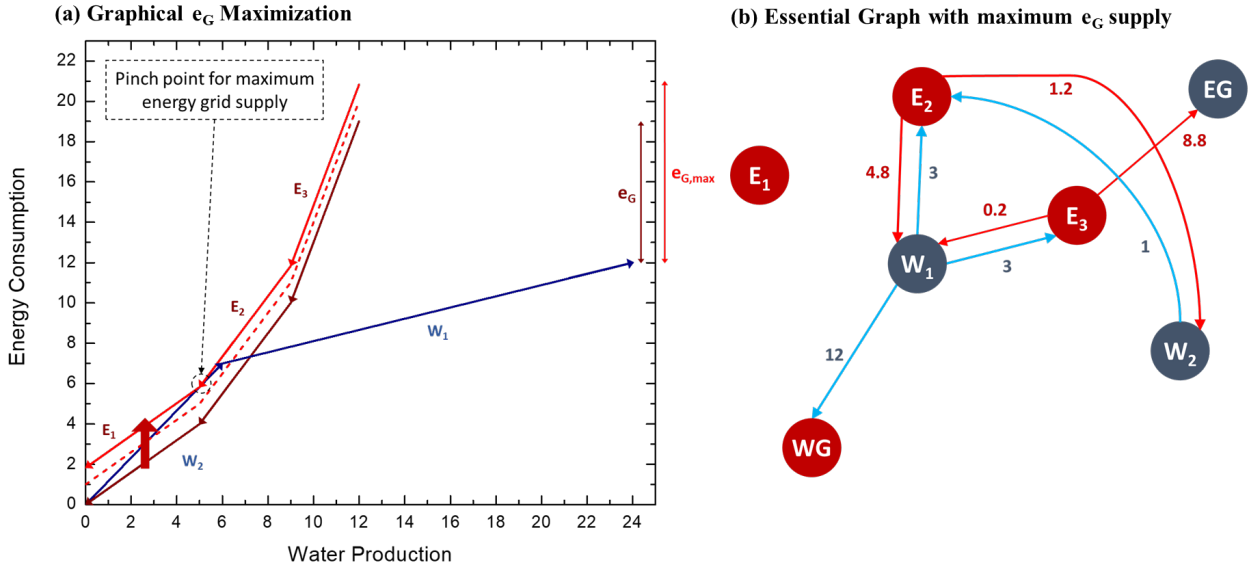

Figure 2.7: Procedure for the maximization of energy supply to the grid. (a) Graphical approach using the WEN diagram, and (b) the resultant nexus configuration that delivers maximum energy supply to the grid for the motivating example problem.

Figure 2.7b shows the resulting nexus configuration that delivers maximum energy to the grid for the motivating example problem. Since the entire E_1 and a portion of W_2 appear below the pinch point in the revised WEN diagram, we notice that E_1 is now completely eliminated and only the portion of W_2 that is above the pinch point is used producing only 1 water unit at the expense of 1.2 energy unit from E_3 in the revised nexus configuration. However, W_1 supplies a total of 18 water units out of which 12 units is delivered to the water grid. This amount is the same as the amount of water that is supplied to the grid in the case of minimum generation. However, the revised nexus configuration now supplies a total of 8 energy units (1 unit from E_2 and 7.8 units from E_3) to the energy grid, which is 25% higher than the amount (7 energy units) for the case of minimum generation. The overall energy generation from all sources is increased by 29% from

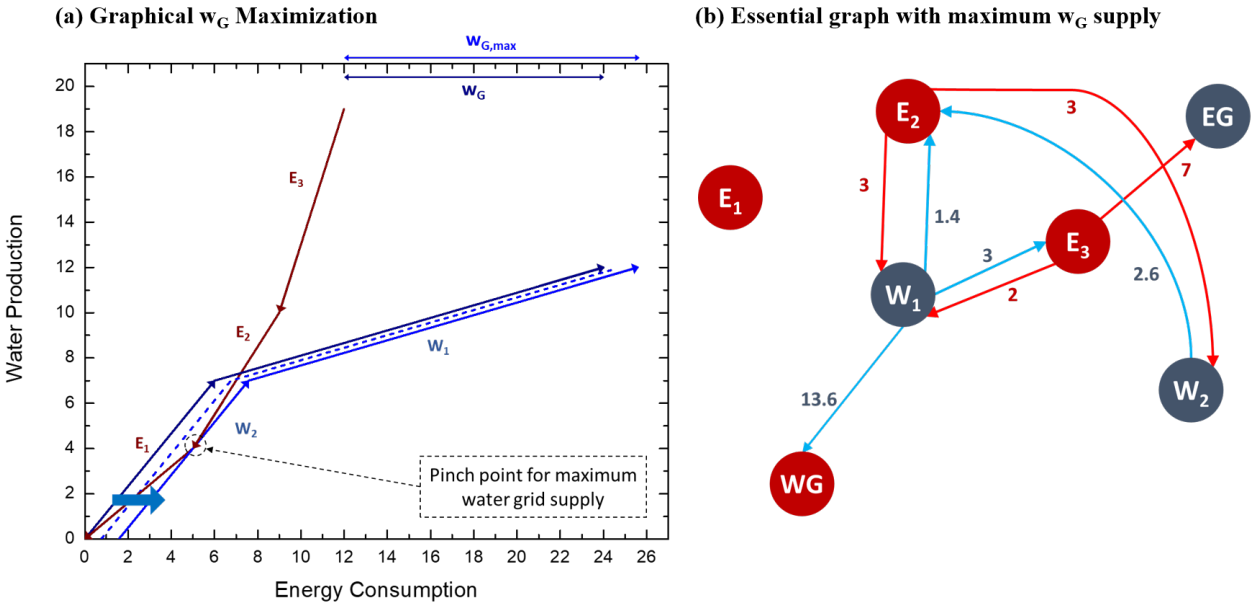

Figure 2.8: Procedure for the maximization of water supply to the grid. (a) Graphical approach using the WEN diagram, and (b) the resultant nexus configuration that delivers maximum water supply to the grid for the motivating example problem.

11.6 to 15 units when compared to the case of minimum generation. The generation of water is also increased by 7.8% from 16.7 to 18 units to compensate for the increased energy. However, the generation of energy and water are still less than those compared to the base case (Figure 2.1).

The nexus configuration that supplies maximum energy to the grid (Figure 2.7b) is also different than the configuration for minimum generation (Figure 2.4b). For instance, both E_2 and E_3 contribute to the energy grid in the case of maximum supply, while only E_3 contribute to the energy grid in the case of minimum generation. Furthermore, the generation capacity of E_2 is now increased by more than 130% from 2.6 units to 6 units. The water grid can be similarly maximized, while keeping the energy grid constant. Similar procedure is followed to maximize the supplies to the water grid, by shifting the water composite curve to the right (Figure 2.8).

2.3.3 Nexus Optimization in the Presence of Restricted Matches

The presence of prohibited connections may or may not increase the size of the essential part of the nexus graph. Therefore, we now describe a method to account for matching constraints and

measure their effects, if there is any, on nexus optimization. To obey any completely restricted matches, we need to rearrange the WEN diagram in the same way as described in steps 1-3 in the minimization of total generation section. The essential nexus obtained after these steps is the lower bound to the possible reduction of the total generation, and the redundant part of the unconstrained nexus is an upper bound to the part of the nexus that can be eliminated.

The result obtained from unrestricted matching is still applicable, and hence there will be no change in the size of the essential nexus graph, if

1. the restricted match is not present in the WEN diagram,

2. the restricted match appears only at the redundant part of the WEN diagram, and

3. the requirements of the sink of a prohibited source-sink match can be satisfied by other source(s) that are present in the essential nexus. Similarly, the amount produced by the source of a prohibited source-sink match can be completely delivered to other sink(s) that are present in the essential nexus.

Case (i) can be easily inferred – since if the current connectivity of the essential nexus is feasible, then the essential nexus is the minimum possible. For example, it can be seen from Figure 2.9a that even if W_1 cannot provide energy to E_1, then the entire nexus configuration is not affected. In case (ii), irrespective of the restriction, the essential nexus remains unaffected. Lastly, case (iii) is demonstrated in Figure 2.9, where energy source E_2 cannot provide energy to water source W_1. E_1 also supplies energy to W_1 below the overlap, however there is no need to take this redundant section into account. The part of E_2 above the overlap can be replaced by E_3, given that E_3 provides its energy to W_1 and E_2 supplies to the energy grid. Then, replacing E_2 with E_3 will satisfy the connectivity constraint and the essential nexus will remain unaffected.

When the source in a prohibited source-sink match cannot be replaced by another source from the essential part of the nexus graph, we need to redesign the WEN diagram. This can be done by including either a source or a sink from previously redundant portion of the nexus graph. While this provides opportunities for new allowable matching, this also increases the size of the essential

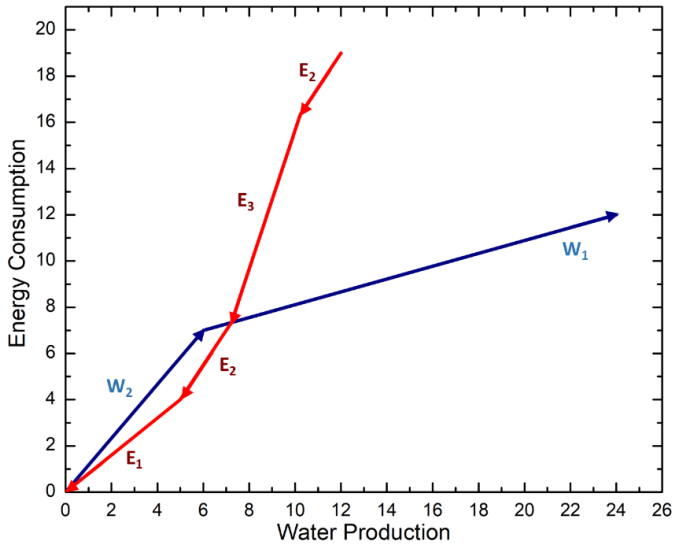

Figure 2.9: Revised WEN diagram to address prohibited match $W_1 - E_2$ for the case where the essential nexus is unaffected. As an illustration, we consider that the energy flow from E_2 to W_1 is prohibited for some operational reasons. The revised WEN diagram is obtained by substituting the part of E_2 providing energy to W_1 above the overlap with E_3. As a result, E_3 provides more energy to W_1 compared to the unconstrained case, and E_2 provides its energy to the energy grid. Therefore, the essential nexus remains unaffected in terms of size.

graph and require more generation. These are illustrated in Figures 2.9a,b. Here, we consider that the water flow from W_1 to E_2 is prohibited for some operational reasons. The revised diagram in Figure 2.10a is obtained by substituting the part of W_1 providing water to E_2 above the overlap, with W_2. After the replacement, a portion of W_1 enters the redundant part of the nexus, while a portion of W_2 is used in the essential nexus. Therefore, the essential nexus increases in size compared to the unconstrained case. We can also revise the WEN diagram by substituting the part of E_2 receiving water from W_1 above the overlap with E_1, as shown in 2.10b. In this case, the sink of the infeasible matching is substituted. After the replacement part of E_2 has to enter the redundant part of the nexus, and E_1 enters the essential nexus. Therefore, the essential nexus increases in size compared to the unconstrained case. The effect on the essential subgraph given by Figure 2.10b is less when compared to the one shown in Figure 2.9a. Therefore, we finally the configuration corresponding to the one shown in Figure 2.9b.

In general, the following rules apply to ensure minimum impact on the essential part of the

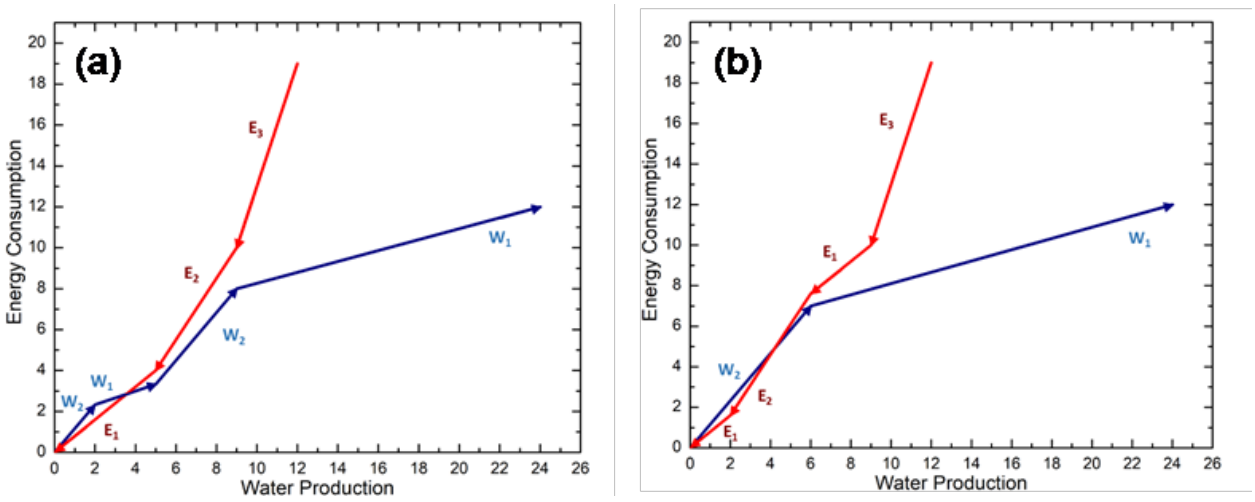

Figure 2.10: Revised WEN diagram to address prohibited match $W_1 - E_2$ for the case where the essential nexus is affected. We can revise the WEN diagram in two ways: (a) by substituting the part of W_1 providing water to E2 above the overlap with W_2, or (b) by substituting the part of E_2 receiving water from W1 above the overlap with E_1. The effect on the increase is reduced in (b) compared to (a), and therefore, we finally select (b).

nexus graph: (i) an energy source is substituted by an admissible energy source with the closest lower slope, and (ii) a water source is substituted by an admissible water source with the closest higher slope.

2.3.4 Nexus Optimization in the Presence of Quality Requirements

The presence of quality specifications can be dealt with appropriate mixing of multiple water sources in order to satisfy the required impurity concentration by the sinks. Again, we first construct the WEN diagram without considering any quality specifications. Then, we identify the matches which do not satisfy the sink requirements. Note that we need to only focus on the essential part of the nexus graph for this check.

As an illustration, let us revisit the motivating example. While the base case remains the same, we now further impose an impurity level for each water source (in ppm) and a maximum allowable impurity level (in ppm) for each water sink. These values are provided in Table 2.1. We notice that W_2 still can supply water to all sinks ($E_1 - E_3$), as the impurity level is lower than the maximum impurity tolerance of the sinks. According to Figure 2.4, W_1 should also provide all the water that

E_3 requires to operate (3 water units), if there were no quality restrictions. However, under the new quality specifications, W_1 alone cannot provide water to E_3, since W_1 has a higher impurity (200 ppm) level than the maximum allowable level for E_3 (100 ppm). Therefore, we need to mix a part of W_1 with a part of W_2 that has much lower impurity level, before we can send it to satisfy the water demand of E_3. The relative amounts of W_1 and W_2 for mixing can be determined using a method similar to lever arm rule for mixing.

Table 2.1: Quality specifications for the motivating example of WEN base case.

Energy Source	**Water Withdrawn**	**Energy Produced**	**Intensity** (ϕ_E)	**Maximum Allowed Impurity** (q_E)
E_1	5	4	1.250	400 ppm
E_2	4	6	0.667	200 ppm
E_3	3	9	0.333	100 ppm
Water Source	**Water Produced**	**Energy Consumed**	**Intensity** (ϕ_W)	**Output Impurity Level** (q_W)
W_1	6	7	1.167	200 ppm
W_2	18	5	0.278	50 ppm

Such a mixing is demonstrated in Figure 2.11 with blue dotted line. To obtain the minimum essential nexus, we have to find the minimum fraction of W2 that is required to satisfy the quality specifications. This is obtained by solving the impurity concentration balance and the total water balances together. These balances for the example case are given as

$$W_{23} + W_{13} = 3 \tag{2.3}$$

$$q_{W_2} \cdot W_{23} + q_{W_1} \cdot W_{13} = q_{E_3} \cdot 3 \tag{2.4}$$

where, $W_{23}, W_{13} \geq 0$, is the amount of water provided to E_3 from W_2 and W_1, respectively. q_{W_1} and q_{W_2} are the qualities of water from W_1 and W_2, which are 200 ppm and 50 ppm, respectively. Furthermore, q_{E_3} is the maximum allowable impurity level, which is 100 ppm. For these values of impurity levels, Eqs. 2.3-2.4 lead to the following solution: 2 units of water from W_1 should be mixed with 1 unit of water from W_2 to satisfy both the water demand and quality specifications of E_3.

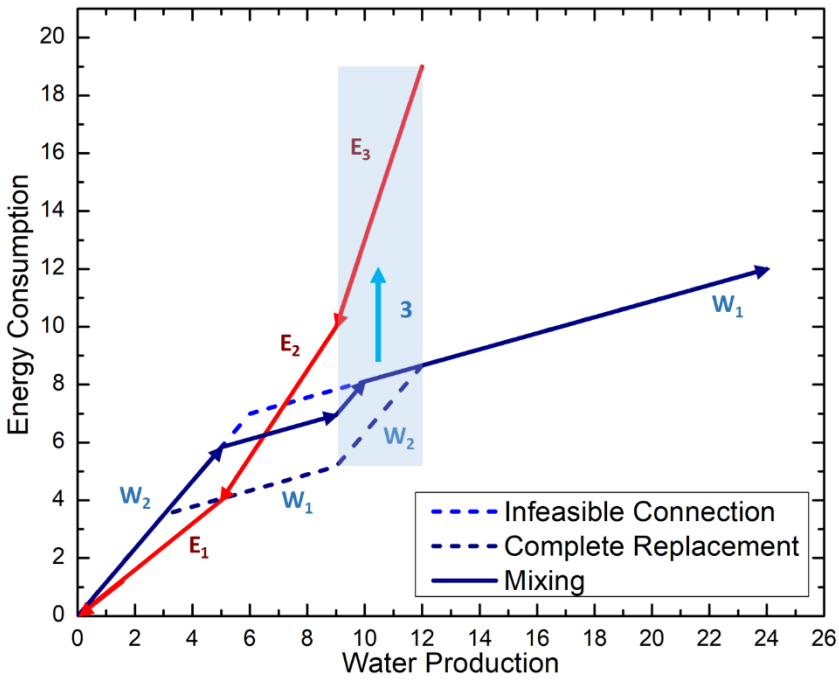

Figure 2.11: Revised WEN diagram to satisfy the quality specification of E_3. The extremes of complete replacement (due to restriction matching) and infeasible matching (base case) are demonstrated.

2.4 Results on Regional WEN Optimization

So far, we have provided a graph-theoretical representation of the water-energy nexus as well as a pinch-like graphical method that enables us to obtain the essential nexus configurations for minimum generation or grid supplies maximization. In this section, we attempt to analyze and optimize WEN using case studies on existing infrastructures at a regional level. In this scale, the external energy resources correspond to the system's primary fuels, like crude oil, nuclear fuel, natural and shale gas, etc. The external water resources are the freshwater found in surface or underground aquifers, but also brackish or seawater. The water sources, which are also energy sinks, for a regional nexus are the purifying, desalinating and distributing facilities that obtain the water resources from the environment and deliver it to water sinks and to the water grid. The regional energy sources, which are also water sinks, correspond to the processing facilities that treat crude fuels, but also power plants that use energy primary resources to generate electricity.

These fuel and electricity outputs are delivered to energy sinks and to the energy grid to satisfy the system's energy demands. The system of reference can be a town, a county, a state, a country, or a region.

The country of Spain offers an extended and diverse pool of energy and water sources, including open-loop cooled power plants, biofuels and desalination, due to its uneven climate. Fuel, power and water data, assorted by source were acquired for 2013 ([6, 7, 5]), along with literature intensity factors [8]. The total fossil energy utilized was 8,907,520 TJ. From fossil energy along with renewables, 285,632 GWh of electricity was generated. By using maximum values of intensity factors (withdrawal) and a 45/55 ratio of open loop and closed loop cooling in power plants, it was calculated that 26,750 Mm3 of water was utilized for energy. Analytically, 7,878 Mm^3 was utilized solely for fuel, while 18,878 Mm^3 are withdrawn for fuel which was used for power generation.

In total, 38,106 Mm^3 of water was estimated to have been withdrawn of which, 78% corresponds to surface water treatment, 18% to groundwater treatment, and the rest 4% to desalinated water. For the desalination plants the maximum capacity was used. It was estimated, that 25,335 GWh of power was required for water generation. These data are presented in Appendix A (Tables A.1,A.2), and further information can be found at [8].

The resulting WEN diagram was constructed for power generation sources and water sources (Figure 2.12). There is overlapping between the intensive sources of Spain's nexus, which correspond to open-loop nuclear power plant, and seawater desalination. In particular, 11,652 GWh of nuclear power (4%) and 2,691 Mm3 of desalinated water (7%) can be omitted from the network, while the grid demands for power and water are still satisfied. For average values of intensity factors, the redundant subsystem corresponds to 11,279 GWh (3.9%) and 1,906 Mm^3 (5%) from total generation.

In Figure 2.13, the alternative scenario of using the biofuels produced in Spain for electricity generation instead of transportation and heating sources as a news system is demonstrated on the energy-water diagram. In this case, there is significant overlapping of the curves and a redundant

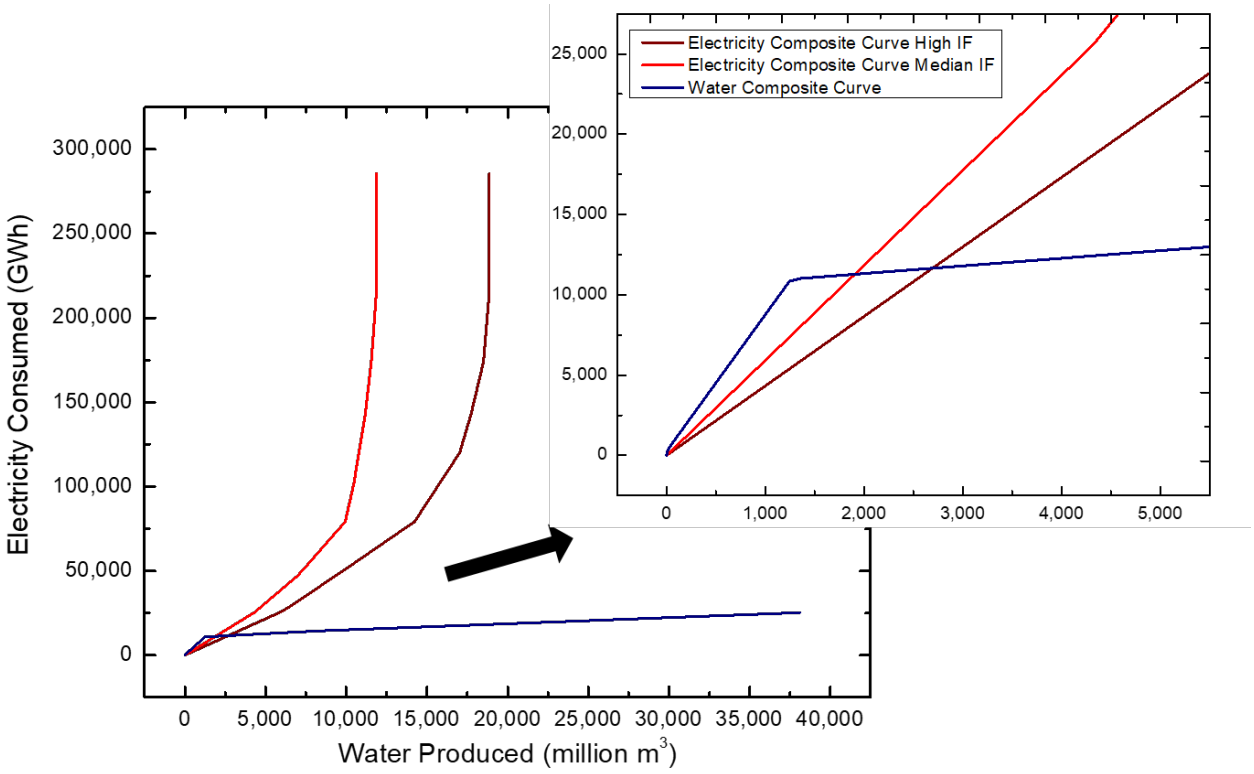

Figure 2.12: Water-energy nexus diagram for electricity and water sources for the case study on Spain. The red curve corresponds to the electricity composite curve that was obtained with median values of the water intensity factors. The dark red curve corresponds to the electricity composite curve that was obtained with maximum values of the water intensity factors. The water composite curve, depicted in blue color, was derived using maximum values of energy intensity factors.

loop exists due to the presence of seawater desalination and biofuel power generation. Almost 8,000 million Mm^3 of water and 20,000 GWh of electricity could be subtracted from the network without affecting the grid supplies of the hypothetical system. This indicates, that seawater desalination should not be combined with biofuels in a nexus in terms of profitability, except from the case of certain technologies being imposed in a system due to environmental and sustainability regulations.

2.5 Summary

We presented a simple, graphical and systematic method for the redesign, retrofit and optimization of complex water-energy nexus using the concept of a water-energy nexus (WEN) diagram.

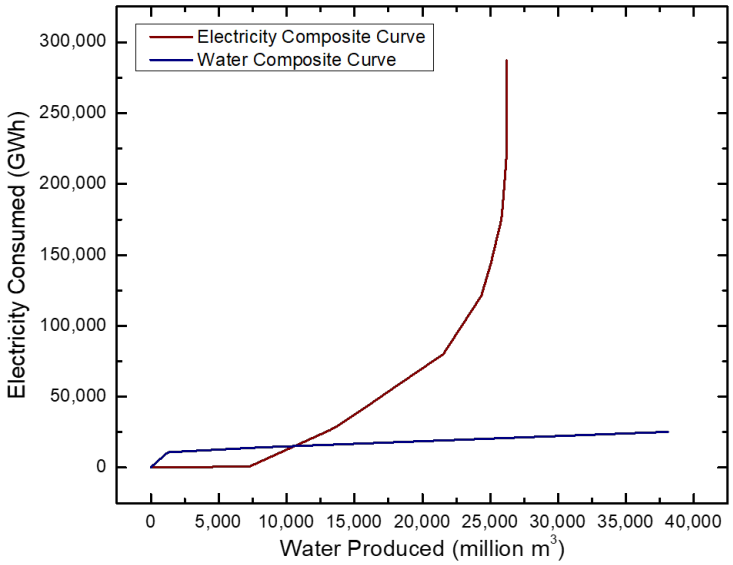

Figure 2.13: Water-energy nexus diagram for electricity and water sources of Spain, using biofuels for electricity generation.

Several useful results from the graph theory are also extracted for nexus analysis. We demonstrated that a nexus can be represented as a directed bipartite graph with water and energy flows. While the graph-theoretic approach characterizes the properties of optimal nexus configurations, further works are needed to develop subsequent algorithms to identify redundant subsystems. However, we provided a graphical technique to identify redundant subsystems and redesign a nexus for optimal resource generation and utilization. Using the WEN diagram it is possible to answer the following questions: (i) how to systematically identify and eliminate redundant cycles, flows and entities within a nexus for sustainability, (ii) how to systematically design a nexus with minimum generation/extraction of water and energy resources from the environment, and (iii) how to systematically design a nexus for maximum yield of water and energy that can be supplied to external demands. It is worthwhile to note that the graphical procedure presented here is based on concepts that are similar to the ones used in pinch analysis for solving individual water and energy targeting problems. However, a key difference is that this work essentially addresses the water and energy integration simultaneously by considering the interactions between two networks. It was observed that depending on the objective, the optimal configurations of a nexus could be signifi-

cantly different. For conceptual development of the approach, we considered simplistic scenarios with aggregated sources and sinks. While conceptually it is possible to apply the same framework for scenarios with many sources and sinks, the variability in the results would depend on the accuracy of the input data provided, rather than the size of the nexus system. Therefore, future work should be directed to more realistic design and optimization of large-scale nexus systems when accurate descriptions of all sources and sinks are available. Lastly, while we did not take the economics of retrofitting a nexus into account, further refinement of the results can be done by performing a cost-benefit analysis.

3. SUPERSTRUCTURE-BASED REGIONAL WEN DESIGN[1]

The previous chapter addresses the interdependence analysis within a WEN and focuses on the energy and water sources and consumers of a WEN. Except from nexus interdependence, there can be other factors such as economic or transportational constraints that do not allow for complete elimination of redundant subsystems. In this chapter, the superstructure-based optimal design of complex regional WENs is addressed to balance the trade-offs between economics, interdependence, and sustainability.

In order to come up with the optimal water-energy nexus for a region the entities acting upon it are first defined. Given are:

- a pool of available energy and water resources in a region that can be withdrawn,
- a set of final energy and water sinks with end-use fuel, power and water demands to be satisfied,
- a pool of intermediate processing energy and water sources that can be allocated, with different generating technologies and varying utilization of resources.

The decisions to be determined include the combination of processing plants (binary variables of selection), their nominal generation. The model also determines the connectivity (binary variables of existence), and the nominal flow rates of the connecting streams. The objective is to minimize the total annualized cost for the planning horizon, comprised of the fixed investment cost, capital cost and operating cost components.

3.1 Water-Energy Nexus Superstructure

To address this problem, a water-energy nexus superstructure is constructed, where all different nodes are represented, and all potential connections are demonstrated (Figure 3.1). It is evident,

[1]Reproduced in part with permission from [9] Tsolas, S. D., Karim, M. N., & Hasan, M. M. F. (2019). Systematic Design, Analysis and Optimization of Water-Energy Nexus. In Computer Aided Chemical Engineering, vol. 47, pp. 227-232. Elsevier

that the WEN graph is part of the WEN superstructure. The WEN design problem differs from conventional supply chains and pooling problems, as there are two competing products (energy and water), which must be exchanged between the intermediate facilities (sources).

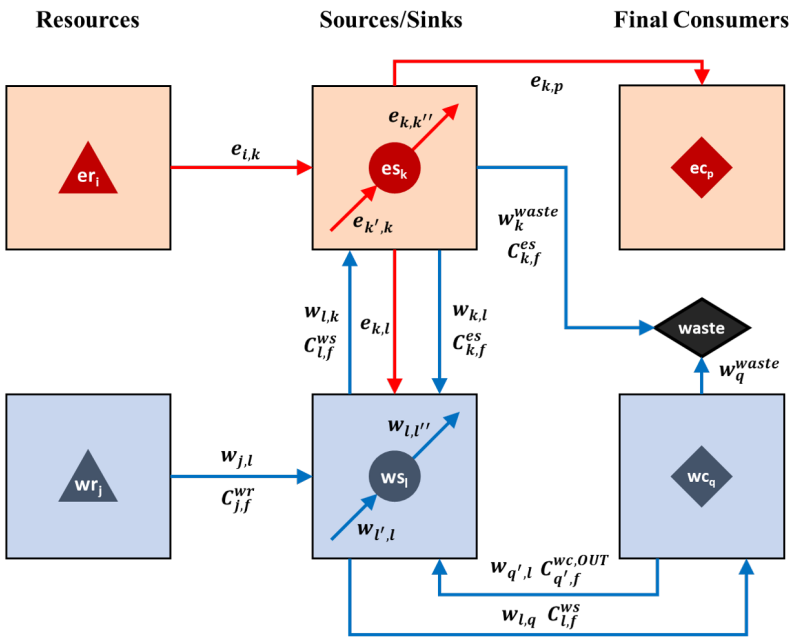

Figure 3.1: The Water-Energy Superstructure depicts regional system as a three-echelon supply chain.

Given is a set of energy resources I that are available in a region. These resources include underground fossil fuels, like crude oil, coal, natural gas reserves or shale gas formations with a fixed availability era_i. These can be also renewable energy resources, like solar and wind power. In that case, the availability is infinite.

In the water side, a set of available water resources J is available in the same region. These can be surface water from lakes and rivers, fresh and brackish groundwater, as well as seawater. There is also an availability parameter associated with each resource wra_j, which expresses the environmentally allowable withdrawal limit from the ecosystem's water reserves. In addition, the water withdrawn from each resource has F impurities present with $C_{j,f}^{wr}$ concentration, that need

to be removed for the water to be usable by the sinks. The energy and water resources are captured on the resources block in Figure 3.1.

Given is a set of end-use energy consumers P, with fixed demands ecd_p. These can be different kind of fuels, like diesel, ethanol, natural gas, LNG and also electricity. There must be a correspondence between the final consumers of different kinds and the energy resources. Hence, if there is a demand for natural gas or LNG, there must be a present natural gas or shale gas reserve in the same region.

In the water side, a set of end-use water consumers Q is defined, with fixed demands wcd_q and specified maximum impurity concentration levels C_p^{wc} that need to be satisfied. These consumers represent the various agricultural, commercial and residential sinks within a regional nexus. Because of the different type of the water usage from the sinks, the quality standards are also different. For example, domestic freshwater must be of greater quality than irrigation water. In addition, there is a recovery fraction β_q^{rec} and fixed outlet concentrations $C_{q,f}^{wc,out}$ that define the amount and quality of the water reclaimed from the final consumers. The energy and water consumers are the terminating nodes in Figure 3.1.

Finally, the intermediate facilities correspond to the sources defined in Chapter 2. For each energy source K there is an associated conversion factor β_k which is the ratio of the output clean fuel or power to the incoming crude fuel or fuel input respectively. Furthermore, an intensity factor is associated with every energy source and expresses the water requirement in terms of withdrawal, ϕ_k^{with} and consumption, ϕ_k^{cons}.

For each water source L there is an associated intensity factor ϕ_l^{cons}, expressing the energy requirement for water generation and purification. In addition, a removal ratio for $rr_{l,f}^{ws}$ is available for every water source, expresses the purifying capability for contaminant f. The total water coming out of a water source, ws_l has a concentration value for every impurity f present, $C_{l,f}^{ws}$. The energy and water sources are the intermediate blocks in Figure 3.1. Last but not least, there is a node representing a waste disposal site, where any untreated streams are deposited.

As it can be inferred from the figure, energy sources k receive energy streams from the re-

sources i, produce energy and provide it to other energy sources k', water sources l and the final consumers. The same way, water sources l, obtain water from the water resources j and reclaimed water from the consumers q, purify it and distribute it to other water sources l', energy sources k and to water final consumers p. Each water stream contains its own impurity concentration level.

3.2 Model Formulation

Following the superstructure description, the water-energy nexus is mathematically modeled as an MINLP problem. The model is governed by the total energy and water balances in the different entities. In addition, component balances for the different impurities must hold, as well as the removal and contamination equations must hold, for the concentration of the various to be calculated. Along with the variables upper and lower bounds definitions, the allowable limits of impurities' concentrations are also imposed. We also utilize the theoretical targets for the intermediate streams from the graph-theoretic work.

3.2.1 Balance Constraints

The general equations governing the generalized WEN problem are listed below. These are mainly the balances of energy and water along with the demands of the sinks, which are connected with the supplies of the sources via the intensity factors. The rest are the bounds of generating capacities, as well as some specifications of the networks that can be imposed.

Energy resource i availability: The total energy withdrawn from resource i must satisfy the supply availability:

$$\sum_{k} e_{i,k} \leq era_i \qquad \forall\, i \,\epsilon\, I \tag{3.1}$$

Water resource j availability: The total water withdrawn from resource j must satisfy the supply availability:

$$\sum_{l} w_{j,l} \leq wra_j \qquad \forall\, j \,\epsilon\, J \tag{3.2}$$

Energy source/water sink k

Energy balance: The energy intake to an energy source comes from energy resources and other

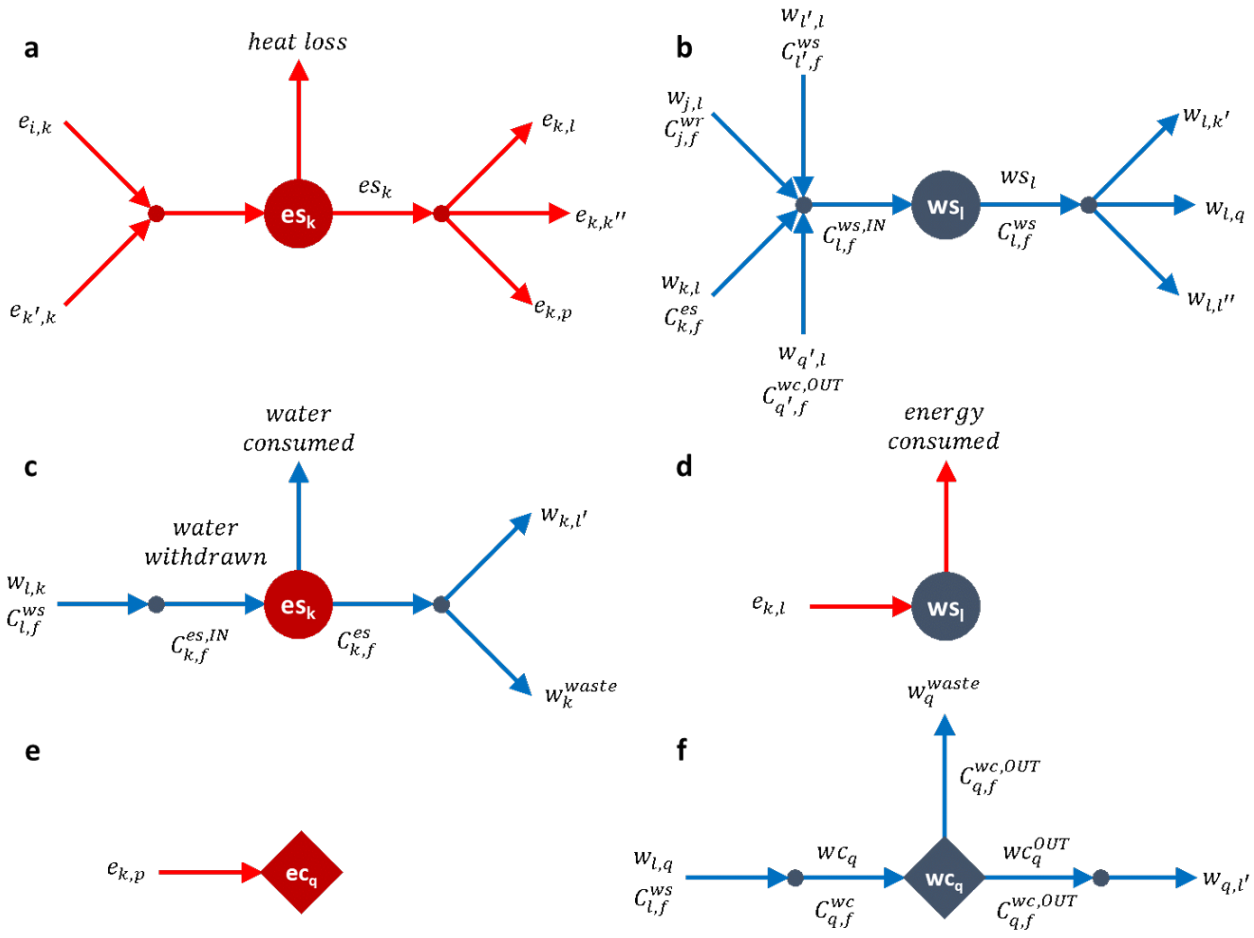

Figure 3.2: Analysis of incoming and outgoing streams for every node within the WEN superstructure.

water sources k and is converted converted to output power or fuels. This output energy is supplied to the water sources l, the end-use energy consumers p and other energy sources k'.

$$\beta^{es}_k \cdot \left(\sum_i e_{i,k} + \sum_{\substack{k' \\ k' \neq k}} e_{k',k} \right) = es_k \qquad \forall\, k \,\epsilon\, K \tag{3.3}$$

$$es_k = \sum_l e_{k,l} + \sum_p e_{k,p} + \sum_{\substack{k' \\ k' \neq k}} e_{k,k'} \qquad \forall\, k \,\epsilon\, K \tag{3.4}$$

Water withdrawal: The water intake to an energy source comes from water sources l and must

satisfy the water requirements of power and fuel production of energy source k:

$$\phi_k^{ewith} \cdot es_k = \sum_l w_{l,k} \qquad \forall\, k \,\epsilon\, K \tag{3.5}$$

Water balance: The water withdrawn by an energy source k is partly lost in the energy plant and the rest returns to other water sources l' and to the waste disposal:

$$\sum_l w_{l,k} = \phi_k^{econs} \cdot es_k + \sum_{\substack{l' \\ l' \neq l}} w_{k,l'} + w_k^{waste} \qquad \forall\, k \,\epsilon\, K \tag{3.6}$$

Input contaminant balance: The concentration of the f contaminant is obtained by the mixing of the input water streams to energy source k:

$$C_{k,f}^{es,IN} \cdot \sum_l w_{l,k} = \sum_l C_{l,f}^{ws} \cdot w_{l,k} \qquad \forall\, k \,\epsilon\, K \tag{3.7}$$

Water quality deterioration: The f contaminant concentration is increased as the water passes through energy source k:

$$C_{k,f}^{es} = \left(1 + cr_{k,f}^{es}\right) \cdot C_{k,f}^{es,IN} \qquad \forall\, k \,\epsilon\, K,\ f \,\epsilon\, F \tag{3.8}$$

Water source/energy sink l

Total water balance: The water intake to water source l comes from water resources i, other water sources l', reclaimed water from final consumers q and recovered water from energy sources k. The total water generated from the water source is supplied to other energy sources k', final water consumers q' and other water sources l'':

$$\sum_j w_{j,l} + \sum_{\substack{l' \\ l' \neq l}} w_{l',l} + \sum_q w_{q,l} + \sum_k w_{k,l} = ws_l \qquad \forall\, l \,\epsilon\, L \tag{3.9}$$

$$ws_l = \sum_{\substack{k' \\ k' \neq k}} w_{l,k'} + \sum_q w_{l,q} + \sum_{\substack{l' \\ l' \neq l}} w_{l,l'} \qquad \forall\, l \,\epsilon\, L \tag{3.10}$$

Input contaminant balance: The concentration of the f contaminant is obtained by the mixing of the input water streams to water source l:

$$C_{l,f}^{ws,IN} \cdot ws_l = \sum_j C_{i,f}^{wr} \cdot w_{j,l} + \sum_{\substack{l' \\ l' \neq l}} C_{l',f}^{ws} \cdot w_{l',l} + \sum_q C_{q,f}^{wc,OUT} \cdot w_{q,l} + \sum_k C_{k,f}^{es} \cdot w_{k,l} \qquad \forall l \, \epsilon \, L, \; f \, \epsilon \, F \tag{3.11}$$

Water quality improvement: The f contaminant concentration is reduced as the water passes through water source l is treated:

$$C_{l,f}^{ws} = (1 - rr_{l,f}) \cdot C_{l,f}^{ws,IN} \qquad \forall \, l \, \epsilon \, L, \; f \, \epsilon \, F \tag{3.12}$$

Energy consumption: The total energy intake from the energy sources k to a water source l is used to satisfy the energy requirements of water generation:

$$\phi_l^w \cdot ws_l = \sum_k e_{k,l} \qquad \forall \, l \, \epsilon \, L \tag{3.13}$$

Energy final consumer p

Energy demand satisfaction: The total energy delivered to the final consumer p must satisfy the consumer's demand:

$$\sum_k e_{k,p} \geq ecd_p \qquad \forall \, p \, \epsilon \, P \tag{3.14}$$

Water final consumer q

Inlet contaminant balance: The concentration of the f contaminant is obtained by the mixing of the input water streams to water consumer q:

$$C_{q,f}^{wc} \cdot \sum_l w_{l,q} = \sum_l C_{l,f}^{ws} \cdot w_{l,q} \qquad \forall \, q \, \epsilon \, Q, \; f \, \epsilon \, F \tag{3.15}$$

Water demand satisfaction: The total water delivered to the final consumer q must satisfy the

demand:

$$\sum_{l} w_{l,q} \geq wcd_q \qquad \forall\, q \,\epsilon\, Q \tag{3.16}$$

Water quality satisfaction: The contaminant f concentration must satisfy the tolerance level of the final sink:

$$C_{q,f}^{wc,IN} \leq C_{q,f}^{wc,U} \qquad \forall\, q \,\epsilon\, Q,\ f \,\epsilon\, F \tag{3.17}$$

Total water delivered: The total water intake to a water final consumer q is defined:

$$wc_q^{IN} = \sum_{l} w_{l,q} \qquad \forall\, q \,\epsilon\, Q \tag{3.18}$$

Outlet water streams: The total water delivered on consumer q is used and it is partially lost, partially disposed as waste and also partially recollected and is also reclaimed as waste and sent back to water sources for treatment:

$$wc_q^{IN} = wc_q^{lost} + wc_q + w_q^{wc,waste} \qquad \forall\, q \,\epsilon\, Q \tag{3.19}$$

The amount of water that is lost is determined by the loss fraction:

$$w_q^{lost} = \beta_q^{loss} \cdot wc_q^{IN} \qquad \forall\, q \,\epsilon\, Q \tag{3.20}$$

The amount of wastewater that is recovered is determined by the recovery fraction:

$$wc_q = \beta_q^{rec} \cdot wc_q^{IN} \qquad \forall\, q \,\epsilon\, Q \tag{3.21}$$

Finally, the wastewater that is disposed without being treated is what remains from the previous streams:

$$w_q^{waste} = \left(1 - \beta_q^{loss} - \beta_q^{rec}\right) \cdot \sum_{l} w_{l,q} \qquad \forall\, q \,\epsilon\, Q$$

3.2.2 Logical Constraints

The binary variables z_k, z_l correspond to the allocation decision of sources k, l respectively, in order to account for the fixed part of the capital cost. The binary variables $z_{a,b}$ correspond to the existence of connecting stream from entity a to b. The following constraints dictate the existence of plants and streams according to their connectivity.

Energy source k

Selection of energy source - incoming energy streams: If energy source k is not selected, there can be no incoming energy streams:

$$z_{i,k} \leq z_k \qquad \forall\, i \epsilon I,\, k \epsilon K \tag{3.22}$$

$$z_{k',k} \leq z_k \qquad \forall\, k' \neq k,\, k \epsilon K \tag{3.23}$$

Existence of incoming energy streams - energy source: If no incoming streams reach energy source k, then the source cannot be selected:

$$\sum_i z_{i,k} + \sum_k z_{l,k} \geq z_k \qquad \forall\, k \epsilon K \tag{3.24}$$

Selection of energy source - outgoing energy streams: If energy source k is not selected, there can be no outgoing energy streams:

$$z_{k,p} \leq z_k \qquad \forall\, k \epsilon K,\, p \epsilon P \tag{3.25}$$

$$z_{k,k'} \leq z_k \qquad \forall\, k,\, k' \neq k \epsilon K \tag{3.26}$$

$$z_{k,l} \leq z_k \qquad \forall\, k \epsilon K,\, l \epsilon L \tag{3.27}$$

Existence of outgoing energy streams - energy source: If no outgoing streams span from energy

source k, then the source cannot be selected:

$$\sum_{p} z_{k,p} + \sum_{\substack{k' \\ k' \neq k}} z_{k,k'} + \sum_{l} z_{k,l} \geq z_k \qquad \forall\, k \,\epsilon\, K \tag{3.28}$$

Selection of energy source - water streams: If energy source k is not selected, there can be no incoming or outgoing water streams:

$$z_{l,k} \leq z_k \qquad \forall\, i \,\epsilon\, I,\; k \,\epsilon\, K \tag{3.29}$$

$$z^{w}_{k,l} \leq z_k \qquad \forall\, k \,\epsilon\, K,\; l \,\epsilon\, L \tag{3.30}$$

$$z^{waste}_{k} \leq z_k \qquad \forall\, k \,\epsilon\, K \tag{3.31}$$

The opposite disjunction, hence if there are no incoming water streams to energy source k, then k cannot be selected does not hold. There are cases, where an energy source can have zero water requirements, like wind or solar power plants. The corresponding binary relations are imposed for the water sources and their adjacent water and energy streams. The same disjunctions are expressed for water sources l.

3.2.3 Problem feasibility in terms of intensity

To ensure that the energy requirements of water generation, and the water requirements of energy generations are satisfied the following constraints are imposed. This is obtained from the graph-theoretic work, and the source sets k, l are ordered in decreasing intensity factors.

$$\sum_{k} \sum_{l} e_{k,l} \geq \sum_{l} \phi_l \cdot max \left[0,\, min \left(ws^{U}_{l},\, \sum_{q} wcd_q - \sum_{l'=1}^{l-1} ws^{U}_{l'} \right) \right] \tag{3.32}$$

$$\sum_{l} \sum_{k} w_{l,k} \geq \sum_{k} \phi^{with}_{k} \cdot max \left[0,\, min \left(es^{U}_{k},\, \sum_{p} ecd_p - \sum_{k'=1}^{k-1} es^{U}_{k'} \right) \right] \tag{3.33}$$

3.2.4 Distance Constraints

In order to include the transportation cost of fuels, power and water in the total economic objective of the problem we need to define the distance variables between the potential sources k and l, and the fixed entities like i, j, p, q.

$$d_{i,k} = \sqrt{(x_i^{er} - x_k^{es})^2 + (y_i^{er} - y_k^{es})^2} \qquad \forall\, i \epsilon I,\ k \epsilon K \tag{3.34}$$

$$d_{j,l} = \sqrt{\left(x_j^{wr} - x_l^{ws}\right)^2 + \left(y_j^{wr} - y_l^{ws}\right)^2} \qquad \forall\, j \epsilon J,\ l \epsilon L \tag{3.35}$$

$$d_{k,l} = \sqrt{(x_k^{es} - x_l^{ws})^2 + (y_k^{es} - y_l^{ws})^2} \qquad \forall\, k \epsilon K,\ l \epsilon L \tag{3.36}$$

$$d_{k,k'} = \sqrt{(x_k^{es} - x_{k'}^{es})^2 + (y_k^{es} - y_{k'}^{es})^2} \qquad \forall\, k,\ k' \neq k \epsilon K \tag{3.37}$$

$$d_{l,l'} = \sqrt{(x_l^{ws} - x_{l'}^{ws})^2 + (y_l^{ws} - y_{l'}^{ws})^2} \qquad \forall\, l,\ l' \neq l \epsilon L \tag{3.38}$$

$$d_{k,p} = \sqrt{\left(x_k^{es} - x_p^{ec}\right)^2 + \left(y_k^{es} - y_p^{ec}\right)^2} \qquad \forall\, k \epsilon K,\ p \epsilon P \tag{3.39}$$

$$d_{l,q} = \sqrt{\left(x_l^{ws} - x_q^{wc}\right)^2 + \left(y_l^{ws} - y_q^{wc}\right)^2} \qquad \forall\, l \epsilon L,\ q \epsilon Q \tag{3.40}$$

3.2.5 Non-overlapping Constraints

Additional constraints must be imposed for non-communicating entities. For example, there is no stream connecting energy resource i with water source l, and the corresponding distance is not defined, since it does not contribute to the objective function. However, we still need to ensure that those entities will not overlap and keep a minimum distance.

$$\sqrt{(x_i - x_l)^2 + (y_i - y_l)^2} \geq D_{low} \qquad \forall\, i \epsilon I,\ l \epsilon L \tag{3.41}$$

$$\sqrt{(x_j - x_k)^2 + (y_j - y_k)^2} \geq D_{low} \qquad \forall\, j \epsilon J,\ k \epsilon K \tag{3.42}$$

$$\sqrt{(x_k - x_q)^2 + (y_k - y_q)^2} \geq D_{low} \qquad \forall\, k \epsilon K,\ q \epsilon Q \tag{3.43}$$

$$\sqrt{(x_l - x_p)^2 + (y_l - y_p)^2} \geq D_{low} \qquad \forall\, l \epsilon L,\ p \epsilon P \tag{3.44}$$

3.2.6 Lower and upper bounds of variables

The decision variables are bounded by user-specified production and transportation limits. If a processing plant is chosen to be designed, its generating capacity is bounded by its production upper limit. Similarly, if a stream supply is chosen to be allocated, its transportation capacity must be bounded by a transportation upper limit. The upper limits are multiplied with the corresponding binary variables of selection for each processing node or connecting stream. The min operators are utilized for the parameters to provide tighter bounds.

$$es_k \leq z_k \cdot es_k^U \qquad \forall\, k \epsilon K \tag{3.45}$$

$$e_{i,k} \leq z_{i,k} \cdot min\left(era_i,\, \frac{es_k^U}{\beta_k}\right) \qquad \forall\, i \epsilon I,\, k \epsilon K \tag{3.46}$$

$$e_{k,l} \leq z_{k,l} \cdot min\left(es_k^U,\, \phi_l \cdot ws_l^U\right) \qquad \forall\, k \epsilon K,\, l \epsilon L \tag{3.47}$$

$$e_{k,p} \leq z_{k,p} \cdot min\left(es_k^U,\, ecd_p\right) \qquad \forall\, k \epsilon K,\, p \epsilon P \tag{3.48}$$

$$ws_l \leq z_l \cdot ws_k^U \qquad \forall\, k \epsilon K \tag{3.49}$$

$$w_{j,l} \leq z_{i,k} \cdot min\left(wra_j,\, \frac{ws_l^U}{\beta_l}\right) \qquad \forall\, j \epsilon J,\, l \epsilon L \tag{3.50}$$

$$w_{l,k} \leq z_{k,l} \cdot min\left(ws_k^U,\, \phi_l^{with} \cdot es_k^U\right) \qquad \forall\, l \epsilon L,\, k \epsilon K \tag{3.51}$$

$$w_{k,l} \leq z_{k,l}^w \cdot \left(\phi_k^{with} - \phi_k^{cons}\right) \cdot es_l^U \qquad \forall\, k \epsilon K,\, l \epsilon L \tag{3.52}$$

$$w_{l,q} \leq z_{l,q} \cdot min\left(ws_l^U,\, wcd_q\right) \qquad \forall\, l \epsilon L,\, q \epsilon Q \tag{3.53}$$

3.2.7 Objective function

The objective function can obtain a generic form, where the total generation of energy and water from the sources and their corresponding binaries, are to be minimized.

$$
\begin{aligned}
z = & \sum_{k} (z_k + es_k) + \sum_{l} (z_l + ws_l) + \sum_{i} \sum_{k} (z_{i,k} + e_{i,k} \cdot d_{i,k}) + \sum_{j} \sum_{l} (z_{j,l} + w_{j,l} \cdot d_{j,l}) + \\
& + \sum_{k} \sum_{l} \left(z_{k,l} + e_{k,l} \cdot d_{k,l} + z^{w}_{k,l} + w_{k,l} \cdot d_{k,l}\right) + \sum_{l} \sum_{k} (z_{l,k} + w_{l,k} \cdot d_{l,k}) + \\
& + \sum_{k} \sum_{p} (z_{k,p} + e_{k,p} \cdot d_{k,p}) + \sum_{l} \sum_{q} (z_{l,q} + w_{l,q} \cdot d_{l,q} + z_{l,q} + w_{l,q} \cdot d_{l,q})
\end{aligned}
\tag{3.54}
$$

The economic objective function consists of the different cost expressions, resource supply cost, source capital and operating cost, transportation cost, revenue of the final products sales and waste disposal cost.

$$
\begin{aligned}
z = & Supply\_cost^{er} + Supply\_cost^{wr} + Gen\_cost^{es} + Gen\_cost^{ws} + \\
& + Trans\_cost^{e} + Trans\_cost^{w} + Waste\_cost
\end{aligned}
\tag{3.55}
$$

$$
Supply\_cost^{er} = \sum_{i} \sum_{k} ersc_{i,k} \cdot e_{i,k} \tag{3.56}
$$

$$
Supply\_cost^{wr} = \sum_{j} \sum_{l} wrsc_{j,l} \cdot w_{j,l} \tag{3.57}
$$

$$
Gen\_cost^{es} = \sum_{k} (EFC_k \cdot z_k + EOC_k \cdot es_k) \tag{3.58}
$$

$$
Gen\_cost^{ws} = \sum_{l} (WFC_l \cdot z_l + WOC_l \cdot ws_l) \tag{3.59}
$$

$$
\begin{aligned}
Trans\_cost^{e} =& k_F \cdot \Bigg[\sum_i \sum_k \left(eftc_{i,k} \cdot z_{i,k} \right) + \sum_k \sum_l \left(eftc_{k,l} \cdot z_{k,l} \right) + \sum_k \sum_{k'} \left(eftc_{k,k'} \cdot z_{k,k'} \right) + \\
&+ \sum_k \sum_p \left(eftc_{k,p} \cdot z_{k,p} \right) \Bigg] + \sum_i \sum_k eotc \cdot e_{i,k} + \sum_k \sum_l eotc_{k,l} \cdot e_{k,l} + \\
&+ \sum_k \sum_{k'} eotc_{k,k'} \cdot e_{k,k'} + \sum_k \sum_p eotc_{k,p} \cdot e_{k,p}
\end{aligned}
\tag{3.60}
$$

$$
\begin{aligned}
Trans\_cost^{w} =& k_F \cdot \Bigg[\sum_j \sum_l \left(wftc_{j,l} \cdot z_{j,l} \right) + \sum_k \sum_l \left(wftc_{k,l} \cdot z^{w}_{k,l} \right) + \\
&+ \sum_l \sum_k \left(wftc_{l,k} \cdot z_{l,k} \right) + \sum_l \sum_{l'} \left(wftc_{l,l'} \cdot z_{l,l'} \right) + \\
&+ \sum_l \sum_q \left(wftc_{l,q} \cdot z_{l,q} \right) + \sum_q \sum_l \left(wftc_{q,l} \cdot z_{q,l} \right) \Bigg] + \\
&+ \sum_j \sum_l wotc_{j,l} \cdot w_{j,l} + \sum_k \sum_l wotc_{k,l} \cdot w_{k,l} + \sum_l \sum_k wotc_{l,k} \cdot w_{l,k} + \\
&+ \sum_l \sum_{l'} wotc_{l,l'} \cdot w_{l,l'} + \sum_l \sum_q wotc_{l,q} \cdot w_{l,q} + \sum_q \sum_l wotc_{q,l} \cdot w_{q,l}
\end{aligned}
\tag{3.61}
$$

3.3 Case Study on Jack County (TX)

For the WEN superstructure optimization, a Texas county was investigated in the year of 2015. The county has a population of 9,236, and a major city (Jacksboro) in the middle of the region. Plant-level data were acquired for power generation [U.S. Energy Information Administration]. The input-output conversion was available, along with the location of the plants. There is one natural gas and three wind parks operating in the region, with installed capacities of 1,280, 150, 120, and 110 MW respectively. The natural gas plant has an estimated intensity factor of 0.22 gal/KWh. The wind parks have no water requirement. In 2015, a measured of 11,455, 1,365, and 751, and 1,154 GWh of power were generated, requiring 1,512 MGal of water. There are no gas processing facilities in the county. It is assumed that, the fuel needed for power generation is obtained from other counties as a resource. The locations of the energy sources are fixed and are illustrated in Figure 3.3, with red circles.

Water generation data were available by source (surface, groundwater, reuse) and consumption sector (municipal, manufacturing, mining, steam electric, irrigation, livestock) [TWDB]. Since there are no plant-level data, we assume that three major water facilities provide water to the county, specifically to two major consumers of (domestic, agricultural), along with the requirements for energy generation. The locations of the two water resources (surface and groundwater) and the two water consumers can be seen in Figure 3.3, with blue triangles and blue squares respectively. The optimal locations of the three water facilities will be determined by the solution of the problem. The three water sources in 2015, were estimated to produce 1,662, 136 and 0.65 MGal respectively, with 0.0014, 0.0018 and 0.009 Kwh/gal requirement of power. Thus, 2,557 MWh of electricity was needed. In total, the consumer demands were 6,553 GWh of power (the city in the middle of the region), 319 MGal of residential water, and 250 MGal of irrigation water.

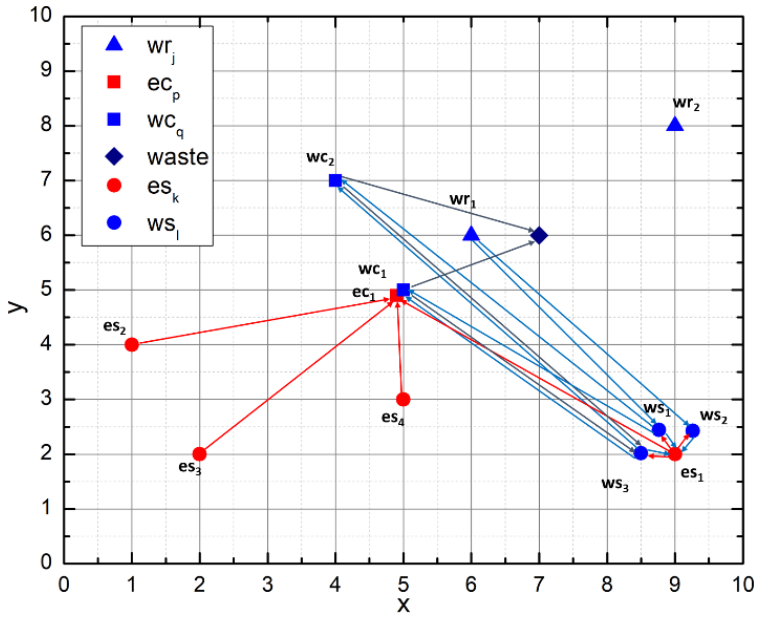

Figure 3.3: Optimal WEN result for regional planning

The objective in this case study was to obtain the minimum generation from the sources, and the optimal connectivity and the locations of the water sources to satisfy the existing demands. The resulting nexus has decreased power and water generation, as the second water resource and the

third water source were omitted from the nexus, and no reuse of water was necessary. The ratio of water recovery was also a variable to be determined. For the scenario of increased water demands (600 and 500 MGal), the resulting nexus is depicted in Figure 8. No groundwater (wr_2) is utilized in the nexus, but all three water sources are chosen to operate. Source ws_3 receives wastewater from the consumers, with a recovery ratio of 80%. Finally, all three sources provide water and receive energy from the natural gas power plant and are allocated close to each other.

4. RESILIENCE-AWARE DESIGN [1]

In this chapter we explore the operational and economical performance of interconnected supply chain networks against connectivity disruptions. We first revisit the definition of network resilience and demonstrate the trade-off between economic optimization and system robustness. We then introduce operation- and economics-based metrics to quantify the resilience of existing infrastructures against connectivity disruptions. Following this, we develop a mathematical programming-based framework for the resilience-aware design of interconnected networks. We then demonstrate the applicability of our framework on an illustrative example for grass-root and retrofit analyses and investigate the effect of nexus interdependence. Finally, we perform a resilience analysis to a regional WEN in the state of Texas.

4.1 Trade-offs between network efficiency and resilience

Cost-optimal WEN configurations do not always result in resilient supply chains against disruption events. For a WEN to be tolerant against disruptions, it should be designed to operate and deliver only for nominal demands. To demonstrate this notion, assume a simplified version of the WEN superstructure-based design model (Figure 4.1).

The superstructure is comprised of three echelons. The suppliers echelon (I, J) corresponds to the physical locations of underground crude fossil fuels and raw water reserves or seawater. Here, I and J are the set of energy and water resources, respectively. The resources are extracted by power plants and water treatment facilities to generate useful products to satisfy the demands of consumers. Here, P and Q are the sets of total energy and water consumers, respectively. They also represent the consumers echelon. Between the suppliers and consumers echelons, we have the facilities echelon, which consists of the interconnected energy (K) and water (L) facilities. The power plants (K) act as energy sources and water sinks. The water treatment and distribution

[1] Reproduced in part from a manuscript that has been submitted for publication: Tsolas, S. D. & Hasan, M. M. F. (2021). Resilience-Aware Design of Interconnected Supply Chain Networks with Application to Water-Energy Nexus. *Submitted for Publication.*

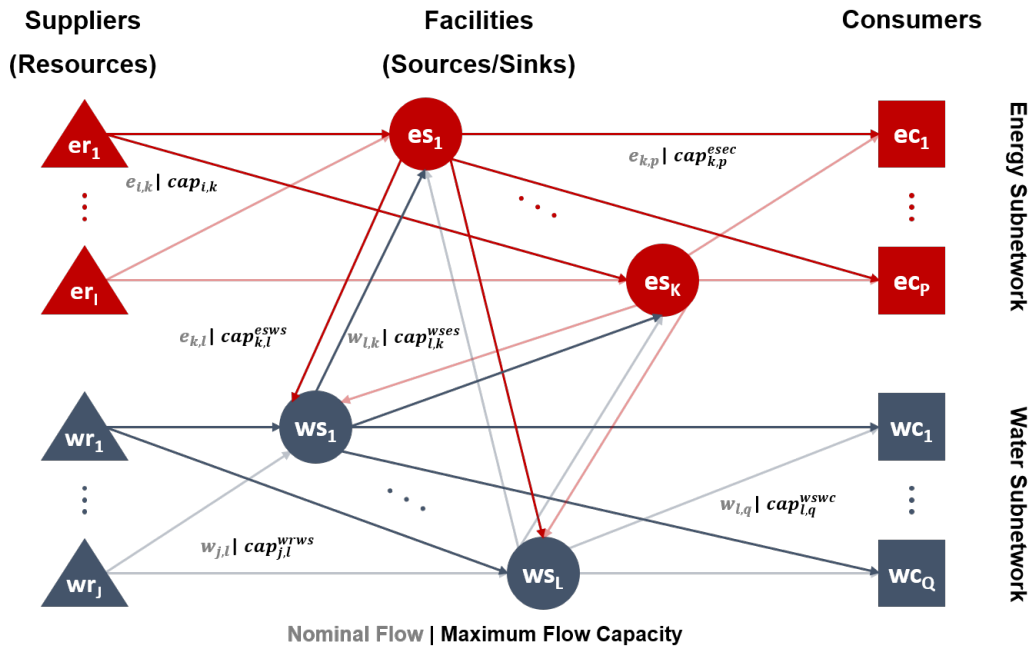

Figure 4.1: Water-energy nexus synthesis superstructure. A WEN can be modeled as a dual-product interconnected supply chain with energy and water as the two products. The superstructure is comprised of three echelons: suppliers echelon (I, J), facilities echelon (K, L), and consumers echelon (P, Q).

facilities (L) are water sources, acting also as energy sinks. The water sources receive energy from the energy sources and the energy sources receive required water from the water sources. With this, we define the nominal WEN design problem as follows.

4.1.1 Motivating example

We now demonstrate the superstructure-based WEN design using a small example. Let us consider that the initial given superstructure is comprised of two energy resources ($|I| = 2$), two water resources ($|J| = 2$), four potential energy sources ($|K| = 4$), four potential water sources ($|L| = 4$), two energy consumers ($|P| = 2$), and two water consumers ($|Q| = 2$). For this motivating example the generation variables are expressed in energy units (eu) and water units (wu). The capacities for generation and transportation are expressed in eu per year and wu per year. Consequently, the operational times for the energy and water sources are 1 year (τ_y^{es}, τ_y^{ws}). The availability (era_i) of the two energy resources is 160 eu. The availability of the water resources

is 180 wu. The resource purchasing cost ($ersc_i$) is \$0.5 per eu and \$0.6 per eu for the two energy resources. The resource purchasing cost ($wrsc_j$) is \$0.55 per wu and \$0.65 per wu for the two water resources. The energy demands (ecd_p) is 90 eu for each of the two energy consumers, while the water consumer demands (wcd_q) are 130 and 100 wu for the two water consumers. The value of the annualization factor (κ_F) is 0.1 per year. The fixed cost of energy transportation ($EFTC$) is \$80 for each connection. The capital cost ($EVTC$) is \$3 per eu/y, and the variable cost of transportation ($EOTC$) is \$1.5 per eu. For the water product, the fixed transportation cost ($WFTC$) is \$90 per connection, the capital cost ($WVTC$) is \$2 per wu/y, and the variable transportation cost ($WOTC$) is \$1 per wu. The parameter values for the potential energy and water sources are presented in **Table 4.1**.

Table 4.1: Operational and cost parameters for the illustrative example.

		Energy Sources k			
Parameter	**Units**	k=1	k=2	k=3	k=4
Conversion Factor, β_k	-	0.86	0.88	0.90	0.92
Intensity Factor, ϕ_k	wu/eu	0.02	0.03	0.04	0.05
Fixed Cost, EFC_k	\$	90	103	94	85
Capital Cost, EVC_k	\$/(eu/y)	0.9	0.4	0.7	0.5
Operating Cost, EOC_k	\$/eu	0.45	0.2	0.35	0.25
Available Capacity, CAP_k^{es}	eu/y	110	110	110	110
		Water Sources l			
Parameter	**Units**	l=1	l=2	l=3	l=4
Conversion Factor, β_l	-	0.96	0.92	0.94	0.95
Intensity Factor, ϕ_l	eu/wu	0.03	0.04	0.05	0.06
Fixed Cost, WFC_l	\$	120	100	115	105
Capital Cost, WVC_l	\$/(wu/y)	0.8	0.65	0.7	0.85
Operating Cost, WOC_k	\$/wu	0.4	0.325	0.35	0.425
Available Capacity, CAP_l^{ws}	wu	125	125	125	125

While the superstructure consists of all plausible entities and all plausible connections, it can be modeled and optimized to find an optimal configuration with minimum cost. The selected WEN entities are a subset of the initial superstructure. Specifically, the cost-optimal network selects

energy sources $k = 2$, $k = 4$ and water sources $l = 1$ and $l = 2$. These, along with the selected connecting streams are demonstrated in Figure 4.2. Energy resource $i = 1$ supplies source $k = 2$ with 112 units. Energy source $k = 1$ receives a total of 112 units, and produces 99 units according to its conversion factor of 0.88. The generated units are distributed to satisfy the demands of 9 units to water sources $l = 1, 2$ and 90 units to consumer $p = 1$. The demand of consumer $p = 2$ is fully covered by plant $k = 4$. Similarly, water resources supply resources to plants $l = 1$ and $l = 2$, which are utilized to generate products to be supplied to sources $k = 2$, $k = 4$, and consumers $q = 1$ and $q = 2$.

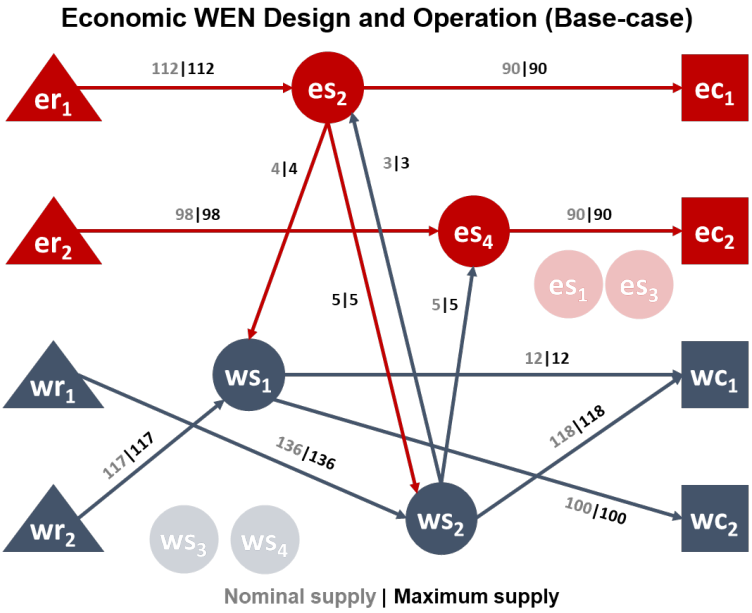

Figure 4.2: Illustrative motivating example of a nominal WEN design and operation problem. The network is comprised of 2 energy and water resources, 4 energy and water sources, and 2 consumers for each product.

This network corresponds to the minimum cost for the given initial superstructure (Base-case network). The nominal and maximum designed supplies are shown on Figure 4.2. Since there was no consideration for any disruption events, the operating variables (nominal supply) are equal to the design variables (maximum supply).

4.1.2 Motivating Example under Connectivity Failures

After the nominal case, let us now consider the ability of given interconnected networks to withstand single-connectivity disruptions. These disruptions correspond to edge failures, where one established connection has its flow completely restricted. These edge failures can be caused by routine maintenance errors, random failures, and natural disasters, like floods, fires and earthquakes.

Assume that due to a disruption, the energy connection $e_{k=2,p=1}$ fails and cannot supply 90 units to ec_1 anymore. This renders consumer ec_1 to be unreachable from the energy sources. Not meeting the demands results in commercial losses, and emergency supplies should be designed on the spot, which also entails additional expenditures. In addition, if energy consumer ec_1 was supplied by other sources, namely via $e_{k=4,p=1}$, there is no margin for excess generation from plant $k = 4$ or excess transportation capacity $cap^{esec}_{k=4,p=1}$.

In order for a network to withstand connectivity disruptions without any external or emergency supplies, alternative routes must be available for flows to be redirected to. The alternative routes entail that every energy and water consumer should be reachable from at least two energy and water sources, respectively. Every source should also supply to more than one customer. The same observation holds for the connection links between the sources and the resources. In addition, the infrastructure should have excess generation and transportation capacities installed, such that the load of a disrupted connection can be compensated by the uninterrupted connections of any affected facility. For example, if connection $w_{l=1,q=1}$ was disrupted, and if the rest of the connections from water source $l = 1$ had 12 units of additional capacity (e.g. $cap^{wswc}_{l=2,q=1} = 130$), then the network would be still feasible. Then, the residual 12 units required by consumer $q = 1$ could be satisfied by water source $l = 2$.

The last concept corresponds to the capacity factor of the energy and water treatment facilities. It is defined as the fraction of nominal (operational) generation to the maximum designed generation capacity. Capacity factor equal to one corresponds to the least-over-design case. Lower capacity factor increases the total cost, but also provides with reserve generation (and transporta-

tion), which increases the resilience of the operation.

4.2 Resilience Metrics for Existing Infrastructures

In order to systematically analyze the resilience of a given supply chain under single-connectivity disruptions, we define the following indices:

1. **Network Structural Robustness** ρ is the ability of a supply chain network to maintain full feasibility after any connection is disrupted. Specifically, it is the fraction of single-connectivity failures for which the rest of the network is still feasible.

2. **Operational Resilience** θ corresponds to a network's ability to satisfy the consumer demands after edge failures. Analytically, it is the average fraction of demand satisfaction across all single-connectivity failures.

3. **Excess Nexus Capacity** ξ corresponds to the maximum excess fraction of the total demands that can be satisfied when there are no disruptions and the system operates at maximum capacity.

We can calculate the three resilience metrics for given interconnected networks. To obtain Network Structural Robustness ρ, we run a minimization problem for every designed supply connection failure. In each run, the corresponding connection has its flow imposed to be zero, and the rest of the sources and the connections are allowed to operate at their maximum capacities. Then, we check the feasibility of the resultant network and repeat this process for all the existing connections. Here, ρ is defined as follows:

$$\rho = \frac{Number\,of\;feasible\,subnetworks\,after\,connectivity\,failure}{Total\,number\,of\,connections}. \tag{4.1}$$

For θ, we run a maximization problem to calculate the maximal supplies to the consumers ($e'_{k,p}$ and $w'_{k,p}$) for every designated connection failure. We calculate θ as the average fraction of

consumer demands (ecd_p, wcd_q) satisfied across all connection failures:

$$\theta_c = \frac{0.5}{|P|} \cdot \sum_p \sum_k \frac{e'_{k,p}}{ecd_p} + \frac{0.5}{|Q|} \cdot \sum_q \sum_l \frac{w'_{l,q}}{wcd_q}, \qquad \forall\, c \in C \tag{4.2}$$

$$\theta = \frac{1}{|C|} \sum_{c \in C} \theta_c, \qquad C = \{I \times K\}, \{J \times L\}, \{K \times L\}, \{L \times K\}, \{K \times P\}, \{L \times Q\}. \tag{4.3}$$

θ_c is the connection-specific operational resilience and is the fraction of demands satisfied, after connection c fails. Set C corresponds to the set of all designed connections of the existing infrastructure.

For ξ, we run a maximization problem to calculate the maximal supplies to the consumers ($e"_{k,p}$ and $w"_{l,q}$) without any connection failures. ξ is a metric of the system's over-design. Specifically, it is the fraction of the additional demands that can be satisfied and it is calculated as follows:

$$\xi = \frac{0.5}{|P|} \cdot \sum_p \sum_k \frac{e''_{k,p} - ecd_p}{ecd_p} + \frac{0.5}{|Q|} \cdot \sum_q \sum_l \frac{w''_{l,q} - wcd_q}{wcd_q}\,. \tag{4.4}$$

4.2.1 Resilience analysis and reinforcement of motivating example

The resulting WEN of the motivating example (base-case) has ρ equal to zero, since there are not any reserve capacities (capacity factor equal to one) and because the cost minimization results in minimum connectivity. To improve the resilience of the network there must be appropriate provisions to account for potential disruptions in the designed connections. We now solve again the same WEN problem, but we impose a capacity factor of 60% on the generation and transportation design. In addition, we impose the consumers to be reachable by at least two intermediate sources.

The resulting network is demonstrated in Figure 4.3a where the nominal and the maximum supplies are displayed. In this case, the connectivity is increased compared to the minimum cost case from 13 to 16 connections. The cost is also increased by 10%. It is clear that there is 40% margin from the nominal to the maximum transportation capacities. In this case, if stream $e_{k=2,p=1}$ is disrupted the rest of the network is able to withstand the connectivity disruption. This connection failure is demonstrated in Figure 4.3b along with the redirected supplies.

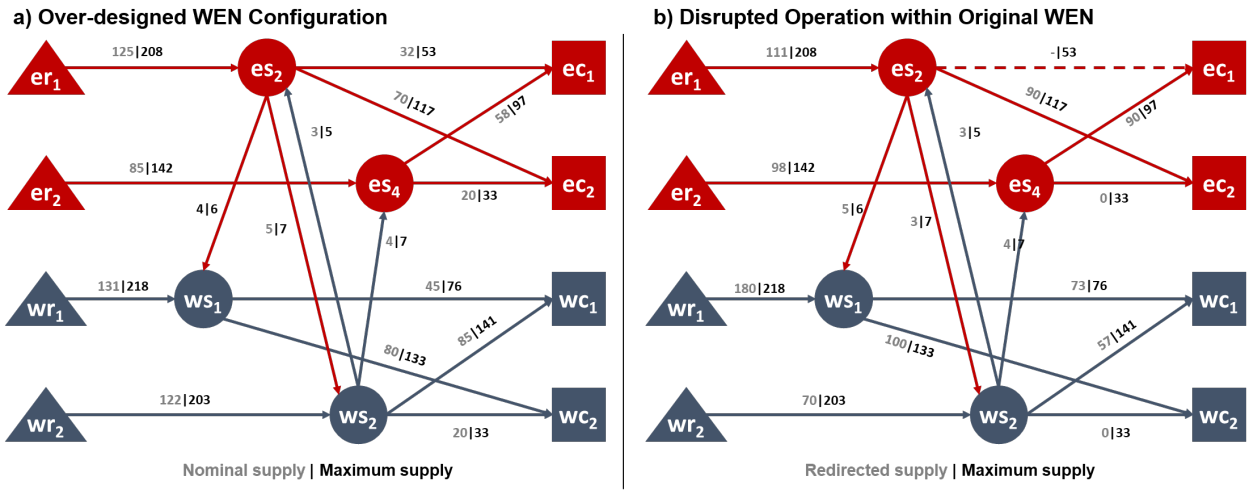

Figure 4.3: Modified WEN of motivating example with user-specified over-design for resilience reinforcement. (a) Nominal operation with increased connectivity and decreased capacity factor imposing for increased resilience, (b) Reconfigured WEN operation under failure of connection $e_{k=2,p=1}$ within the original design capacities.

Network structural robustness ρ is calculated as 25% ($= 4/16$), meaning that only 4 out of the 16 designed connections can be disrupted without affecting the rest of the network. The operational resilience θ is 92% and the additional capacity ξ is 45%. This means that across all single-connectivity failures 92% of the demands are satisfied on average, and without any connectivity disruptions the system can provide 45% additional energy and water supplies to the consumers.

4.2.2 Identification of Critical Connections

Operational resilience can be utilized to identify the most critical WEN connections. The effect of connection c failure on the nominal operation of the supply chain is measured by θ_C. Specifically, the imbalance on the network created by disruption of connection c is pushed to the consumer echelon by maximizing the consumer supplies of the remaining network.

In Figure 4.4 the distribution of operational resilience for the designed connections of the modified motivating example is demonstrated. The demand fraction θ_C that can be satisfied, if edge c fails, is inversely proportional to the criticality of the corresponding connection. In the example, connections 5 ($e_{i=1,k=2}$), 12 ($w_{j=2,l=2}$), 14 ($e_{k=2,l=2}$), and 15 ($w_{l=2,k=2}$) have the greatest impact on

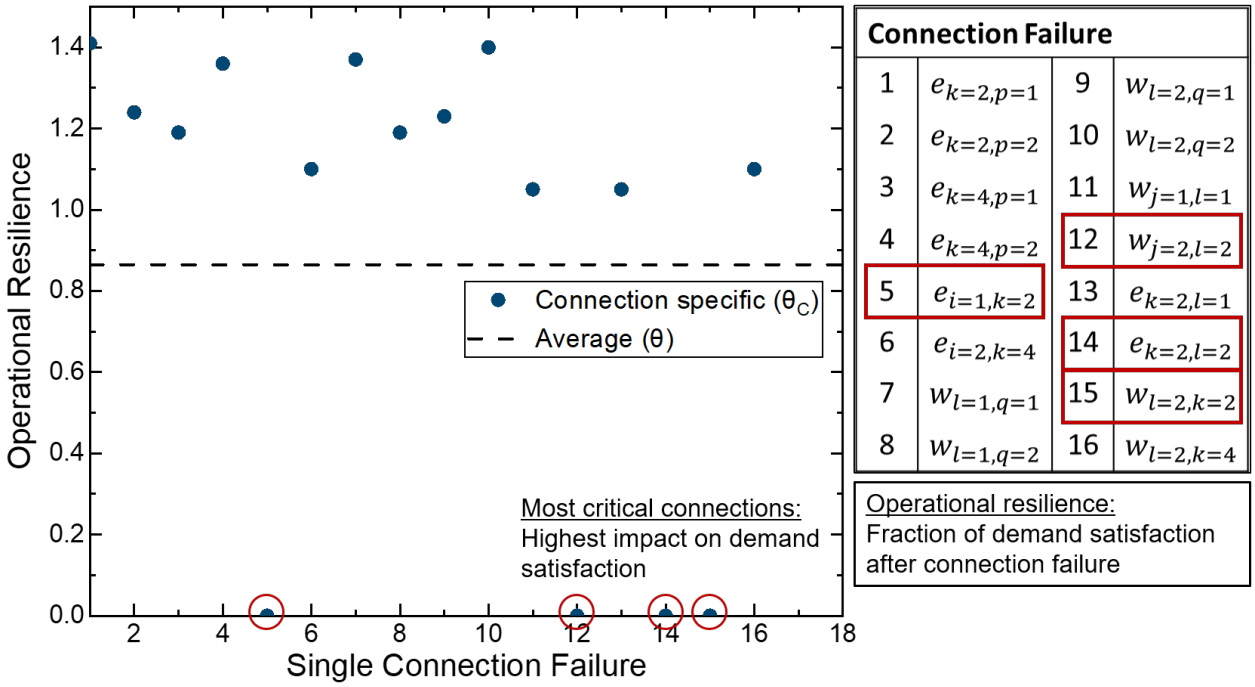

Figure 4.4: Average (θ) and connection-specific (θ_c) operational resilience for the modified motivating example (4.3). Lower fractions of demand satisfaction (θ_c) after connection failure correspond to more critical connections. The average operational resilience (θ) should be closer to 1 for more resilient interconnected networks.

the network's performance. Two of the most impactful connections correspond to streams between resources and sources. Interestingly, the other two connections have very low capacities and operating flows but correspond to the intermediate exchange streams between the two sub-networks. This demonstrates also the effect of nexus interdependence on network resilience.

4.2.3 Minimum Cost of Resilience (MCOR)

We saw in the previous example that over-designing a supply chain infrastructure with increased connectivity and capacities is improving the performance of the supply chains during disruption events. However, it is also induces increased infrastructure investments. To compate

So far, we have addressed the post-design resilience analysis of interconnected networks, using a WEN design problem. The previous WEN result was an example of a heuristic approach towards the resilience reinforcement of a WEN supply chain. Clearly, by keep increasing the min-

imum connectivity and lowering the capacity factor, the resulting WEN resilience will be further improved. However, the corresponding total infrastructure cost will increase as well, as the WEN is even more over-designed. In order to guarantee that structural robustness $\rho = 100\%$ and operational resilience $\theta = 100\%$, the heuristic over-design will result in excessive cost increase. To calculate the additional infrastructure investments to reinforce a WEN's resilience, we compare it to the nominal design, which is also the most economical and least resilient. This increased cost of the resilient design compared to the minimal cost nominal design is defined as minimum cost of resilience ($MCOR$):

$$MCOR = \frac{Resilient\,Design\,Cost(\rho, \theta, \xi) - Nominal\,Design\,Cost}{Nominal\,Design\,Cost}\,. \tag{4.5}$$

Remarks:

1. Adequate over-design may be required to improve the resilience of interconnected networks.
2. Increased connectivity compared to minimum cost design provides alternative routes for flows to be redirected in connectivity failure events.
3. Decreased capacity factor provides flexibility for excess generation and transportation compensating for disrupted connections.
4. These strategies improve resilience by enhancing the robustness and the redundancy of a supply chain network.
5. To avoid uncontrolled over-design for a desired degree of resilience, the potential disruptions must be considered in the design phase of interconnected supply chain networks.

4.3 Resilience-aware Design

In this section we develop a mathematical-programming approach to account for WEN resilience from the conceptual design phase and guarantee minimum over-design. The model also incorporates the resilience indices which can be imposed or deduced based on demand violation penalizing. The resilience-aware design problem statement is as follows: Given:

1. a set of available energy and water resource suppliers in a region (type and withdrawal limit)
2. a set of final energy and water consumer centers (clean fuel, power and water demands),
3. a pool of potential intermediate processing energy and water sources or facilities (generation technologies, conversion and intensity factors, costs)

Determine:

1. which resources to be utilized and withdrawn to produce the required power, fuels, and water
2. which energy and water sources to be selected
3. optimal network connectivity
4. how much energy and water to be generated in each facility
5. how much energy and water to be transported by each connection or transportation link
6. the maximum generation and transportation capacities.

The optimization objective is to minimize the total cost, but also guarantee a predicted degree of resilience against the single-connectivity failures. For grass-root designs there are not any pre-existing facilities or connections, and all the sources (K, L) are proposed to be part of the resilient network. On the other hand, for retrofitting cases part of the superstructure might correspond to an existing network. In this case the existing facilities have already some initial fixed capacities. The optimizer will decide whether to expand the existing facilities/connections capacities, and/or to allocate new entities from the given superstructure.

4.3.1 Multi-scenario formulation

The traditional minimum-cost supply chain design problem is expanded over all potential disruption scenarios. Each scenario $s \in S$ corresponds to the failure of one potential WEN connection. The total number of scenarios is equal to maximum potential designed connections of a given

superstructure, and is given by

$$|S| = \sum_{m_1 \in M^{in}} I_{m_1} \cdot K_{m_1} + 2 \cdot K \cdot L + \sum_{m_2 \in M^{out}} K_{m_2} \cdot P_{m_2} + \sum_{n_1 \in N^{in}} J_{n_1} \cdot L_{n_1} + \sum_{n_2 \in N^{out}} L_{n_2} \cdot Q_{n_2}.$$

We use the subsets $I_{m_1}, J_{n_1}, K_{m_1}, K_{m_2}, L_{n_1}, L_{n_2}, P_{m_2}, Q_{n_2}$ in the operating balances, so that only the connections exchanging products $m_1 \in M^{in}, m_2 \in M^{out}, n_1 \in N^{in}, n_2 \in N^{out}$ will be defined. For example, the stream variables $(z_{i,k}, cap^{eres}_{i,k}, e_{i,k,s})$ will only be defined for the connections between nodes i, k that correspond to the same product m_1. The total number of disruption scenarios $|S|$ reduce, depending on the allowable connections derived from the appending sets. The operating variables and the operating balances are formulated for every scenario $s \epsilon S$.These operating scenario-dependent balances are depicted below.

$$\sum_{k \in K_{m_1}} e_{i,k,s} \leq era_i \qquad \forall\, i \in I_{m_1},\, m_1 \in M^{in},\, s \in S \tag{4.6}$$

$$\beta^{es}_k \cdot \sum_{i \in I_{m_1}} e_{i,k,s} = es_{k,s} \qquad \forall\, k \in K_{m_1},\, m_1 \in M^{in},\, s \in S \tag{4.7}$$

$$\phi^{es}_k \cdot es_{k,s} = \sum_{l} w_{l,k,s} \qquad \forall\, k \in K,\, s \in S \tag{4.8}$$

Equation (4.6) ensures that the withdrawal limit of the resources is always satisfied. Equation (4.7) calculates the generation from the energy sources based on a conversion factor β^{es}_k. Equation (4.8) ensures that the requirements of energy generation for source k are supplied by the water sources. Similar balances are utilized for the water resources and sources (Eqs (4.9)-(4.11)).

$$\sum_{l \in L_{n_1}} w_{j,l,s} \leq wra_j \qquad \forall\, j \in J_{n_1},\, n_1 \in N^{in},\, s \in S \tag{4.9}$$

$$\beta^{ws}_l \cdot \sum_{j \in J_{n_1}} w_{j,l,s} = ws_{l,s} \qquad \forall\, l \in L_{n_1},\, n_1 \in N^{in},\, s \in S \tag{4.10}$$

$$\phi^{ws}_l \cdot ws_{l,s} = \sum_{k} e_{k,l,s} \qquad \forall\, l \in L,\, s \in S \tag{4.11}$$

The scenario-dependent operating variables are bounded by the common design variables. The

operating variables ($es_{k,s}, ws_{l,s}$) express the generation of energy and water in an annual basis. The capacity variables are multiplied with the capacity factor cf_k^{es}, cf_l^{ws} and the operational time within a year of operation (τ_y^{es}, τ_y^{ws}). For example, if the generating capacity for the energy sources (cap_k^{es}) is expressed in MW, then the yearly operation time (τ_y^{es}) is 8,760 h. Similarly, if the water source generating capacity (cap_l^{ws}) is expressed in mgd, then τ_y^{ws} will be 365 days.

$$es_{k,s} \leq cf_k^{es} \cdot cap_k^{es} \cdot \tau_y^{es} \qquad \forall\, k \in K,\, s \in S \tag{4.12}$$

$$e_{i,k,s} \leq cap_{i,k}^{eres} \cdot \tau_y^{es} \qquad \forall\, i \in I_{m_1},\, k \in K_{m_1},\, m_1 \in M^{in},\, s \in S \tag{4.13}$$

$$e_{k,l,s} \leq cap_{i,k}^{esws} \cdot \tau_y^{es} \qquad \forall\, k \in K,\, l \in L,\, s \in S \tag{4.14}$$

$$e_{k,p,s} \leq cap_{k,p}^{esec} \cdot \tau_y^{es} \qquad \forall\, k \in K_{m_2},\, p \in P_{m_2},\, m_2 \in M^{out},\, s \in S \tag{4.15}$$

$$ws_{l,s} \leq cf_l^{ws} \cdot cap_l^{ws} \cdot \tau_y^{ws} \qquad \forall\, l \in L,\, s \in S \tag{4.16}$$

$$w_{j,l,s} \leq cap_{j,l}^{wrws} \cdot \tau_y^{ws} \qquad \forall\, j \in J_{n_1},\, l \in L_{n_1},\, n_1 \in N^{in},\, s \in S \tag{4.17}$$

$$w_{l,k,s} \leq cap_{l,k}^{wses} \cdot \tau_y^{ws} \qquad \forall\, l \in L,\, k \in K,\, s \in S \tag{4.18}$$

$$w_{l,q,s} \leq cap_{l,q}^{wswc} \cdot \tau_y^{ws} \qquad \forall\, l \in L_{n_2},\, q \in Q_{n_2},\, n_2 \in N^{out},\, s \in S \tag{4.19}$$

Incorporation of Structural Robustness ρ: Every scenario corresponds to a potential connection from the initial superstructure that can be disrupted. The following constraints fix the operating variables of any missing link to zero, for the corresponding scenario.

$$e_{a^*,b^*,s^*} = 0, \qquad (a^*,\, b^*,\, s^*) \in O_{i,k,s}^{eres}, O_{k,l,s}^{esws}, O_{k,p,s}^{esec} \tag{4.20}$$

$$w_{c^*,d^*,s^*} = 0, \qquad (c^*,\, d^*,\, s^*) \in O_{j,l,s}^{wrws}, O_{l,k,s}^{wses}, O_{l,q,s}^{wswc} \tag{4.21}$$

Subsets $O_{i^*,k^*,s^*}^{eres}, O_{k^*,l^*,s^*}^{esws}, O_{k^*,p^*,s^*}^{esec}, O_{j^*,l^*,s^*}^{wrws}, O_{l^*,k^*,s^*}^{wses}, O_{l^*,q^*,s^*}^{wswc}$ append every stream to one scenario at a time. For example, the stream connecting energy resource supplier $i = 1$ to energy source $k = 1$ is fixed to be zero only for scenario $s = 1$. For scenario $s = 2$ stream $i = 1, k = 2$ has zero supply, and the same scenario-connection matching is continued until $s = I \cdot K$. As a result, the allocating subset is created $O_{i,k,s}^{eres} = \{(1,1,1), (1,2,2), (1,3,3), ..., (|I|, |K|, |I| \cdot |K|)\}$.

Then, for streams connecting energy sources k to water sources l the mapping subset $O^{esws}_{k,l,s}$ is created accordingly: $O^{esws}_{k,l,s} = \{(1,1,|I|\cdot|K|+1),...,(|K|,|L|,|I|\cdot|K|+|K|\cdot|L|)\}$. These constraints that impose the operating supplies of the streams belonging to the scenario subsets to be zero, combined with constraints (4.6-4.11) ensure that WEN balances hold across all scenarios of disruptions. Thus, the network maintains its feasibility under connectivity disruptions from the design phase. Finally, the optimizer will determine the cost-minimum common maximum capacity variables $\left(cap^{es}_{k}, cap^{eres}_{i,k}, ...\right)$ that will bound the different values of operating variables across all scenarios with equations (4.12-4.19).

Incorporation of Operational Resilience θ: To take into account for demand satisfaction from external resources, we introduce variables $\theta^{e}_{p,s}$ and $\theta^{w}_{q,s}$, which correspond to the demand fractions of consumers p, q that are satisfied by the network in each disruption scenario s. These also correspond to the operational resilience (θ), which are now decision variables depending on each scenario. The external grid supplies are equal to $(1-\theta^{e}_{p,s})$ and $(1-\theta^{w}_{q,s})$ for consumers p and q respectively. Thus, we allow demands not be satisfied completely by the network, and penalize the unsatisfied demands in the objective function.

$$\sum_{k\in K_{m_2}} e_{k,p,s} = \theta^{e}_{p,s}\cdot ecd_p \qquad \forall\, p\in P_{m_2},\, m_2\in M^{out},\, s\in S \tag{4.22}$$

$$\sum_{l\in L_{n_2}} w_{l,q,s} = \theta^{w}_{q,s}\cdot wcd_q \qquad \forall\, q\in Q_{n_2},\, n_2\in N^{out},\, s\in S \tag{4.23}$$

Logical Constraints: The design variables are bounded by user-specified production limits. If a processing plant is selected, its generating capacity is bounded by its production upper limit. Similarly, if a stream supply is chosen to be allocated, its transportation capacity must be bounded by a transportation upper limit. The upper limits are multiplied with the corresponding binary variables of selection for each processing facility or connecting stream. The transportation upper limit is taken as a function of the resource availabilities, generation upper bounds, and consumer

demands.

$$cap_k^{es} \leq z_k \cdot CAP_k^{es} \qquad \forall\, k \in K \tag{4.24}$$

$$cap_{i,k}^{eres} \leq z_{i,k} \cdot min\left(\frac{era_i}{\tau_y^{es}},\, \frac{CAP_k^{es}}{\beta_k}\right) \qquad \forall\, i \in I_{m_1},\, k \in K_{m_1},\, m_1 \in M^{in} \tag{4.25}$$

$$cap_{k,l}^{esws} \leq z_{k,l} \cdot min\left(CAP_k^{es},\, \phi_l \cdot CAP_l^{ws} \cdot \frac{\tau_y^{ws}}{\tau_y^{es}}\right) \qquad \forall\, k \in K,\, l \in\, L \tag{4.26}$$

$$cap_{k,p}^{esec} \leq z_{k,p} \cdot min\left(CAP_k^{es},\, \frac{ecd_p}{\tau_y^{es}}\right) \qquad \forall\, k \in K_{m_2},\, p \in P_{m_2},\, m_2 \in M^{out} \tag{4.27}$$

$$cap_l^{ws} \leq z_l \cdot CAP_l^{ws} \qquad \forall\, l \in L \tag{4.28}$$

$$cap_{j,l}^{wrws} \leq z_{j,l} \cdot min\left(\frac{wra_j}{\tau_y^{ws}},\, \frac{CAP_l^{ws}}{\beta_l}\right) \qquad \forall\, j \in J_{n_1},\, l \in L_{n_1},\, n_1 \in N^{in} \tag{4.29}$$

$$cap_{l,k}^{wses} \leq z_{l,k} \cdot min\left(CAP_l^{ws},\, \phi_l^{with} \cdot CAP_k^{es} \cdot \frac{\tau_y^{es}}{\tau_y^{ws}}\right) \qquad \forall\, l \in L,\, k \in K \tag{4.30}$$

$$cap_{l,q}^{wswc} \leq z_{l,q} \cdot min\left(CAP_l^{ws},\, \frac{wcd_q}{\tau_y^{ws}}\right) \qquad \forall\, l \in L_{n_2},\, q \in Q_{n_2},\, n_2 \in N^{out} \tag{4.31}$$

The binary variables z_k^{es}, z_l^{ws} determine the selection of energy k and water l sources respectively. The following constraints dictate the existence of facilities and streams according to their selected connectivity. Equation (4.32) ensures that if source k is not selected, there can be no incoming streams from i supplier. Equation (4.33) dictates that if no incoming streams from suppliers reach facility k, then it cannot be selected. Similarly, equations (4.34)-(4.36) ensure the consistent selection of source k and outgoing streams k, l and k, p.

$$z_{i,k} \leq z_k^{es} \qquad \forall\, i \in I_{m_1},\, k \in K_{m_1},\, m_1 \in M^{in} \tag{4.32}$$

$$\sum_{i \in I_{m_1}} z_{i,k} \geq z_k^{es} \qquad \forall\, k \in K_{m_1},\, m_1 \in M^{in} \tag{4.33}$$

$$z_{k,p} \leq z_k^{es} \qquad \forall\, k \in K_{m_2},\, p \in P_{m_2},\, m_2 \in M^{out} \tag{4.34}$$

$$z_{k,l} \leq z_k^{es} \qquad \forall\, k \in K,\, l \in L \tag{4.35}$$

$$\sum_{p \in P_{m_2}} z_{k,p} + \sum_{l} z_{k,l} \geq z_k^{es} \qquad \forall\, k \in K_{m_2},\, m_2 \in M^{out} \tag{4.36}$$

Finally, equation (4.37) ensures that if source k is not selected, there can be no incoming water streams from water source l.

$$z_{l,k} \leq z_k^{es} \qquad \forall\, l \in L,\, k \in K \tag{4.37}$$

The same logical constraints hold for the water network connections and facilities and expressed via Equations (4.38)-(4.43).

$$z_{j,l} \leq z_l^{ws} \qquad \forall\, j \in J_{n_1},\, l \in L_{n_1},\, n_1 \in N^{in} \tag{4.38}$$

$$\sum_{j \in J_{n_1}} z_{j,l} \geq z_l^{ws} \qquad \forall\, l \in L_{n_1},\, n_1 \in N^{in} \tag{4.39}$$

$$z_{l,q} \leq z_l^{ws} \qquad \forall\, l \in L_{n_2},\, q \in Q_{n_2},\, n_2 \in N^{out} \tag{4.40}$$

$$z_{l,k} \leq z_l^{ws} \qquad \forall\, l \in L,\, k \in K \tag{4.41}$$

$$\sum_{q \in Q_{n_2}} z_{l,q} + \sum_{k} z_{l,k} \geq z_l^{ws} \qquad \forall\, l \in L_{n_2},\, n_2 \in N^{out} \tag{4.42}$$

$$z_{k,l} \leq z_l^{ws} \qquad \forall\, k \in K,\, l \in L \tag{4.43}$$

Objective function: The objective is minimizing the total annual cost of the supply chain, comprised by the material supply costs, the plants generating and supply transportation costs. The cost expression is split into four components: (i) the fixed cost, which is a linear function of the binaries of selection, (ii) the design cost, which is a function of the maximum capacity variables, (iii) the operating cost which is a function of the operating variables, and (iv) the penalty cost for external supplies (unsatisfied demands).

$$z = FC + DC + OC + PC \tag{4.44}$$

The first two components (FC and DC) depend on the selection and the design variables respec-

tively, and are scenario independent.

$$
\begin{aligned}
FC = & \sum_{k} EFC_k \cdot z_k^{es} + \sum_{l} WFC_l \cdot z_l^{ws} + \\
& EFTC \cdot \left(\sum_{i} \sum_{k} z_{i,k} + \sum_{k} \sum_{l} z_{k,l} + \sum_{k} \sum_{p} z_{k,p} \right) + \\
& WFTC \cdot \left(\sum_{j} \sum_{l} z_{j,l} + \sum_{l} \sum_{k} z_{l,k} + \sum_{l} \sum_{q} z_{l,q} \right)
\end{aligned} \tag{4.45}
$$

$$
\begin{aligned}
DC = & \sum_{k} EVC_k \cdot cap_k^{es} + \sum_{l} WVC_l \cdot cap_l^{ws} + \\
& EVTC \cdot \left(\sum_{i} \sum_{k} cap_{i,k}^{eres} + \sum_{k} \sum_{l} cap_{k,l}^{esws} + \sum_{k} \sum_{p} cap_{k,p}^{esec} \right) + \\
& WVTC \cdot \left(\sum_{j} \sum_{l} cap_{i,k}^{eres} + \sum_{l} \sum_{k} cap_{l,k}^{wses} + \sum_{l} \sum_{q} cap_{l,q}^{wswc} \right)
\end{aligned} \tag{4.46}
$$

The operating cost OPC_s varies across all different scenarios, so we minimize the average operating cost across the scenarios (OC) in Eqs. (4.47)-(4.48):

$$
\begin{aligned}
OPC_s = & \sum_{i} \sum_{k} ersc_i \cdot e_{i,k,s} + \sum_{j} \sum_{l} wrsc_j \cdot w_{j,l,s} + \sum_{k} EOC_k \cdot es_{k,s} + \\
& \sum_{l} WOC_l \cdot ws_{l,s} + \sum_{i} \sum_{k} EOTC \cdot e_{i,k,s} + \sum_{k} \sum_{l} EOTC \cdot e_{k,l,s} + \\
& \sum_{k} \sum_{p} EOTC \cdot e_{k,p,s} + \sum_{j} \sum_{l} WOTC \cdot w_{j,l,s} + \sum_{l} \sum_{k} WOTC \cdot w_{l,k,s} + \\
& + \sum_{l} \sum_{q} WOTC \cdot w_{l,q,s} \qquad \forall\, s \,\epsilon\, S
\end{aligned} \tag{4.47}
$$

$$
OC = \frac{1}{|S|} \sum_{s} OPC_s \tag{4.48}
$$

The last cost component is the penalty cost (PC) for the unsatisfied energy and water demands by the network. It is calculated as the average demand violation across the disruption scenarios. The unsatisfied energy and water product demands are penalized with λ, which is the cost per unit

product amount. The penalty cost can be viewed as the total cost of external product purchasing to compensate for unsatisfied demands, and is formulated as follows:

$$PC = \frac{\lambda}{|S|} \cdot \sum_{s} \left(\sum_{p} (1 - \theta^{e}_{p,s}) \cdot ecd_p + \sum_{q} (1 - \theta^{w}_{q,s}) \cdot wcd_q \right) \tag{4.49}$$

4.4 Results: Revisiting Illustrative Example

To demonstrate the effects of resilience-aware design on the cost of interconnected networks, we revisit the illustrative example. Recall that the minimum-cost design (Figure 4.2) was not immune to single-connectivity failures. Also, note that the minimum cost WEN model has 421 equations and 225 variables (72 binaries). This network did not consider resilience in the design phase (no disruption scenarios) and is referred as base-case network. The resilience-aware model, on the other hand, consists of 6,909 equations and 5,013 variables (72 binaries), due to the multi-scenario expansion (number of scenarios $|S| = 64$). The MILP problem is solved using CPLEX 12.10.0.0 as the solver in GAMS 31.1.0 platform. The models are solved within 0.1% relative optimality gap.

4.4.1 Grass-root resilient design

We first solve the multi-scenario formulation for grass-root resilient design (no pre-existing facilities) for different parametric values of the penalty coefficient λ and observe the resulting costs, network configurations, and resilience metrics. It is worth noting that the solution time to achieve 0.1% optimality gap increases with λ, from minutes to a maximum of 8.5 hours. Note that the base-case network for the same problem (Figure 4.2) is obtained in seconds, due to the absence of scenarios.

The distribution of the total network costs and their components is presented in Figure 4.5a. We observe three regimes of network configurations. For low penalties, there is no need for a network to be created, since it is more cost-effective to supply all the demands from external grids. For intermediate penalties, there are contributions from both the network and the external supplies. In

the last regime, where the penalty is high, there is no dependence on the external grid, as the nexus can self-satisfy all demands for all disruption events. Note that, the total cost is 13.6% greater than the base-case, which corresponds to the MCOR for the last regime.

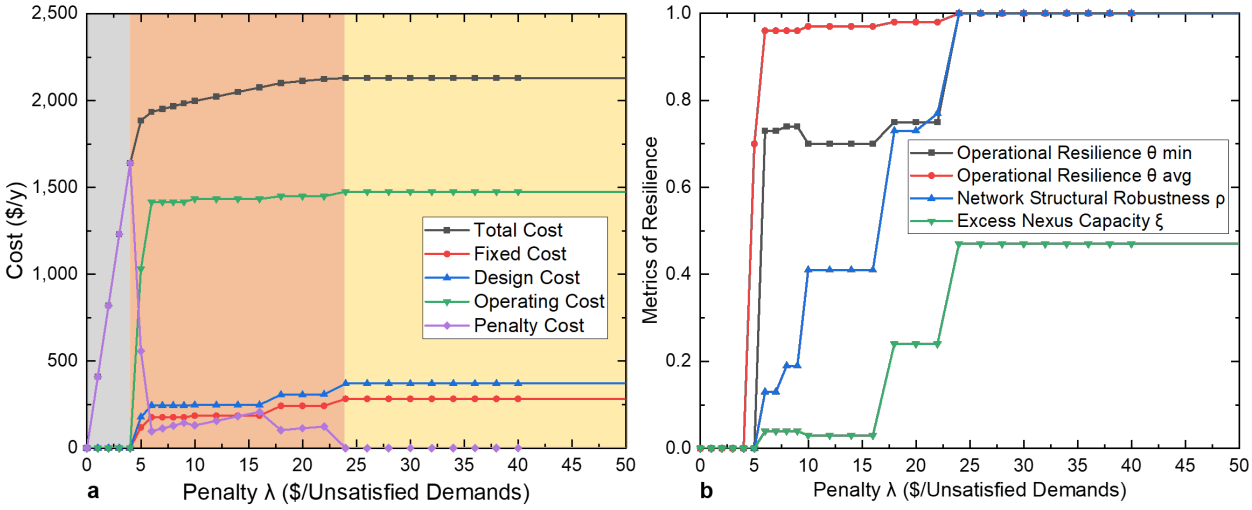

Figure 4.5: Application of resilient grass-root WEN design: (a) Total cost and cost components distribution for different values of λ, (b) Resilience metrics of resulting WEN for different values of λ.

Similar observations can be drawn from the distribution of the resilience metrics for increasing penalties (Figure 4.5b). For $\lambda \leq 5$, all the metrics are zero in the no-network regime. In the intermediate regime, the resilience metrics increase with λ, as the network obtains more proactive provisions. In the third regime, the operational resilience θ and the nexus structural robustness ρ are both equal to one. This entails that there is no dependence on external grids to satisfy the consumer demands. It also means that the network can withstand all network single-connectivity disruptions and maintain feasibility. In the absence of connectivity disruptions, the WEN network can satisfy 47% additional demands (ξ) if operated at maximum capacities.

In Figure 4.6, the progression of the network structure is demonstrated for increasing λ. In the first shaded region, a network is not required to satisfy the demands, hence there are no designed connections or energy/water facilities. As λ increases, a network is needed that continues

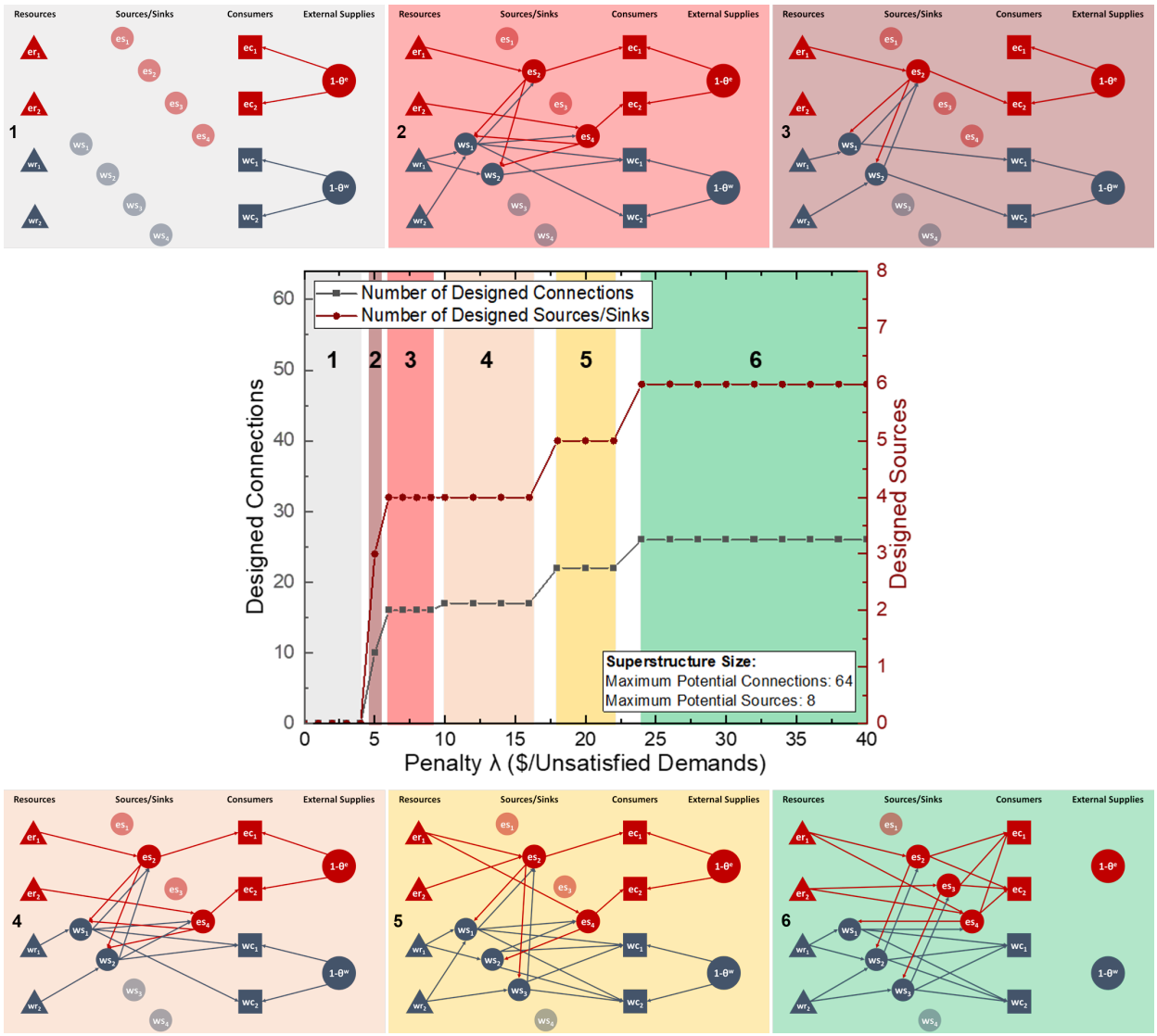

Figure 4.6: Network progression and connectivity distribution for parametric values of λ. As λ increases the network is less dependent on external supplies and the total numbers of the sources and the connection links increase.

to grow in size as more connectivity is required to increase its resilience. In the extreme cases of low and very high penalties, the network is completely dependent and independent from external grids, respectively. Plateaus can be observed in the network progression curves, where there are no changes in the corresponding network configurations. Similar plateaus can be spotted in Figure 4.5a, since the fixed cost component is proportional to the binary variables for sources and connections selection. For the same plateaus, the corresponding total cost increases due to a steady ramp

in the penalty cost. Since the configuration of the nexus remains constant, the demands satisfied from external grids remain constant as well, and the penalty cost increases due to the increasing penalty λ. Only when the last value of λ supersedes a threshold value, the augmented penalty cost forces the network to increase in size and resilience. This also explains that during the next design cost plateau, the penalty cost ramp starts from a lower point.

4.4.2 Zero Nexus Interdependence

We now explore the effect of nexus interdependence on the infrastructure resilience. We postulate the same initial superstructure ($|I| = 2$, $|J| = 2$, $|K| = 4$, $|L| = 4$, $|P| = 2$, $|Q| = 2$) with zero intensity factors of the energy and water sources (ϕ_k^{es}, ϕ_l^{ws}). This results in no water requirements from the energy sources and vice versa (Eqs. (8),(11)). Even not imposed, the resulting intermediate exchange streams obtain zero flows, capacities, and selection variables ($e_{k,l} = cap_{k,l}^{esws} = z_{k,l} = 0$). The two supply chains are independent from each other, and the total potential connections to be designed reduce from 64 to 32. The same holds for the disruption scenarios ($|S| = 32$). The resulting multi-scenario MILP problem consists of 3,581 equations and 2,581 variables. Finally, due to the absence of interdependence, the two product supply chains can be solved as two separate design problems. This also results in the model converging to the 0.1% optimality gap in under a minute.

In this case, with increasing λ the resulting supply chain shifts faster across the three resilience regimes. The 100% self-sufficiency and resilience region is achieved at $\lambda \geq 14$, while for the first case it was achieved for $\lambda \geq 24$. The corresponding network is presented in Figure 4.7a. The expected absence of the intermediate streams can be seen on the diagram. The total cost is 7% lower than in the interdependent case, since there is no additional generation from the sources to satisfy the sinks, and there are no contributions from the intermediate connections $e_{k,l}$ and $w_{l,k}$. Finally, the maximum additional demands (ξ) that can be satisfied with full operation is 27%.

In the non-interdependent case the 100% operational resilient configuration (high λ region) requires 12% infrastructure investments (MCOR) compared to its non-resilient alternative. In the case of the interdependent WEN, the MCOR for 100% operational resilience was 13.6%, which is

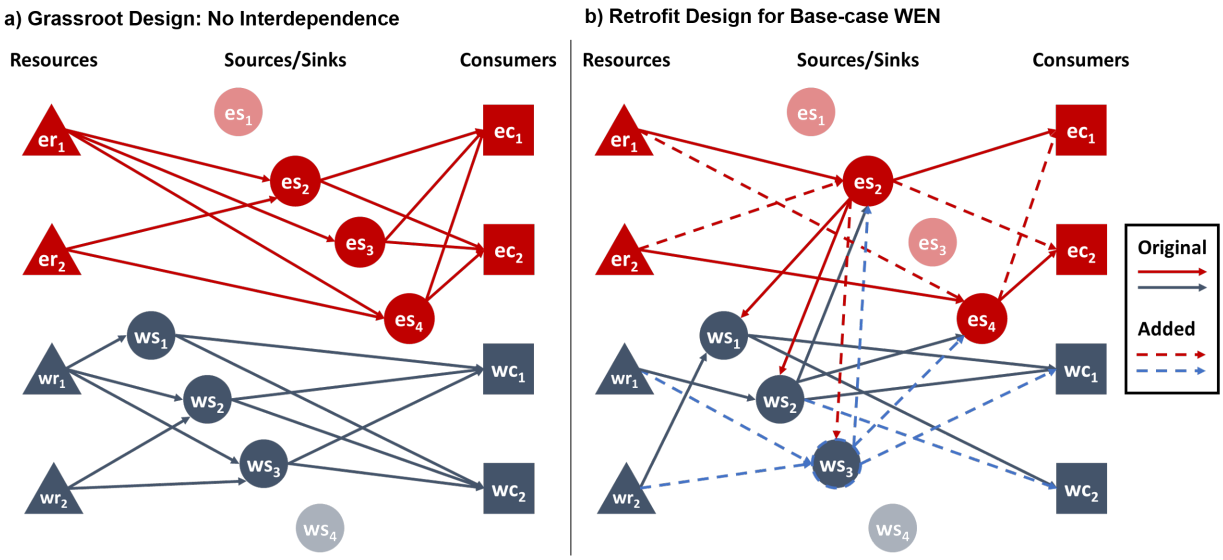

Figure 4.7: Comparison of 100% resilient supply chain network configurations. (a) Grass-root design without nexus interdependence, (b) WEN retrofit for resilience of the minimum-cost network as existing infrastructure.

a result of the additional connections that need to be accounted for.

4.4.3 Resilience-aware Retrofitting

Lastly, we utilize our resilience-aware design framework for the optimal retrofitting of an existing WEN. We start with the base-case network (Figure 4.2) and identify the selected sources and connections as an existing infrastructure, that needs its resilience to be improved. We also provide the rest of the initial superstructure as potential additions. We solve the multi-scenario formulation by fixing the capacity lower bounds of the existing sources and connections to the base-case's values. As a result, the optimizer will choose to increase the connectivity or introduce new sources from the rest of the initial superstructure to account for the existing (and expanded) network's connectivity disruptions. The computations for this case converge in a matter of minutes, since half of the initial superstructure is already provided as a lower bound solution.

In Figure 4.7b we present the high penalty (100% resilient) retrofitted WEN. We have utilized straight and dashed lines to identify the base-case original and the expanded connections and facilities. The base-case WEN consists of 2 energy and 2 water sources, and 13 connections. After

the retrofitting-for-resilience, one additional water source is added, and the total connections are 24. For comparison, the 100% resilient WEN for the grass-root design case can be seen in Figure 4.6.6. The cost of the 100% resilient retrofitted WEN is \$2,168, which is higher than the grass-root case (\$2,130). In addition, this regime is achieved at much higher penalty, $\lambda \geq 100$. Finally, the maximum demands that can be satisfied at maximum operation (ξ) is 32%, which is lower than the first case (47%).

These difference across the three cases can be seen in the comparison of the MCOR. In every case, we solve for the base-case corresponding network. We then calculate MCOR as the normalized difference between the base-case cost and the multi-scenario solution cost. The base-case cost for grass-root and retrofitting cases is the and equal to \$1,875. We demonstrate the MCOR distribution with λ. It is evident that, the no interdependence supply chain achieves 100% resilience in lower λ. It also requires the minimum relative cost increase to reinforce the resilience of the given initial superstructure.

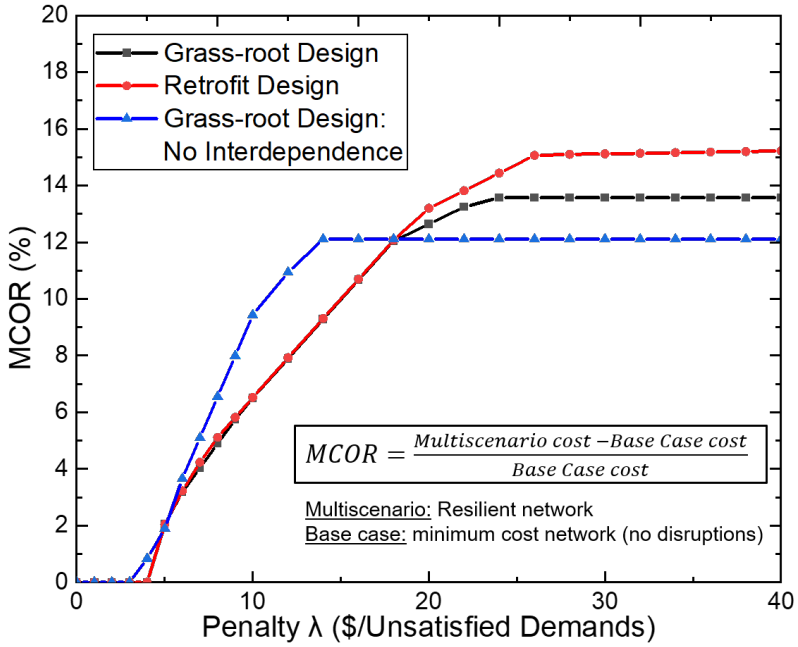

Figure 4.8: Minimum cost of resilience (MCOR) distribution for parametric penalty coefficient λ. The three curves correspond to the three applications of the resilience-aware design framework: (i) Grass-root design, (ii) Retrofitting-for-resilience, (iii) No interdependence supply chain design

MCOR for retrofitting is 15.6%, while a grass-root resilient WEN requires 13.6% additional investments compared to the base case. This is because, there exists already a non-resilient network which was not initially designed for resilience. It is worth noting, that the more expensive case (retrofitting) results in less additional demand satisfaction (ξ). Inversely, for the same cost constraints, we expect the retrofit case to result in lower resilience metrics than the grass-root case. Finally, we can deduce that grass-root MCOR provides the theoretical minimum additional network investments for a given initial superstructure, compared to the base case WEN. Retrofitting MCOR provides the actual minimum additional investments to improve an existing base-case WEN for the same superstructure.

4.5 Case Study on Bexar County WEN

We now demonstrate the resilience-aware design of an actual regional WEN. The investigated system is Bexar county, which surrounds the city of San Antonio with a population of 1.928 million. We collected plant-level data for power generation from U.S. Energy Information Administration [153, 1]. In 2016, approximately 11,720 GWh were generated across 15 power plants of a total 4,800 MW installed capacity. These utilize four major resources (natural gas, coal, land-fill gas, solar power) and generate power with corresponding power plants.

On the water side, facility-specific data for the water treatment (water sources) were not available to the authors' knowledge. Instead, we obtained from Texas Water Development Board (TWDB) the historical estimates of water usage [154], assorted by resource and consumer type. Specifically, the region utilized 18,000 MGal of surface water, 88,000 MGal of groundwater, and 27,000 MGal of reused water. These were treated to supply 96,000 Mgal to residential consumers, 4,300 MGal to irrigation and livestock, and 3,200 MGal to mining and manufacturing (Mfg). The rest is assumed to be utilized for power generation.

In the case of energy sources we have a clear picture of the number of energy sources. These are 4 natural gas plants (2,540 MW), 2 coal power plants (2,185 MW), 3 LFG power plants (23.8 MW), and 6 solar parks (94.7 MW). Their capacities are evidently unevenly distributed across the different technologies. In addition, we need to assume the number of water treatment facilities for

this case study. Assuming no power imports or exports, we calculate the energy demand as the total power produced minus the power consumed by the water sources. This is calculated using average values of intensity factors of surface, groundwater, and wastewater treatment, at a total of 720 GWh. We can then infer how much power was dedicated for electricity consumers, which is estimated at 11,000 GWh.

The current system capacities are not enough to guarantee 100% resilience and the upper limits of energy/water production and resource availabilities were leading to infeasibilities in the multi-scenario formulation. In addition, Bexar relies heavily on 4 power plants of two types (natural gas, coal) and groundwater treatment. This uneven generation across technologies creates challenges for the resilience reinforcement. As a result, we suggest additional capacities for energy and water generation. We introduce additional LFG plant and solar parks capacities. For water treatment, we introduce additional surface water and wastewater treatment capacities. The same holds for the resources that will need to be withdrawn.

4.5.1 Initial superstructure

The superstructure for the case study (Figure 4.9) consists of: 4 energy resources ($|I| = 4$), 8 energy sources ($|K| = 8$), 6 potential water sources ($|L| = 6$), 2 energy consumers ($|P| = 2$), and 4 water consumers ($|Q| = 4$). These include 2 natural gas plants, 2 coal power plants, 2 landfill-gas power plants, and 2 solar parks. For the water sources, we assume 2 potential surface water treatment facilities, 2 groundwater treatment, and 2 wastewater treatment. The capacity and capacity factors of the energy and water sources are aggregated to two sources of each product, with proportional values as the case of 2016. These are discussed in more detail below. We assume that major energy consumers of the region are two, and can be further viewed as power distributors. Similarly, we assume that the region has four major water consumers (residential, commercial, livestock/irrigation, mining/manufacturing).

The total energy resource products are four ($|M^{in}| = 4$), corresponding to natural gas ($m_1 = 1$), coal ($m_1 = 2$), LFG ($m_1 = 3$), solar power ($m_1 = 4$). The energy resources corresponding to the products are appended in subsets I_{m_1} as follows: $I_{m_1=1} = \{i = 1\}, I_{m_1=2} = \{i = 2\}, I_{m_1=3} =$

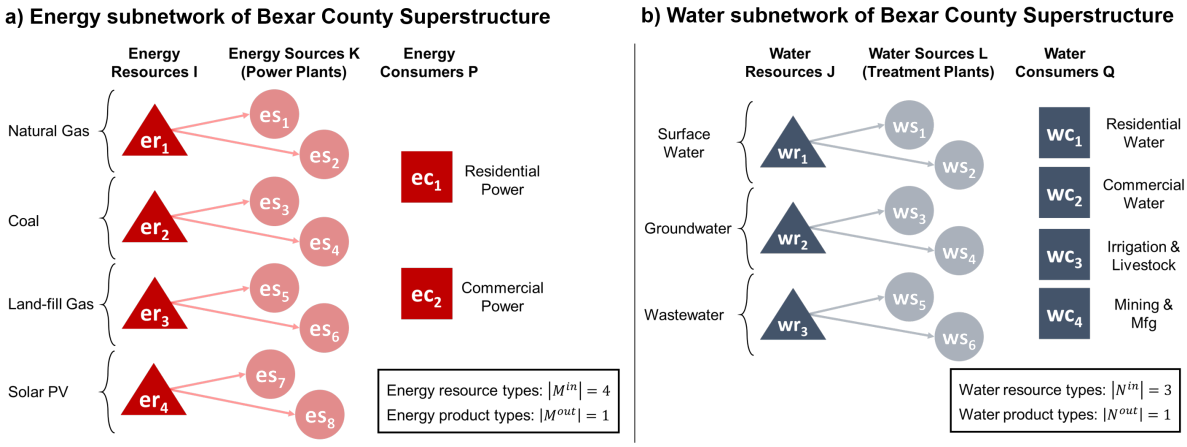

Figure 4.9: Summary of available resources, potential sources and consumers in Bexar County. (a) Energy sub-network of regional WEN, (b) Water sub-network of regional WEN.

$\{i = 3\}, I_{m_1=4} = \{i = 4\}$. Similarly, the energy sources are appended to their corresponding input products (K_{m_1}) as follows: $K_{m_1=1} = \{k = 1, 2\}, K_{m_1=2} = \{k = 3, 4\}, K_{m_1=3} = \{k = 5, 6\}, K_{m_1=4} = \{k = 7, 8\}$. The energy sources produce only one energy product ($|M^{out}| = 1$), and the consumers only receive power. So the product appending sets for the sources and consumers (K_{m_2}, P_{m_2}) are created as follows: $K_{m_2=1} = \{k = 1, 2, 3, 4, 5, 6, 7, 8\}, P_{m_2=1} = \{p = 1, 2\}$. Similarly, there are three water resource types ($|N^{in}| = 3$), corresponding to surface water ($n_1 = 1$), groundwater ($n_1 = 2$), and wastewater ($n_1 = 3$). The water resources corresponding to the products are appended in subsets J_{n_1} as follows: $J_{n_1=1} = \{j = 1\}, J_{n_1=2} = \{j = 2\}, J_{n_1=3} = \{j = 3\}, J_{n_1=4} = \{j = 4\}$. Similarly, the water sources are appended to their corresponding input types (L_{n_1}) as follows: $L_{n_1=1} = \{l = 1, 2\}, L_{n_1=2} = \{l = 3, 4\}, L_{n_1=3} = \{l = 5, 6\}$. We assume that there is no water mixing across different water quality streams at their sinks. The water sources produce one quality of treated water and supply to all the consumers ($|N^{out}| = 1$). So the product appending sets for the sources and consumers (L_{n_2}, Q_{n_2}) are created as follows: $L_{n_2=1} = \{l = 1, 2, 3, 4, 5, 6\}, Q_{n_2=1} = \{q = 1, 2, 3, 4\}$. The initial superstructure is presented in Figure 4.9. The allowable resource-to-source connections are displayed with faded arrows. The sources can supply to all consumers in each sub-network.

The availability of the energy resources is 19,000 GWh of natural gas fuel ($i = 1$), 48,000 GWh

of coal ($i = 2$), 600 GWh of LFG ($i = 3$), and 1,200 GWh of solar power ($i = 4$). The availability of the water resources is 37,000 MGal of surface water ($j = 1$), 88,000 MGal of groundwater ($j = 2$), and 55,000 MGal of wastewater ($j = 3$). The power demand (ecd_p) is 5,600 GWh for both energy consumers. The water demands are 48,800 for consumers 1 and 2, 4,300 MGal for irrigation and livestock ($q = 3$), and 3,200 MGal ofr mining and mfg ($q = 4$).

Table 4.2: Operational and cost parameters for energy and water sources of regional case study[1, 2, 3, 4].

		Energy Sources k			
Parameter	**Units**	k=1,2	k=3,4	k=4,5	k=7,8
Resource/Technology[1]	-	NG	Coal	LFG	Solar
Conversion Factor, β_k	-	0.3490	0.3205	0.2723	0.366
Intensity Factor, ϕ_k^{es}	Gal/kWh	1.652	2.561	0.477	0
Capacity Factor, cf_k^{es}	-	0.29	0.8192	0.663	0.25
Available Capacity, CAP_k^{es}	MW	2540	2185	24	191
Overnight Capital Cost, occ_k	$\$\, MW^{-1}$	1,032	3,600	3,800	2,000
Annual O&M Cost, omc_k	$\$\, MW^{-1}\, y^{-1}$	42,960	141,000	144,000	80,000
Capital Cost[2], EVC_k	$\$\, MW^{-1}\, y^{-1}$	12	33	30	16
Operating Cost, EOC_k	$\$\, MWh^{-1}$	7	5	5	0
		Water Sources l			
Parameter	**Units**	l=1,2	l=3,4	l=5,6	
Resource/Technology[3]	-	SW	GW	WW	
Intensity Factor, ϕ_l^{ws}	$MWh/MGal$	1.4	1.8	6	
Available Capacity, CAP_l^{ws}	mgd	100	240	150	
Annualized Capital Cost, WVC_l	$\$\, mgd^{-1} y^{-1}$	30,000	60,000	120,000	
Operating Cost, WOC_l	$\$\, MGal^{-1}$	300	400	600	

[1] NG: Natural Gas, LFG: Land-fill Gas

[2] $EVC_k = \kappa_F \cdot occ_k + omc_k$, $\kappa_F = 0.03y^{-1}$

[3] SW: Surface Water, GW: Groundwater, WW: Wastewater

The energy generation and transportation variables are expressed in MWh. The generating and transportation capacities ($cap_k^{es}, cap_{i,k}^{eres}, ...$) are expressed in MW, and the annual operational time for energy is 8,760 h (τ_y^{es}). The water generation and transportation variables are expressed in MGal. The generating and transportation capacities ($cap_l^{ws}, cap_{j,l}^{wrws}, ...$) are expressed in mgd, and the annual operational time for water is 365 d (τ_y^{ws}). The energy resource supply cost ($ersc_i$) is

equal to \$21 per MWh for natural gas ($i = 1$), \$21 per MWh for coal ($i = 2$), \$17 per MWh for landfill-gas ($i = 3$), and \$0 per MWh for solar power ($i = 4$). These values are obtained by spot prices for each fuel converted with its heat content. The water rights purchase cost ($wrsc_j$) is taken as \$100 per MGal for surface untreated water ($j = 1$), \$50 per MGal for groundwater ($j = 2$), and \$0 for wastewater ($j = 3$). The capacity factor of the power plants are given based on the historical maximum utilization of the energy sources' nameplate capacity [1]. The capacity factors for water sources is taken 1, as they can operate at 100% of their capacities. The conversion factors of the water sources (β_l^{ws}) are also taken as 1, as we assume no macroscopic water losses at the treatment plants. The parameters for the potential energy and water source are presented in Table 4.2, with operational and cost coefficients [2, 3, 4]. The fixed cost of energy and water (EFC, WFC) sources is taken as \$1,000,000 per year per facility. Similarly, the fixed cost of transportation of energy and water ($EFTC$, $WFTC$) is assumed to be 500,000 per year per installed connection. These coefficient values may seem high but the total fixed cost is far lower than the capital and operating costs of the sources and their connections. These values act as an incentive to obtain lower number of connections and facilities. The capital cost of energy transportation ($EVTC$) is \$139 per MW per year, while the variable cost ($EOTC$) is \$20 per MWh [155]. The capital cost of water transportation ($WVTC$) is \$20,000 per mgd per year, and the variable cost ($WOTC$) is \$100 per MGal.

4.5.2 Regional WEN resilience analysis

This superstructure gives rise to an MILP consisting of 33,347 equations and 25,833 variables (164 binary). The number of potential allowed connections is 150 ($|S| = 150$). If there was no energy and water type differentiation and all connections were allowed the number of scenarios would be 186. The corresponding minimum cost model consists of 716 equations and 503 variables (164 binary). The computational time limit is set to 10 hours and the relative optimality gap to 0.1%. The base case model was solved in seconds. The multi-scenario formulation did not converge within the time limit, and the final relative gap achieved was 0.25%. For this case study, we do not allow external grid supplies, so we impose that the operational resilience will be 100%

($\theta_e = \theta_w = 1$). As a result, the penalty cost (PC) is zero regardless of the value of λ.

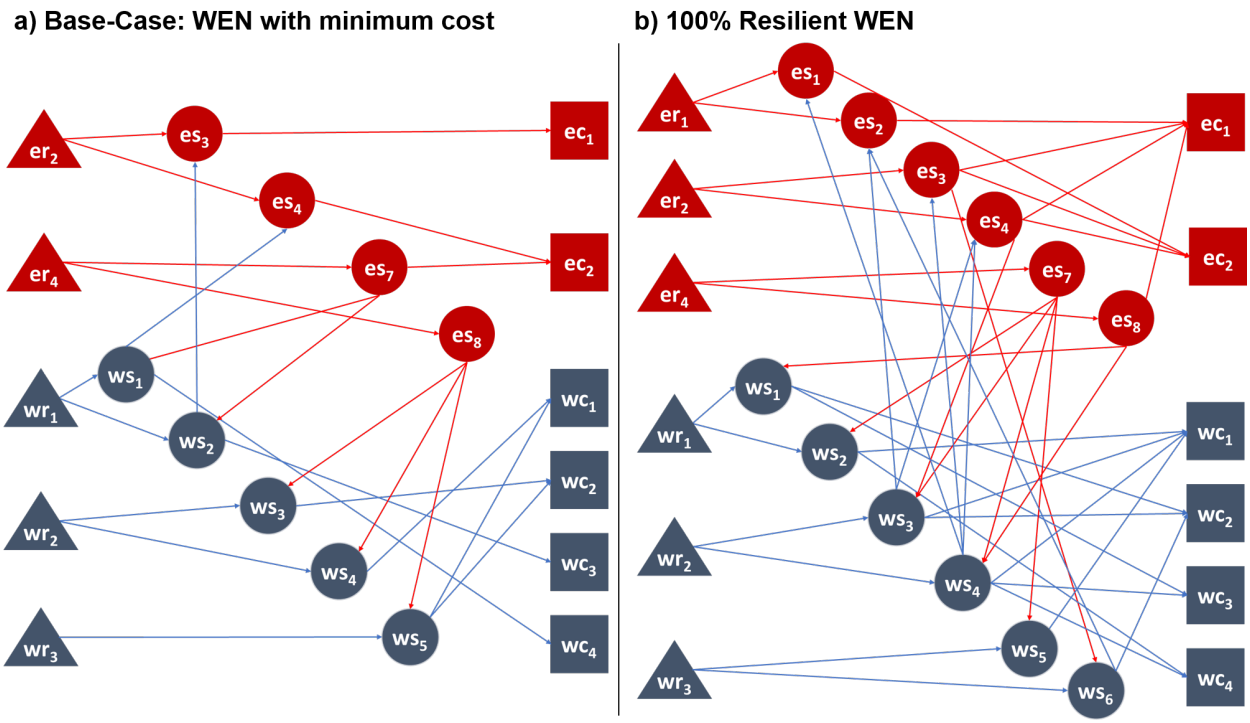

Figure 4.10: Optimized network configurations for regional WEN of Bexar County. (a) Non-resilient minimum cost WEN for Bexar superstructure, (b) Resilient WEN configuration that is fully immune to single-connectivity disruptions.

We first obtain the minimum cost WEN for the given superstructure (Figure 4.10a). The total cost of the infrastructure is \$1,209 million per year. The resulting WEN consists of four energy sources, including 2 coal power plants ($k = 3, 4$) and the 2 solar parks ($k = 7, 8$). The selected water sources are 2 surface treatment plants, 2 water treatment plants, and 1 wastewater treatment plant ($l = 1, 2, 3, 4, 5$). The installed connections are 25. The 100% resilience solution yields a total cost of \$1,385 million. This leads to a MCOR of 14.6% additional investments. In order to account for the potential connectivity disruptions, the all the potential energy sources are utilized ($k = 1, 2, 3, 4, 7, 8$), except from the LFG plants. All the water sources have been utilized as well in order to account for the potential disruption scenarios. The selected connections have also increased to 44. We can infer that the original provided superstructure relies heavily on the water

sources, as they are almost all utilized for the resilient design and operation. Specifically, the energy sources have allocated 1,061 MW and 1,101 MW of natural gas power plants, 769 MW of each coal power plant, and 95 MW of each solar park. The water sources have allocated 50 mgd of each surface water treatment plant, 120 mgd of each groundwater treatment plant, and 67 and 75 mgd of wastewater treatment plants.

4.6 Summary

We developed a multi-scenario optimization-based framework to analyze and design resilient interconnected supply chain networks. We introduced several resilience quantification metrics to the framework and used them to analyze the capability of a given infrastructure to withstand single-connectivity disruptions. We observed that the operational resilience metric could be used to identify the critical connecting streams based on the impact of their failure on the consumer demands satisfaction. To compare among different resilience enhancement strategies and different degrees of over-design, we introduced the minimum cost of resilience (MCOR), which tracks the cost of infrastructure investment that is needed to transform a supply chain to be resilient. Our mathematical programming-based decision-making accounts for the resulting WEN's resilience starting from the design phase. The mathematical model takes into account the performance metrics and guarantees minimum over-design and MCOR. That is, compared to heuristic approaches for resilience reinforcement, the solution of the multi-scenario model provides minimum additional total cost. Inversely, for a fixed network budget the resulting supply chain network yields maximum resilience.

The proposed optimization framework was demonstrated first on an illustrative example for resilience-aware grass-root and retrofit designs. We observed that low penalties for demand violations resulted in simpler or zero network configurations but gives away the chance for local resource management. Higher penalties result in more resilient and self-sufficient network configurations. The grass-root resilient design yielded lower MCOR than the retrofitting case, since there are no pre-existing facilities and connections. We also explored the effect of nexus interdependence by comparing the resilient designs with zero intensity factors. Absence of interdependence reduced

the total cost, the MCOR, and the critical penalty threshold for which the fully resilient network is obtained. The resilience-aware design results in higher tolerance towards demand increases (ξ) in nominal operation. We lastly investigated the resilience-aware design of a regional WEN in a county of Texas. We obtained a fully resilient WEN to single-connectivity failures with an MCOR of 14.56%, compared to the minimum cost configuration for the region. We learned that it is important to evenly distribute the capacities of the energy and water treatment facilities as much as possible. This indicates that distributed manufacturing (vs. centralized large processing) is more favorable for the resilient design of a nexus and other interconnected supply chains.

To conclude, our framework can be applied for the resilience analysis and reinforcement of any type of interdependent or isolated supply chain. As a result, supply chains can be protected against single-connectivity failures, coming from natural disasters such as floods, fires, earthquakes, and hurricanes. Our framework can be used to identify critical components and optimal resilience improvement strategies (retrofitting) with minimum additional investments. It is then up to the decision makers to review such strategies and provide funding and incentives for the protection of its infrastructures. The computational burden for the resilient design is still a challenge due to the multi-scenario expansion, especially in the absence of product differentiation. However, this increase is common in multi-period design and operation of supply chains. Further research is needed to improve the solution efficiency of our model to be able to solve large-scale problems.

5. SURVIVABILITY-AWARE DESIGN [1]

The disruptions and prolonged lockdowns that followed the COVID-19 pandemic have brought to light the vulnerabilities of many supply chains in the food, manufacturing, chemicals, health, energy and other sectors. Similar disruptions can also result from natural disasters (e.g., earthquakes, floods and hurricanes), political instabilities and war, restrictions on commercial activities, sanctions, and trade disputes. These are examples of systemic shocks that can perturb the productivity and operation of a supply chain enough to eventually move it away from equilibrium, thereby suffering from significant economic losses and, in the worst case, permanent shut down.

In this chapter we introduce economic survivability (ES) and discuss its attributes under different disruption events. We then incorporate ES as a an alternative economic objective in the design of multi-regional, multi-period supply chain networks. Finally, we explore the effect of regional interconnectedness on global and localized ES, along with the effect of over-designing for increased demands.

5.1 Economic Survivability

Economic survivability (ES) is the ability to maintain a net positive economic worth or keeping it above a threshold value in the presence of sudden but then prolonged reduction in demands, prices or resource availability. In the context of reduced demand, ES can be also computed as the fraction of the nominal demand for which the supply chain breaks even (i.e., the point where the total expense equals the total revenue, thereby resulting in a net-zero cash flow without profit margin). Consider a supply chain, for example, that is designed to deliver a product with a nominal demand of D_0 units. The fixed and operating costs of producing each unit are α_{FC} and α_{OC}, respectively. Furthermore, the selling price of each unit is α_R. The fixed cost per unit product is amortized with respect to the time basis of nominal demand D_0. To be profitable at the nominal

[1] Reproduced in part with permission from [10] Tsolas, S. D. & Hasan, M. M. F. (2021). Survivability-Aware Design and Optimization of Distributed Supply Chain Networks in the Post COVID-19 Era. *Journal of Advanced Manufacturing and Processing.*

condition, the supply chain must satisfy the following condition:

$$D_0(\alpha_R - \alpha_{FC} - \alpha_{OC}) \geq 0. \tag{5.1}$$

Now, consider that there is a demand reduction at time t onward (see **Figure 5.1a**) such that the new demand is given by $D_t = \lambda_t D_0$, where λ_t is the fractional decrease of the demand from the nominal value. Following the demand, the production amount is adjusted to a new amount. However, the total fixed cost is unchanged since it is a function of the design capacity and does not vary with variable production rate. While the original supply chain was constructed with a fixed investment of $\alpha_{FC} D_0$, the revenue and operating cost are now reduced to $\alpha_R \lambda_t D_0$ and $\lambda_t \alpha_{OC} D_0$, respectively. Therefore, the condition for staying above the break even point with positive cash flow is now changed to

$$D_0 \left[(\alpha_R - \alpha_{OC}) \cdot \lambda_t - \alpha_{FC}\right] \geq 0. \tag{5.2}$$

In other words, the condition for ensuring ES of the supply chain is given by

$$\lambda_t \geq \frac{\alpha_{FC}}{\alpha_R - \alpha_{OC}}. \tag{5.3}$$

ES corresponds to the fractional change in demand below which a business is not profitable. Therefore, the right-hand side of Eq. 5.3 represents an index for ES, and λ_t represents a survivability threshold. A business survives as long as it meets the condition presented in Eq. 5.3. Understandably, a lower value of $\frac{\alpha_{FC}}{\alpha_R - \alpha_{OC}}$ is desirable. This also means that ES depends on critical economic parameters such as the market prices and the supply chain costs. Internally, a supply chain can improve its ES by reducing the fixed costs and operating expenses. We illustrate this using an example. The amortization or depreciation factor has a considerable impact on the economic survivability. Higher annuitization factor increases the contribution of the fixed cost coefficient per product produced. This leads to increased λ_t and reduced ES. Assume that a product

has a fixed cost of \$2/kg, an operating cost of \$2/kg, and a price of \$5/kg. Therefore, we have $ES = \frac{2}{5-2} = 0.67$. This means that a positive cash flow can be maintained even if the demand reduces suddenly and continue to stay at the new value, as long as the changed demand is within 67% or more of the nominal value. If the business takes a measure that reduces the operating cost from \$2/kg to \$1/kg, the threshold for survivability further reduces to 50%, which means that the company now can economically survive even if the demand is reduced to half of its original value.

We have assumed that the product prices do not change considerably after the demand fluctu-

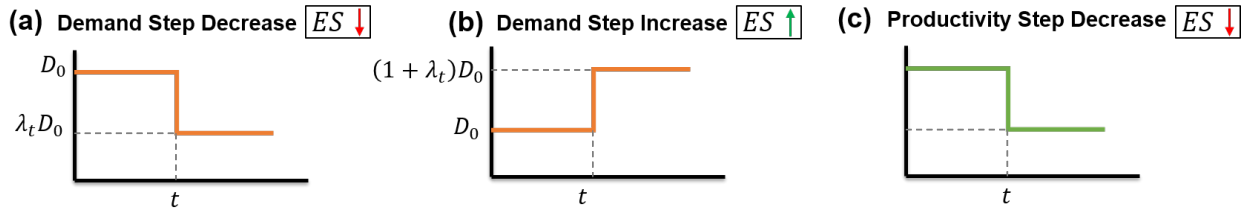

Figure 5.1: Types of systemic shocks and their impact on economic survivability.

ates. In most practical settings, the demand would be affected by the current price and the relative change in consumer patterns. However, we can utilize ES as a theoretical measure to analyze and optimize supply chains for these situations.

ES is also somewhat related to return on investment (ROI). ROI provides a direct measure of the amount of return relative to a particular investment or fixed cost. ES, on the other hand, provides a measure of how costly it is to get a return. It can be used to compare the costs of different investments. ROI is a performance measure used to evaluate the efficiency of an investment only at the nominal case, but ES is a performance measure under changing conditions.

Furthermore, the economic survivability threshold can be viewed as a special case of the break-even point. In economics, the break-even point corresponds to the number of units a business must sell in order for the sales revenue to match the variable and amortized fixed costs. For a supply chain, the break-even point corresponds to the demand that results in a zero net profit. ES is the fraction of the break-even demands to the nominal demands for which the supply chain is

designed. From this definition of ES, we expect that higher economic survivability will result in higher supply chain profitability.

In **Figure 5.1**, we sketch the nature of different systemic shocks and their effect on ES. When a reduction in demand results in a reduction in revenue, the supply chain survivability reduces (**Figure 5.1a**). An unexpected increase in demand may increase the survivability when there is no penalty for demand violation (**Figure 5.1b**). However, there is always a chance that the system is not designed flexibly enough to be able to grab the economic opportunity provided by the excess demands. In the context of pandemics and natural disasters, this may impair the social welfare of a region. A great example is the sudden increase in demands for masks, hand sanitizers and personal protection equipment (PPE) at the onset of COVID-19. Finally, when the demand remains unchanged but the productivity is reduced/restricted, both the social welfare and economic survivability suffer (**Figure 5.1c**). A common strategy to combat disruption events is to overdesign, but in many cases, such excess capacities are not utilized. Such overdesigned supply chains suffer more economic losses in the presence of step decrease in demand that continues for a prolonged time period.

A supply chain may survive a disruption event if there is additional savings/loan/stimulus available to balance out the negative cash flows. The question then becomes how long the company or the supply chain can withstand the disruption before the reserved amount is completely depleted. The updated necessary condition for economic survivability is as follows:

$$\lambda_t \geq \frac{\alpha_{FC} - \alpha_{FS}}{\alpha_R - \alpha_{OC}} \tag{5.4}$$

where, α_{FS} is the fixed savings/loan/stimulus in terms of dollar per unit product amount (\$/kg). This means that the management has a total reserve of $\alpha_{FS} D_0 \tau_{ES}$ (\$) to mitigate the disruption-related losses should the disruption occurs, where τ_{ES} is the additional time (days) that the business can survive until the reserve is depleted completely. If, for some reason, the number of days with negative cash flow exceeds τ_{ES}, then the business will not survive economically. This can

happen if a lockdown continues for a prolonged period. Therefore, for informed decision-making, policymakers can benefit from such analysis of economic survivability. One such policy may include a stimulus that is in proportion to the number of lockdown days, the unit fixed cost and the nominal demands of a business entity. For example, using the same concept that is used in Eq. 5.4, one can compute how much stimulus may be needed to keep a particular business running if there is an imposed reduction of demands or production capacity, for example, to survive over a two-week period of lockdown.

5.2 Incorporating Economic Survivability in Supply Chain Design

We consider the survivability of supply chain networks comprised of four echelons. These echelons are: (i) potential raw material suppliers with known locations and availabilities, (ii) potential manufacturing centers, (iii) potential distribution centers, and (iv) customer centers with fixed locations and demands. We also consider a single product that involves multiple geographically interdependent supply chain components. The interdependence arises due to the fact that the overall supply chain spans across multiple regions (see **Figure 5.2** for an example). The de-

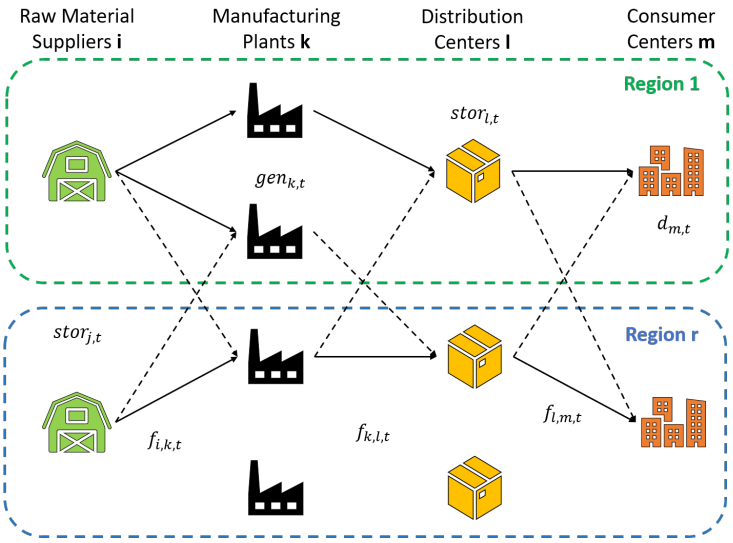

Figure 5.2: Geographically interconnected multi-period supply chain network synthesis superstructure. The supply chain is comprised of 4-echelons: material suppliers, manufacturing centers, distribution centers, and consumer centers. The interdependence arises due to the fact that the overall supply chain spans across multiple regions

cisions that need to be determined include the selection of manufacturing facilities, distribution centers and transportation links, and their maximum capacities. While these capacities are design decisions, the actual operating levels can vary with time. Therefore, we also optimize the time-dependent operating variables. We define three distinct objectives for the mathematical programming formulation: (i) maximization of the total profit, (ii) maximization of global survivability, and (iii) maximization of local regional survivability. The three objectives will be imposed in distinct single-objective optimization problems.

Let $i \in I$ represent supplier i from the set of available raw material suppliers I, $k \in K$ denote processing facility k from the set of potential manufacturing plants K, $l \in L$ denote distribution center l from the set of potential centers L, and $m \in M$ denote customer center m with known demand from the set of all available customers M. We also define a set $t \in T$ of time periods as a representative operational horizon. Finally, we have a set $r \in R$ corresponding to multiple regions, where the facilities can be located. We know the locations of all potential facilities beforehand. Based on these information, we further define the following subsets: $R_I(i,r) \subseteq I \times R$, $R_K(k,r) \subseteq K \times R$, $R_L(l,r) \subseteq L \times R$, and $R_M(m,r) \subseteq M \times R$ to identify the suppliers, processing plants, distribution centers and customer locations that are located in region r. For instance, assume that there are five suppliers ($|I| = 5$) who are located across two regions ($|R| = 2$). Three suppliers ($i = 1, 2, 3$) are allocated in region $r = 1$ and others ($i = 4, 5$) are located in region $r = 2$. Then, the subset allocating the suppliers to the regions is $R_I = \{(1,1), (2,1), (3,1), (4,2), (5,2)\}$. Other subsets are constructed similarly.

We define the following parameters to remain constant when we optimize the supply chain. The maximum availability of the raw material for supplier i at time t is set by $a_{i,t}$. A manufacturing facility k is characterized by a conversion factor β_k that corresponds to its output-to-input productivity ratio. We also fix the maximum available design capacities CAP_k^{gen} and CAP_l^{stor} for the manufacturing plants and distribution centers, respectively. Also, fc_k and fc_l represent the fixed investment of manufacturing center k and distribution center l, respectively. Similarly, the capital cost coefficients are represented by cc_k and cc_l, while the the operating costs of the facilities

are represetned by oc_k and oc_l. The fixed, capital, and variable costs of transportation are given by ftc, ctc, and vtc, respectively. Lastly, we know the selling price of the product for each customer center m, which is denoted as p_m.

The continuous decision variables to be optimized are defined as follows:

$gen_{k,t}$	Product generation from manufacturing center k at time period t,
$stor_{l,t}$	Storage inventory level of distribution center l at time period t,
cap_k^{gen}	Maximum generating capacity of manufacturing plant k,
cap_l^{stor}	Maximum storage capacity of distribution center l,
$f_{i,k,t}$	Product flow from supplier i to manufacturing plant k at time period t,
$f_{k,l,t}$	Product flow from manufacturing plant k to distribution center l at time period t,
$f_{l,m,t}$	Product flow from distribution center l to customer center m at time period t,
$cap_{i,k,t}$	Maximum transportation capacity from supplier i to manufacturing plant k,
$cap_{k,l,t}$	Maximum transportation capacity from manufacturing plant k to distribution center l,
$cap_{l,m,t}$	Maximum transportation capacity from distribution center l to customer center m,
RFC_r	Fixed cost of investment of facilities in region r,
RCC_r	Capital cost of investment of facilities in region r,
ROC_r	Operating cost of facilities in region r,
$RREV_r$	Revenue from product sales to the consumers of region r,
FCT	Total fixed cost across all regions,
CCT	Total capital investment across all regions,
OCT	Total operating cost across all regions,
REV	Total revenue from product sales to the consumers,
P	Total profit of the supply chain,
λ_r	Local economic survivability threshold for every region, r
λ_{local}	Average local economic survivability threshold across all regions,
λ_{global}	Global economic survivability threshold across all regions.

We define the following binary variables for the selection of facilities and designed connections. These variables appear also in the fixed cost components:

z_k takes a value of one if manufacturing plant k is selected, zero otherwise;

z_l takes a value of one if distribution centers l is selected, zero otherwise;

$z_{i,k}$ takes a value of one if supplier i supplies to plant k, zero otherwise;

$z_{k,l}$ takes a value of one if manufacturing plant k supplies to distribution center l;

$z_{l,m}$ takes a value of one if distribution center l supplies to to customer center m.

With these variables and parameters, we now describe the model formulation. We include Eq. 5.5 to ensure that the supply of raw material from a supplier does not exceed the available amount $a_{i,t}$. At time t, the raw material is converted to product at processing facility k with a conversion factor β_k. This conversion is enforced in Eq. 5.6. After this, Eq. 5.7 ensures the material balance for the outgoing flow of product from each facility k to all distribution centers. Eq. 5.8 represents the inventory balance at each distribution center l over time. Eq. 5.9 imposes that the inlet flows to a center l plus the previous period's inventory level do not exceed the total inventory capacity. Eq. 5.10 ensures that all the customer demands $d_{m,t}$ are met at all times.

$$\sum_k f_{i,k,t} \leq a_{i,t} \qquad \forall\, i \in I,\, t \in T \tag{5.5}$$

$$\beta_k \cdot \left(\sum_i f_{i,k,t} \right) = gen_{k,t} \qquad \forall\, k \in K,\, t \in T \tag{5.6}$$

$$gen_{k,t} = \sum_l f_{k,l,t} \qquad \forall\, k \in K,\, t \in T \tag{5.7}$$

$$stor_{l,t} = stor_{l,t-1} + \sum_k f_{k,l,t} - \sum_m f_{l,m,t} \qquad \forall\, l \in L,\, t \in T \tag{5.8}$$

$$stor_{l,t-1} + \sum_k f_{k,l,t} \leq cap_l^{stor} \qquad \forall\, l \in L,\, t \in T \tag{5.9}$$

$$\sum_l f_{l,m,t} = d_{m,t} \qquad \forall\, m \in M,\, t \in T \tag{5.10}$$

At any given time t, the actual operating capacities or flows cannot exceed the maximum design capacities. Therefore, we enforce the following capacity constraints for each selected facility:

$$gen_{k,t} \leq cap_k^{gen} \qquad \forall\, k \in K,\, t \in T \tag{5.11}$$

$$stor_{l,t} \leq cap_l^{stor} \qquad \forall\, l \in L,\, t \in T \tag{5.12}$$

$$f_{i,k,t} \leq cap_{i,k} \qquad \forall\, i \in I,\, k \in K,\, t \in T \tag{5.13}$$

$$f_{k,l,t} \leq cap_{k,l} \qquad \forall\, k \in K,\, l \in L,\, t \in T \tag{5.14}$$

$$f_{l,m,t} \leq cap_{l,m} \qquad \forall\, l \in L,\, m \in M,\, t \in T \tag{5.15}$$

The design capacity of a facility must be zero, if it is not selected. When selected, the facility cannot exceed its maximum allowed capacity. These are imposed as follows:

$$cap_k^{gen} \leq z_k \cdot CAP_k^{gen} \qquad \forall\, k \in K,\, t \in T \tag{5.16}$$

$$cap_l^{stor} \leq z_l \cdot CAP_l^{stor} \qquad \forall\, l \in L,\, t \in T \tag{5.17}$$

$$cap_{i,k} \leq z_{i,k} \cdot min(max(a_{i,t}), CAP_k^{gen}) \qquad \forall\, i \in I,\, k \in K,\, t \in T \tag{5.18}$$

$$cap_{k,l} \leq z_{k,l} \cdot min(CAP_k^{gen}, CAP_l^{stor}) \qquad \forall\, k \in K,\, l \in L,\, t \in T \tag{5.19}$$

$$cap_{l,m} \leq z_{l,m} \cdot min(CAP_l^{stor}, max(d_{m,t})) \qquad \forall\, l \in L,\, m \in M,\, t \in T \tag{5.20}$$

We also include several logical constraints to impose the relationships between the binary variables that dictate the selection of various facilities. Specifically, if manufacturing facility k is not selected, then there can be no incoming (i to k) and outgoing (k to l) connections. These restrictions are imposed through Eqs. 5.21 and 5.23. Inversely, if no incoming connections reach manufacturing centers (i to k), the manufacturing center cannot be selected (Eq. 5.22). Similarly, if no supplies stem from each facility (k to l), then it cannot be selected (Eq. 5.24). Similar constraints are expressed for distribution centers l (Eqs. 5.25 - 5.27). Eqs. 5.25 and 5.27 ensure that if a distribution center l is not selected, there can be no incoming or outgoing connections respectively. Finally, a distribution center l cannot be selected, if no incoming (eq. 5.26) or outgoing (eq.

5.28) connections are selected.

$$z_{i,k} \leq z_k \qquad \forall\, i \in I,\, k \in K \tag{5.21}$$

$$\sum_i z_{i,k} \geq z_k \qquad \forall\, k \in K \tag{5.22}$$

$$z_{k,l} \leq z_k \qquad \forall\, k \in K,\, l \in L \tag{5.23}$$

$$\sum_l z_{k,l} \geq z_k \qquad \forall\, k \in K \tag{5.24}$$

$$z_{k,l} \leq z_l \qquad \forall\, i \in I,\, t \in T \tag{5.25}$$

$$\sum_k z_{k,l} \geq z_l \qquad \forall\, l \in L \tag{5.26}$$

$$z_{l,m} \leq z_l \qquad \forall\, l \in L,\, m \in M \tag{5.27}$$

$$\sum_m z_{l,m} \geq z_l \qquad \forall\, l \in L \tag{5.28}$$

The fixed cost of investment of the infrastructure is a linear function of the binary variables of selection, and is determined by the combination of allocated facilities and connectivity (Eqs. 5.29, 5.33). The capital cost of investment is a linear function of the maximum capacities, which are the design variables of the mathematical model (Eqs. 5.30, 5.34). The operating cost is a linear function of the time-dependent operating variables, hence product generation, inventory levels, and supplies (Eqs. 5.31, 5.35). For the calculation of regional cost expressions, we consider only the facilities that belong in each corresponding region. For the fixed, capital, and variable cost of transportation we allocate the cost of each stream to the region of origin facility of that flow. For example, the cost of an inter-regional flow from generating facility $k = 1, r = 1$ to a storage facility $l = 3, r = 2$, will be calculated in the cost expressions of region 1. The revenue of each region is calculated from the sales of the region's consumer centers. A regional supply chain may correspond to geographical entities where there is at least one consumer center for the product under examination. A region can be a city, county or country. It can also span over multiple

countries.

$$RFC_r = \sum_{k \in R_K} fc_k \cdot z_k + \sum_{l \in R_L} fc_l \cdot z_l + ftc \cdot \left[\sum_{i \in R_I} \sum_{k} z_{i,k} + \sum_{k \in R_K} \sum_{l} z_{k,l} + \sum_{l \in R_L} \sum_{m} z_{l,m} \right], \qquad \forall\, r \in R \tag{5.29}$$

$$RCC_r = \sum_{k \in R_K} cc_k \cdot cap_k + \sum_{l \in R_L} cc_l \cdot cap_l + ctc \cdot \left[\sum_{i \in R_I} \sum_{k} cap_{i,k} + \sum_{k \in R_K} \sum_{l} cap_{k,l} + \sum_{l \in R_L} \sum_{m} cap_{l,m} \right], \qquad \forall\, r \in R \tag{5.30}$$

$$ROC_r = \sum_{k \in R_K} oc_k \cdot gen_{k,t} + \sum_{l \in R_L} oc_l \cdot stor_{l,t} + vtc \cdot \left[\sum_{i \in R_I} \sum_{k} \sum_{t} f_{i,k.t} + \sum_{k \in R_K} \sum_{l} \sum_{t} f_{k,l,t} + \sum_{l \in R_L} \sum_{m} \sum_{t} f_{l,m,t} \right], \qquad \forall\, r \in R \tag{5.31}$$

$$RREV_r = \sum_{l} \sum_{m \in R_M} \sum_{t} p_m \cdot f_{l,m,t} \tag{5.32}$$

The expressions for costs and revenue across all regions are given in Eqs. 5.33 - 5.36:

$$FCT = \sum_{r} RFC_r \tag{5.33}$$

$$CCT = \sum_{r} RCC_r \tag{5.34}$$

$$OCT = \sum_{r} ROC_r \tag{5.35}$$

$$REV = \sum_{r} RREV_r \tag{5.36}$$

We define three objective functions in order to demonstrate the relation between total cost,

economic survivability, and the effect of geographical interdependence. The first objective corresponds to the total profit of the whole supply chain across all regions (Eq. 5.37). The second objective is to maximize the global survivability ES^{global} (Eq. 5.38). According to our previous definition of economic survivability, we aggregate the total cost and revenue expressions as in eqs. 5.33 - 5.36, without differentiating across multiple regions. The third objective corresponds to the average local survivability ES^{local}, hence the weighted summation of each region's survivability (Eq. 5.39, 5.40). The fixed and capital costs are annuitized with κ_F.

$$max\, Profit:\ max\, P = REV - \kappa_F \cdot FCT - \kappa_F \cdot CCT - OCT \tag{5.37}$$

$$max\, ES^{global}:\ min\, \lambda_{global} = \frac{\kappa_F \cdot (FCT + CCT)}{REV - OCT} \tag{5.38}$$

$$max\, ES^{local}:\ min\, \lambda_{local} = \frac{1}{|R|} \sum_r \lambda_r \tag{5.39}$$

$$\lambda_r = \frac{\kappa_F \cdot (RFC_r + RCC_r)}{RREV_r - ROC_r} \tag{5.40}$$

To maximize the global (or local) survivability of the supply chain, we minimize the fraction of demand $\lambda_{global}, \lambda_{local}$, since lower demand fraction threshold corresponds to higher ES. This mathematical formulation gives rise to a mixed-integer linear MILP program, when we optimize for the first objective of maximum total profit. When we optimize for maximum global or local economic survivability the resulting program is an MINLP.

To calculate the economic survivability in the model, we use the total revenue REV, fixed cost FCT, capital cost CCT, and operating cost OCT (in dollars). This differs from the unit cost coefficients $\alpha_R, \alpha_{OC}, \alpha_{FC}$ (in dollars per amount of product) used in section 2.

5.3 Case Study on Economic Survivability

In this section we present a numerical example to demonstrate the survivability-aware design of supply chains. We consider a distribution network of three suppliers ($I = 3$), 5 potential manufacturing plant ($K = 5$), 4 distribution centers ($L = 4$), and 3 consumer centers ($M = 3$). The supply chain spans across 3 communicating regions ($R = 3$) and considers 12 time periods ($T = 12$).

The distribution of the given and potential nodes to the corresponding regions is demonstrated in (**Figure 5.3**). The availability ($a_{i,t}$) of the three suppliers is the same for all time periods and equals to 150 ton per month. The selling price (p_m) is \$4 per ton of the product for all consumers. The product demands share the same time-dependent profile for the three consumers and is set to $d_{m,t} = \{100, 105, 110, 90, 90, 95, 100, 95, 105, 110, 100\, tons\, per\, month\}$. The annualization factor (κ_F) is equal to 0.1 per year. The fixed cost of transportation (ftc) is \$80 for each connection. The capital cost of transportation (ctc) is \$3 per ton/month, and the variable cost of transportation (vtc) is \$0.3 per ton. The values of other parameters for the processing facilities and distribution centers are provided in **Table 5.1**. The resulting model consists of 1,244 equations, 811 variables, and 56 binary variables. The models are solved to 0.1% relative optimality gap.

Table 5.1: Parameters for manufacturing facilities and distribution centers.

		Processing Facilities k				
Parameter	**Units**	k=1	k=2	k=3	k=4	k=5
Conversion Factor - β_k	-	0.88	0.92	0.89	0.90	0.91
Fixed Cost - fc_k	\$	98	103	85	100	105
Capital Cost - cc_k	\$/(ton/month)	0.7	0.9	0.6	0.5	0.5
Operating Cost - oc_k	\$/ton	0.07	0.09	0.06	0.05	0.05
Available Capacity - CAP_k^{gen}	ton/month	150	150	150	150	150
		Distribution Centers l				
Parameter	**Units**	l=1	l=2	l=3	l=4	
Fixed Cost - fc_l	\$	95	100	80	100	
Capital Cost - cc_l	\$/(ton/month)	0.5	0.4	0.45	0.5	
Operating Cost - oc_l	\$/ton	0.05	0.04	0.045	0.05	
Available Capacity - CAP_l^{stor}	ton/month	150	150	150	150	

For the first part of the results, we maximize the total profit of the whole supply chain. The resulting profit is equal to $P_{max} = \$433$. The calculated total revenue is $REV = \$1200$, the total fixed cost $\kappa_F FCT = \$129$, the total capital cost $\kappa_F CCT = \$334$, and the total operating cost $OCT = \$304$. The resulting network is demonstrated in **Figure 5.3.1**, and is the most economic configuration. We observe that the network distribution does not take into account the regional

partition of the network, since the profit expression aggregates the cost components from different regions. In this case, the most economical configuration leaves region 1 without any manufacturing plants, and region 3 without any distribution centers.

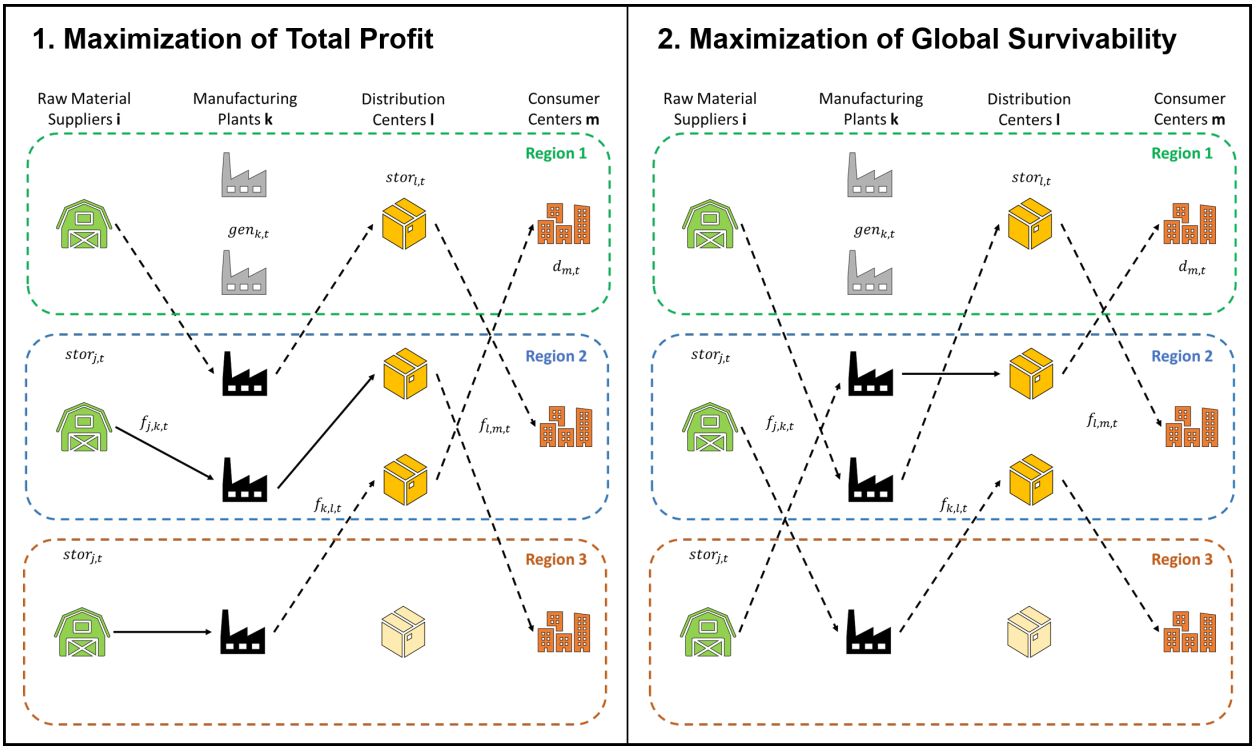

Figure 5.3: Resulting supply chain network connectivity and facility allocation for two distinct optimization objectives. 1) Maximization of total profit for the whole supply chain. 2) Maximization of economic survivability for the whole supply chain.

This observation is inferred also by the calculated values of global and local economic survivabilities shown in **Table 5.2**. The global survivability demand threshold has a value of $\lambda_{global} = 0.516$, meaning that the whole supply chain can withstand 51.6% average demand reductions and still be profitable. However, the values of the local economic survivability ($\lambda_{r=1} = 0.302, \lambda_{r=2} = 1.142, \lambda_{r=3} = 0.295$) are quite unbalanced, compared to the global survivability. This is because the selected facilities and their corresponding costs are also unevenly distributed across the regions. The first and the third regions have not allocated any manufacturing and distribution centers. On

the other hand, the second region has surplus manufacturing and distribution facilities. These additional facilities incur additional regional cost for Region 2 while it receives revenue only from the regional consumers of its own. As a result, Region 2 is over-designed leading to lower local survivability ES, which is characterized by a $\lambda_{r=2}$ value greater than 1. This also means that the break-even demand for Region 2 is higher than the demand for which it receives revenue. Regions 1 and 2 are under-designed and receive flows from Region 2. They also obtain their consumer revenues, which leads to lower ES threshold value compared to the global and average local ES threshold values.

In the second part of our results we maximize the global survivability, by minimizing the demand threshold λ_{global} (**Figure 5.3.2**). We consider again the supply chain as a whole, without regional partitioning. The same facilities are selected and there are only changes in the connectivity of the supply chain network. From the calculated values of total profit and local economic survivability shown in **Table 5.2**, the effect is similar to the first objective result. Maximizing the economic survivability of a supply chain results in maximum profitability. This was expected by the survivability definition, as more profitable supply chains, can withstand increased demand reductions cost-wise.

Table 5.2: Summary of profit and economic survivability results for the three cases.

	Case 1	**Case 2**	**Case 3**
Objective	max Profit	max ES^{global}	max ES^{local}
Profit	P^*_{max}	P_{max}	$98.6\%P_{max}$
λ_{global}	0.516	0.516*	0.522
$\lambda_{r=1}$	0.302	0.301	0.527
$\lambda_{r=2}$	1.142	1.139	0.511
$\lambda_{r=3}$	0.295	0.298	0.526
λ_{local}	0.580	0.579	0.522*

*Optimized decision variable

In the third part, we maximize the average local survivability ES^{local}, by minimizing the average of the individual thresholds $\lambda_{r=1}, \lambda_{r=2}, \lambda_{r=3}$, or λ_{local}. The resulting network is demon-

strated in **Figure 5.4**. In this case, the optimizer still allows inter-regional supplies, but now allocates each region with its own required facilities. In addition, the total profit is calculated as \$427, which corresponds to 98.6% of the maximum potential profit. This profit reduction is also reflected on the decreased global survivability $\lambda_{global} = 0.522$. However, the values of local survivability are more balanced and close to their average and the global survivability ($\lambda_{r=1} = 0.527, \lambda_{r=2} = 0.511, \lambda_{r=3} = 0.526$). This is because, the fixed, capital, and operating costs of the facilities are shared across the different regions more evenly.

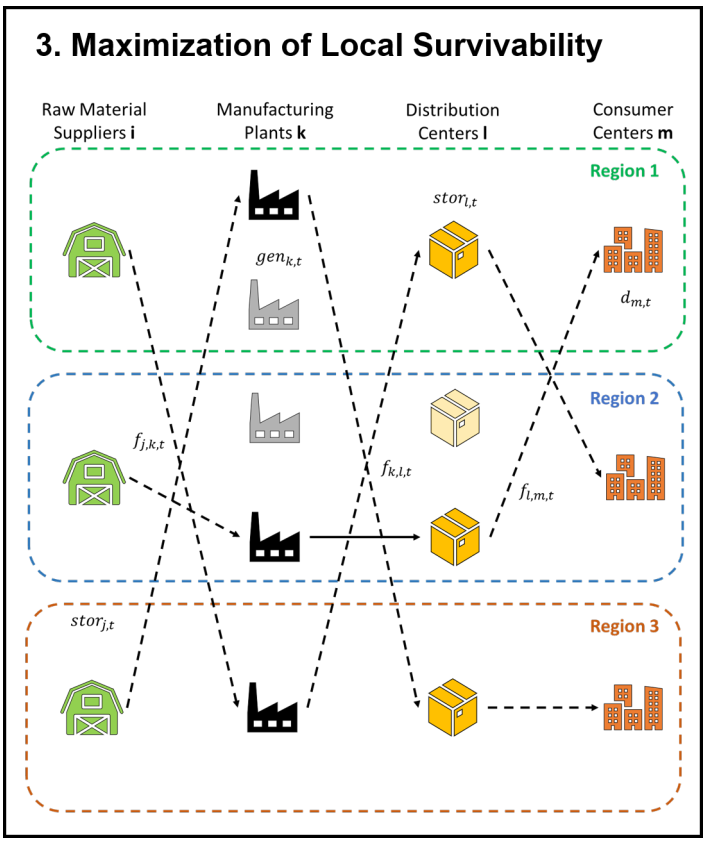

Figure 5.4: Resulting supply chain network and connectivity with maximized local economic survivability ES^{local}.

In the last part of the results, we demonstrate the effect on system profitability and survivability in the case that we need to overdesign the system to satisfy increased demands. To ensure the fea-

sibility of the network in the increased demands scenario, we introduce a duplicate of the operating variables and balances. Representative balances are given below:

$$\beta_k \cdot \sum_i f_{i,k,t}^{feas} = gen_{k,t}^{feas} \qquad \forall\, k \in K,\, t \in T \tag{5.41}$$

$$\sum_l f_{l,m,t}^{feas} = (1+\epsilon) \cdot d_{m,t} \qquad \forall\, m \in M,\, t \in T \tag{5.42}$$

$$gen_{k,t}^{feas} \leq cap_k^{gen} \qquad \forall\, k \in K,\, t \in T \tag{5.43}$$

$$f_{i,k,t}^{feas} \leq cap_{i,k} \qquad \forall\, i \in I,\, k \in K,\, t \in T \tag{5.44}$$

The duplicate balances, maintain system feasibility in the event that we need to satisfy excess demands $(1+\epsilon) \cdot d_{m,t}$. This is expressed in Eq. 5.42. The auxiliary variables must also fall within the bounds of the common design variables $cap_k^{gen}, cap_l^{stor}, cap_{i,k}^{f}, ...$ (Eqs. 5.43-5.44). These variables do not contribute to the cost components directly. However, the values of the design capacity variables will be higher because of Eqs. 5.41-5.42, thus affecting indirectly the fixed cost and the capital cost components FCT', CCT'. The objective is to obtain an optimal supply chain for nominal demands, and be feasible for the scenario of excess demands. As a result, the revenue and the operating cost are calculated using the nominal operating variables. The objective is to maximize the global survivability, by minimizing the demand fraction threshold λ_{global}:

$$min\, \lambda_{global} = \frac{FCT'' + CCT''}{REV - OCT} \tag{5.45}$$

Higher values of ϵ entails that the system design is more conservative. This is due to calculating the revenue for nominal demands, but equipping the system with excess capacities to be able to handle additional demands. Hence, there is a gap introduced between the nominal operating and the design variables, as the auxiliary variables obtain higher values.

We optimize a distribution network of the same size and specifications, but we aggregate the system in one region. We provide parametric values of the excess demands ϵ, and demonstrate the effect on the supply chain's profitability and economic survivability (**Figure ??**). The profitability

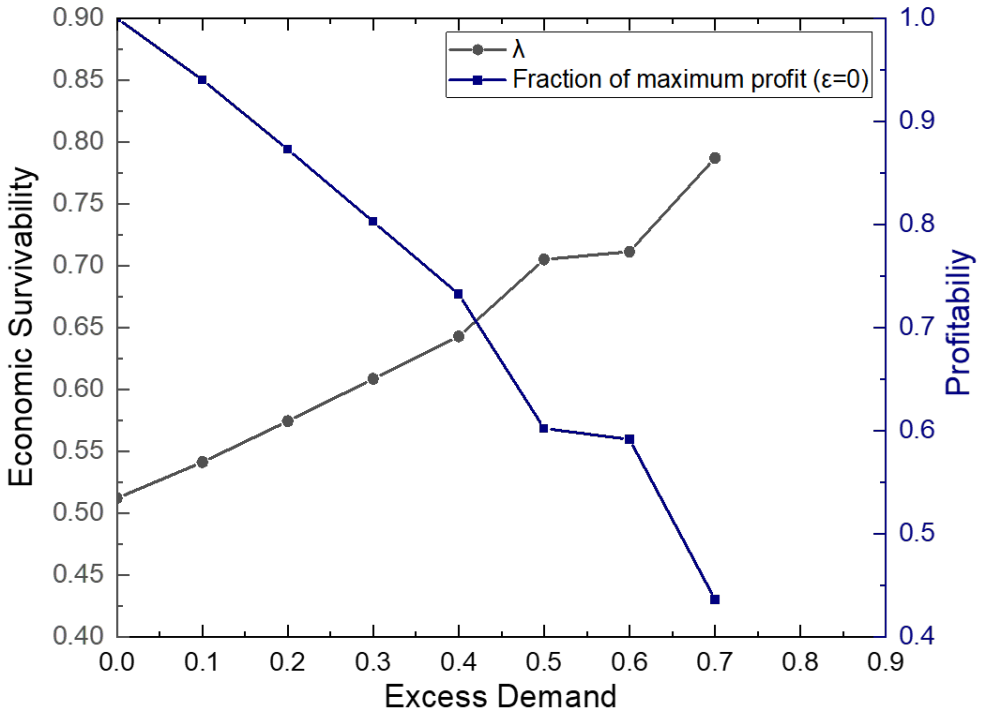

Figure 5.5: Effect of overdesigning for additional demands ϵ on system profitability and survivability.

is calculated as the fraction of the profit of the ϵ-overdesigned network to the maximum potential profit (no overdesign, $\epsilon = 0$). From the igure, we can see that the effect of overdesigning the system is monotonous. The total profitability and economic survivability are decreasing, as we impose the system to be more conservative. The fraction of demand reduction, that the system can handle cost-wise λ is increasing. For example, in the nominal design scenario $(\epsilon = 0)$, the demands can decrease almost by 50% and the system will yield positive profit. Also, in this case the profit is the maximum possible. When the system is designed to satisfy 40% excess demands $\epsilon = 0.4$, the supply chain will be still profitable only for 36% nominal demand reduction $(\lambda = 0.64)$. However, in the expense of total profit, we can ensure that the supply chain could satisfy excess demands in the benefit of social welfare. As a result, increasing ES (or, decreasing λ_t) will make a supply chain network less conservative and, at the same time, less robust. This expands the previous definitions of survivability, which considered survivability only as an extreme case of resilience

and system robustness. The economic survivability allows us to consider the full spectrum of economic performance of supply chains.

For the case of $\epsilon = 0$, the least-overdesigned network is comprised of 6 total facilities and 9 selected transportation links. For ϵ values from 0.1 to 0.4, the configuration remains unchanged with 6 selected facilities and 12 installed connections to compensate in the event of increased demands. It is interesting that for these values the distribution of economic survivability and profitability is linear with respect to parameter ϵ. The network configuration remains the same but the installed maximum capacities of facilities and connections are increased, thereby increasing the capital cost. For ϵ between 0.5 and 0.7, the network configuration changes non-linearly due to changes in the fixed cost component and selection of distinct network configurations. For example, there are 7 total facilities and 13 connections selected for $\epsilon = 0.5$, 6 facilities and 12 connections selected for $\epsilon = 0.6$, and 7 facilities and 15 connections selected for $\epsilon = 0.7$.

In this part of the analysis, we consider ϵ values lower or equal to 0.7, because higher values of excess demands lead to infeasibility for the given problem. This is because of the lack of sufficient processing and storage facilities (which are upper-bounded).

The value of economic survivability is impacted by the economic parameters, namely the product selling prices, the fixed and the capital cost coefficients, and the unit operating costs. In the case of maximum profit, the total revenue (REV) is \$1,200, the total fixed cost ($\kappa_F\, FCT$) is \$129, the total capital cost ($\kappa_F\, CCT$) is \$324, and the total operating cost (OCT) is \$304. These yield a total profit (P) of \$433. This results in λ value of 0.51. Overall, we obtain a profit margin (i.e., the ratio of the net profit over the total revenue) of 36%.

The above result is obtained when the product price (p_m) is \$4 per ton. When we reduce the product price from \$4 to \$3 per ton but keep the total cost to be the same, we observe that λ increases from 0.51 to 0.78, thereby decreasing the economic survivability. If we increase the product price, on the other hand, from \$4 to \$5 per ton, λ decreases to 0.39, thereby increasing the economic survivability. Therefore, we observe a strong positive correlation between product price and the economic survivability.

We further analyze the effect of the relative capital intensity compared to the variable cost. The total cost is comprised of the total investment cost ($\kappa_F\, FCT + \kappa_F\, CCT$) as well as the operating cost (OCT). These terms appear both in the numerator and the denominator in Eq. 5.38. When we solve our case study problem for maximum profit, we found the investment cost to be 60% of the total investment and operating costs, and the value of λ is 0.51. If we enforce the same total cost with a different distribution of 75% investment cost and 25% operating cost, then we obtain a different λ value of 0.57. Therefore, higher investment requirement decreases the economic survivability. This indicates that capital-intensive industries may have lower economic survivability in the face of prolonged disruption events. However, similar industries with larger depreciated capital investments will have higher economic survivability.

Depending on the objective, the network configurations and facility allocations across the regions were different. These differences are due to the selection of facilities across different regions, as observed for Case 1 (maximum profit) and Case 3 (maximum local survivability). We observe a reduction in the total profitability for Case 3. This is because of a more balanced investment portfolio of the supply chain across the regions.

Based on the above results, we summarize our observations as follows:

1. ES can be an alternative performance metric to measure the economic performance of a supply chain under unexpected situations and disruptions that drastically shift the consumer demands.

2. ES can be used to analyze the break-even demand or as a prediction tool for future retrofit designs. Using ES, one can analyze the effect of different demand scenarios of changing demands, disrupted operations, and price forecasts.

3. Maximizing global economic survivability (ES) leads to higher profitability of the supply chain as a whole. Maximizing local economic survivability attempts to normalize and balance the investments on facilities and spanning connections in a more even fashion across multiple regions, in the expense of lower profit.

4. When a region has more production and storage capacities installed compared to its needs, and supplies it to other unequipped regions, it reduces the survivability of that region, while it increases the survivability of the dependent regions.

5. Economic survivability threshold greater than one means that a region is over-designed compared to the demands that it satisfies. It also entails, that its break-even demands are higher than the nominal demands it satisfies. This is because, additional facilities and installed capacities exist to satisfy product exports to other regions.

6. Depending on the initial superstructure's cost parameters, the resulting network may also result in more distributed configurations across the regions. However, maximizing the local survivability, the optimizer will try to balance the allocation of facilities and spanning connections across the regions.

5.4 Summary

Systemic shocks have a huge impact on supply chain profitability, operability and the capacity of distribution networks to maintain demand satisfaction. We introduced the concept of economic survivability as a measure of economic performance in the presence of sudden changes in demands. We defined economic survivability as the fractional change in demand from nominal value, beyond which a network is not anymore profitable. We observed that there is a relation between the economic survivability and the return-on-investment of a business or a supply chain. We then explored the effect of lock-downs and sudden restrictions on region-specific flow of goods within a multi-regional supply chain. We observed that maximizing global survivability and maximizing profitability are synonymous. However, to ensure the local survivability of the supply chain components at each region under regional lock-downs, one needs to balance the allocation of facilities and connections across multiple regions, which comes at a greater expense and reduced profitability. In the case of more balanced local survivability for all regions, the investment costs are distributed more evenly across multiple regions, along with dedicated facilities and connections. We studied the maximization of local survivability when the inter-regional supplies were

still allowed. In the event that the inter-regional supplies are also cut-off, it is easier to establish emergency connections, if every region has the facilities with required capacities to meet its own demands. If a region does not have its own facilities, there arises a need for establishing emergency and costly inter-regional supplies when a systemic shock arrives. Therefore, it is important to evenly allocate infrastructure to ensure the survivability of individual local regions that constitute the overall/global supply chain network. While this may reduce the profit, it ensures the economic sustainability of the overall supply chain in the long run.

6. CONCLUSIONS

In this dissertation, a framework was presented towards improving the sustainability, resilience, and survivability of interconnected networks with an emphasis on water-energy nexus (WEN) applications. The framework was utilized to analyze given WENs and optimally design new systems with the aforementioned targets embedded.

In Chapter 2, the interdependence of a nexus was analyzed via a graph-theoretic approach and a novel WEN diagram. The graphical optimization procedure provided with theoretical targets for minimum generation of regional networks for given grid supplies, and maximized grid supplies for given installed generating capacities. This lead to minimum utilization of resources. The graphical approach can be used as a technology screening tool to provide targets for aggregated analyses and easier superstructure-based optimal designs.

In Chapter 3, a superstructure-based optimization approach was followed to perform economic optimization and consider more complex phenomena affecting the sustainability of regional WENs. In the superstructure, all potential connections and intermediate sources are included, and from the solution of the MINLP model, the optimal combination of sources and connectivity is determined to satisfy the demands of consumers and the availability of resources. The model can handle explicitly contaminants concentrations and location-allocation of intermediate sources. The applicability of the model was demonstrated in a regional case studies.

In Chapter 4, the resilience analysis of a WEN was addressed. Minimum cost of resilience (MCOR) and operation-based resilience metrics were utilized to quantify operational and economic system performance against single-connectivity failures and identify critical connections. MCOR provides with the minimum additional infrastructure investment required to achieve a certain degree of resilience. Incorporation of resilience metrics in a multi-scenario optimization model lead to minimum overdesign and minimum MCOR. It was observed that grass-root resilient designs yielded lower MCOR than the retrofitting MCOR for the same system. The nexus interdependence impacts both the MCOR and the computational performance of the resilience-aware

design activity. Higher tolerance to connectivity disruptions either equips the nexus with excess capacities and connectivity, or increases the dependence from external grid supplies to satisfy the demands for all scenarios. The increased WEN investments are minimum compared to other heuristic-based resilience enhancement techniques, and lead to demand increase tolerance in the event of no disruptions. The resilience analysis was performed on a regional WEN in the state of Texas and showed that a minimum of 14.6% was required for fully immune infrastructure. It was observed that evenly distributing the capacities of the energy and water treatment facilities as much as possible is important for resilience achievement. This indicated that distributed manufacturing (vs. centralized large processing) is more favorable for the resilient design of supply chains.

In Chapter 5, the survivability of profit-driven supply chain networks was addressed. Economic survivability was defined and was used as an alternative profit objective to analyze and predict the performance of supply chains against demand disruptions. Maximizing ES led to solutions of maximum profit. The effect of geographical interdependence was explored, with different the results for maximum global and average local survivability. Maximum global ES did not differentiate across the different regions. On the other hand, maximizing local ES led to more balanced regional investments and facility allocations, but at the expense of total profit. Higher demands satisfied led to lower economic survivability under demand decreases, so the decision-makers should balance the trade-offs between survivability and excess demand satisfaction by thoroughly assessing the probability of positive and negative demand fluctuations. The developed framework and methods can be applied for grass-root and retrofitting cases and were demonstrated in a range of illustrative examples and regional case studies.

6.1 Directions for Future Work

6.1.1 Resilience Analysis Expansion for Facility Disruptions

The proposed resilience-aware framework presented in 4 can be extended to consider failures of whole generating facilities. In this case, the disruption scenario set S will correspond to the potential facilities instead of the potential connections, in the example $S = K$, and the multi-

scenario formulation will reduce in size.

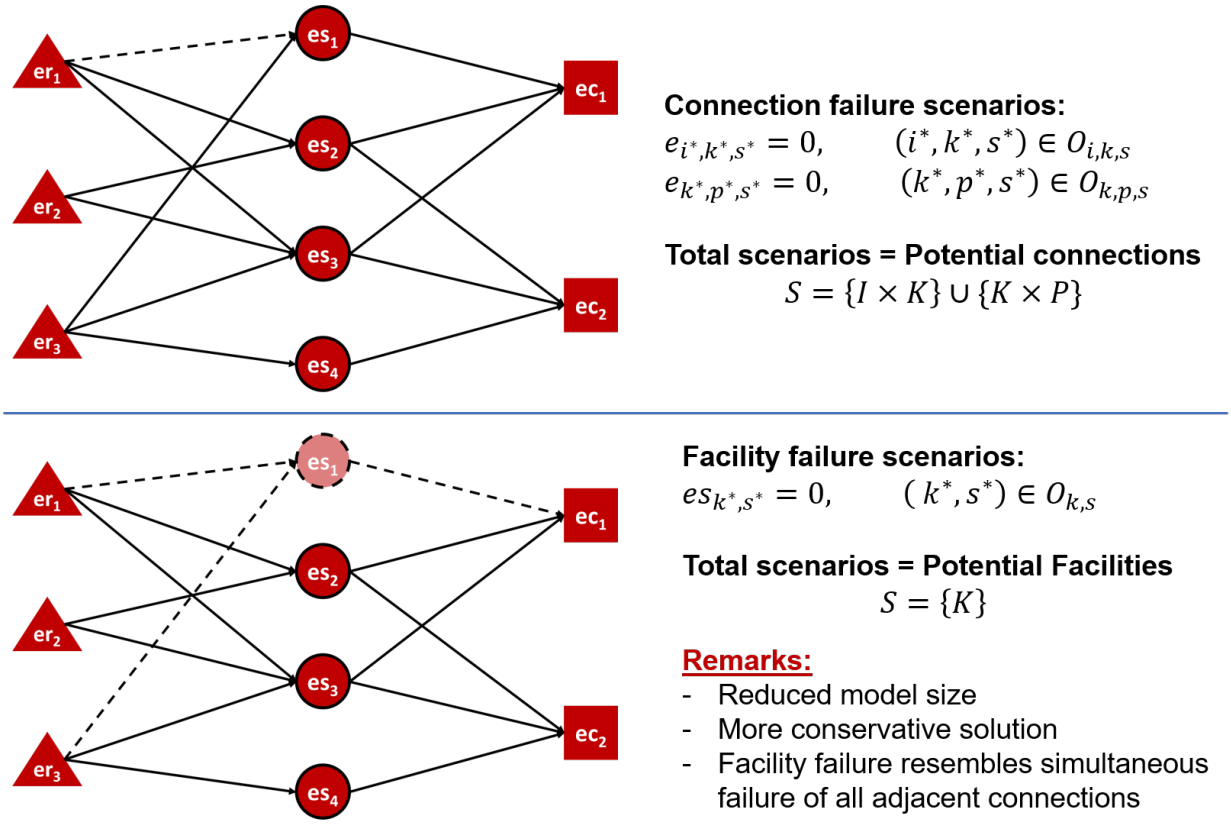

Figure 6.1: Comparison of resilience-aware design between tolerance against connectivity and facility failures. Demonstration and disruption scenario sets for energy subnetwork.

The imposing constraint of disrupted operation will need to be modified for the operating generation of disrupted facilities to obtain zero values, instead of the zero flows of disrupted connections in Chapter 4.

$$e_{k^*,s^*} = 0, \qquad (k^*,\ s^*) \in O^{es}_{k,s} \tag{6.1}$$

It will be worth investigating in future to see the implications of facility disruptions on the resulting network configurations, the resilience metrics and MCOR. Furthermore, the comparison between connectivity-resilience and facility-resilience should be performed to compare the degree

of over-design and cost increase. A facility failure can be viewed as the simultaneous connectivity failures of all its the adjacent connections. Finally, the model is expected to suffer less from the scenario expansion in terms of computation times, due to the reduced number of scenarios. This may also lead to efficient solution strategies for the hard-scaling connectivity resilience, by using information from the faster-obtained facility-resilience solutions.

6.1.2 Holistic framework for all disruption events

while investigating the trade-offs between cost and tolerance to connectivity failures in Chapter 4, it was observed that increased tolerance to connectivity disruptions incurred an increased cost (MCOR), and accounting for connectivity disruptions resulted in a higher (calculated) tolerance against demand increases (ξ). In Chapter 5, the trade-offs between demand decrease threshold leading to positive profit (ES) and the over-design for excess demands (ϵ) were explored. In future endeavors, the proposed resilience- and survivability-aware analyses presented in Chapters 4 and 5, can be combined to a holistic framework to include all potential disruption events (demand decreases, connectivity disruptions, demand increases).

To account for all potential disruption events, the modeling framework presented in Chapter 4 can be extended to explicitly account for nominal operation, connectivity disruptions and demand increase scenarios (Figure 6.2). The scenario set $s \in S$ can be expanded and split into connectivity failures scenarios S_C, nominal operation scenario S_{nom}, and increased demand scenario S_ϵ. The corresponding scenario sets are demonstrated in Figure 6.2. All the operating balances will be expanded for all disruption scenarios S as in Chapter 4. The demand satisfaction constraints will be written separately for the different disruption scenarios. For connectivity disruption scenarios $s \in S_C$, the same constraint as in Chapter 4 is used, with $\theta_{p,s}$ fraction of the demands satisfied. For the nominal operation scenario S_{nom} all the demands are satisfied. Finally, for the demand increase

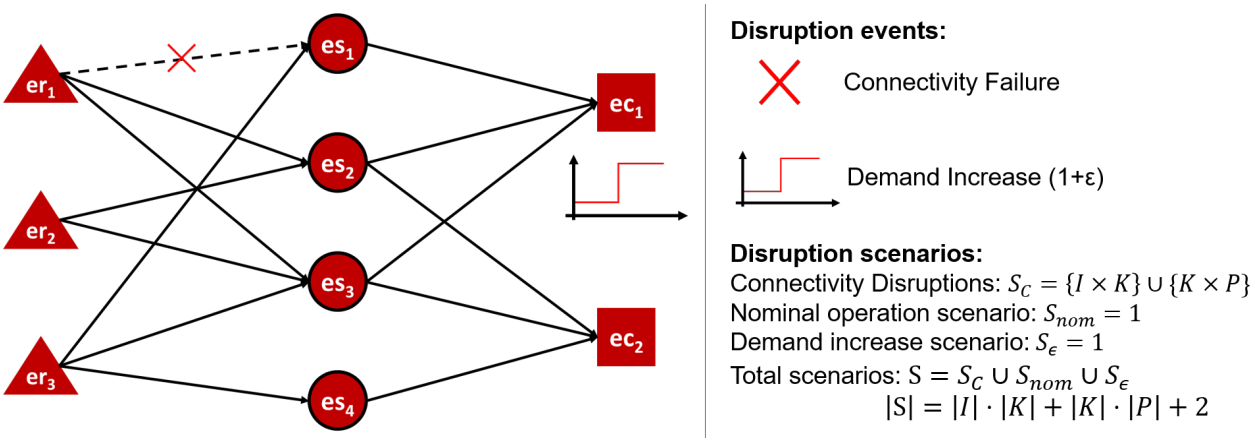

Figure 6.2: Holistic Framework for all potential disruption types along with nominal operation. The scenario set is expanded to include nominal operation and demand increase scenarios.

scenario S_ϵ additional demands $(1+\epsilon)$ will be satisfied.

$$\sum_k e_{k,p,s} = ecd_p \qquad \forall\, p \in P,\ s \in S_{nom} \tag{6.2}$$

$$\sum_k e_{k,p,s} = \theta^e_{p,s} \cdot ecd_p \qquad \forall\, p \in P,\ s \in S_C \tag{6.3}$$

$$\sum_k e_{k,p,s} = (1+\epsilon) \cdot ecd_p \qquad \forall\, p \in P,\ s \in S_\epsilon \tag{6.4}$$

The problem could be posed as a multi-objective optimization, which depending on the values of objective coefficients, would reduce to nominal design (Base-case), resilient against disruptions case, and tolerance to demand increases case. The first objective is minimizing MCOR, where the base case cost (BC) is calculated apriori to normalize the total cost of this formulation. The total cost (TC) is scenario-independent and is comprised of the fixed and capital investments (FC, DC), and the operation cost calculated at the nominal operation scenario (OC_{nom}). The second objective captures penalty cost due to demand violation during connectivity disruptions (S_C). Finally, the third objective corresponds to lost profit in the event of demand increases, so ϵ is maximized. Depending on the penalty and lost profit coefficients ($\lambda_C, \lambda_\epsilon$) and multi-objective coefficients the model will focus on a combination of minimum nominal design cost, performance against connec-

tivity disruptions, and demand increase tolerance.

$$\min = \alpha_1 \cdot MCOR + \alpha_2 \cdot PC + \alpha_3 \cdot LP \tag{6.5}$$

$$\alpha_1 + \alpha_2 + \alpha_3 = 1 \tag{6.6}$$

$$MCOR = \frac{TC - BC}{BC} \tag{6.7}$$

$$TC = FC + DC + OC_{nom} \qquad FC = f_1(z_{i,k}, z_k^{es}, ...), DC = f_2(cap_{i,k}, cap_k^{es}, ...) \tag{6.8}$$

$$PC = \frac{\lambda_C}{|S_C|} \cdot \sum_{s \in S_C} \frac{1}{|P|} \sum_{p \in P} (1 - \theta_{p,s}) \tag{6.9}$$

$$LP = -\lambda_\epsilon \cdot \epsilon \tag{6.10}$$

Lastly, to account for demand decreases for all potential disruption events, the multi-objective optimization can be modified to maximize the economic survivability (ES), by minimizing the modified demand threshold λ. The first objective is the modified economic survivability to consider connectivity disruptions. The fixed and capital investments (FC, DC) are common across all scenarios and for all expressions. The revenue and operating cost (REV_{nom}, OC_{nom}) are calculated for the nominal operating scenario (S_{nom}) and the penalty cost (PC_C) as a function of the connectivity disruption scenarios (S_C). The second objective is the economic survivability threshold in the event of demand increases (λ_ϵ). The revenue and the operating cost are calculated based on the S_ϵ operating variables. The two objectives are normalized by the probabilities of nominal and increased demands (ρ_{nom} and ρ_ϵ).

$$\min z = \rho_{nom} \cdot \lambda + \rho_\epsilon \cdot \lambda_\epsilon \tag{6.11}$$

$$\min = \rho_{nom} + \rho_{epsilon} \tag{6.12}$$

$$\lambda = \frac{FC + DC}{REV_{nom} - OC_{nom} - PC_C} \tag{6.13}$$

$$\lambda_\epsilon = \frac{FC + DC}{REV_\epsilon - OC_\epsilon} \tag{6.14}$$

It is expected that this expanded framework will successfully consider all potential systemic shocks

and balance the trade-offs given the probabilities of occurrence and the penalty coefficients provided by the decision maker.

6.2 List of Publications

1. Tsolas, S. D., Karim, M. N., & Hasan, M. M. F. (2018). Optimization of water-energy nexus: A network representation-based graphical approach. Applied Energy, 224, 230-250.

2. Tsolas, S. D., Karim, M. N., & Hasan, M. M. F. (2019). Systematic Design, Analysis and Optimization of Water-Energy Nexus. In Computer Aided Chemical Engineering, vol. 47, pp. 227-232. Elsevier

3. Tsolas, S. D. & Hasan, M. M. F. (2021). Survivability-Aware Design and Optimization of Distributed Supply Chain Networks in the Post COVID-19 Era. *Journal of Advanced Manufacturing and Processing.*

4. Tsolas, S. D. & Hasan, M. M. F. (2021). Resilience-Aware Design of Interconnected Supply Chain Networks with Application to Water-Energy Nexus. *Submitted for Publication.*

REFERENCES

[1] U.S. Energy Information Administration (EIA), "Electicity analysis & projections." https://www.eia.gov/electricity/data/eia860/. Accessed: May 2021.

[2] National Renewable Energy Laboratory (NREL), "Atb electricity data overview." https://atb.nrel.gov/electricity/2020/. Accessed: May 2021.

[3] J. Arroyo and S. Shirazi, "Cost of brackish groundwater desalination in texas," *Texas Water Development Board*, pp. 1–7, 2012.

[4] C. S. Rogers, *Economic costs of conventional surface-water treatment: A case study of the Mcallen Northwest Facility*. PhD thesis, Texas A & M University, 2010.

[5] International Energy Agency (IEA), "Data and statistics." https://www.iea.org/statistics/statisticssearch/report/?country=SPAIN&product=Balances&year=2013. Accessed: June 2017.

[6] Food and Agriculture Organization of the United Nations (FAO), "Aquastat database." http://www.fao.org/nr/water/aquastat/data/query/. Accessed: June 2017.

[7] P. Palomar and I. Losada, "Desalination in spain: recent developments and recommendations," *Desalination*, vol. 255, no. 1-3, pp. 97–106, 2010.

[8] S. D. Tsolas, M. N. Karim, and M. M. F. Hasan, "Optimization of water-energy nexus: A network representation-based graphical approach," *Applied energy*, vol. 224, pp. 230–250, 2018.

[9] S. Tsolas, M. N. Karim, and M. M. F. Hasan, "Systematic design, analysis and optimization of water-energy nexus," in *Computer Aided Chemical Engineering*, vol. 47, pp. 227–232, Elsevier, 2019.

[10] S. D. Tsolas and M. M. F. Hasan, "Survivability-aware design and optimization of distributed supply chain networks in the post covid-19 era," *Journal of Advanced Manufacturing and Processing*, vol. n/a, no. n/a, p. e10098.

[11] U. DOE, "The water-energy nexus: Challenges and opportunities," *Washington, DC: US DOE. http://energy. gov/downloads/water-energy-nexus-challenges-and-opportunities*, 2014.

[12] A. Boretti and L. Rosa, "Reassessing the projections of the world water development report," *npj Clean Water*, vol. 2, no. 1, pp. 1–6, 2019.

[13] U. E. I. A. (EIA), "Annual energy outlook 2020," *U.S. Department of Energy.https://www.eia.gov/outlooks/aeo/*, 2020.

[14] D. Quagliarotti, "World water day 2012.," *Global Environment*, vol. 4, no. 7-8, pp. 156–163, 2011.

[15] F. Birol, "The outlook for energy demand to 2010," *International Journal of Global Energy Issues*, vol. 11, no. 1/2/3/4, pp. 51–57, 1998.

[16] W. N. Lubega and A. M. Farid, "A reference system architecture for the energy–water nexus," *IEEE Systems Journal*, vol. 10, no. 1, pp. 106–116, 2016.

[17] A. Sieminski *et al.*, "International energy outlook," *Energy information administration (EIA)*, vol. 18, 2014.

[18] S. Kenway, P. Lant, A. Priestley, and P. Daniels, "The connection between water and energy in cities: a review," *Water Science and Technology*, vol. 63, no. 9, pp. 1983–1990, 2011.

[19] A. S. Stillwell, C. W. King, M. E. Webber, I. J. Duncan, and A. Hardberger, "The energy-water nexus in texas," *Ecology and Society*, vol. 16, no. 1, 2011.

[20] F. Kahrl and D. Roland-Holst, "China's water–energy nexus," *Water Policy*, vol. 10, no. S1, pp. 51–65, 2008.

[21] A. Siddiqi and L. D. Anadon, "The water–energy nexus in middle east and north africa," *Energy policy*, vol. 39, no. 8, pp. 4529–4540, 2011.

[22] L. Hardy, A. Garrido, and L. Juana, "Evaluation of spain's water-energy nexus," *International Journal of Water Resources Development*, vol. 28, no. 1, pp. 151–170, 2012.

[23] A. M. Hamiche, A. B. Stambouli, and S. Flazi, "A review of the water-energy nexus," *Renewable and Sustainable Energy Reviews*, vol. 65, pp. 319–331, 2016.

[24] D. J. Garcia and F. You, "The water-energy-food nexus and process systems engineering: a new focus," *Computers & Chemical Engineering*, vol. 91, pp. 49–67, 2016.

[25] J. Dai, S. Wu, G. Han, J. Weinberg, X. Xie, X. Wu, X. Song, B. Jia, W. Xue, and Q. Yang, "Water-energy nexus: A review of methods and tools for macro-assessment," *Applied Energy*, vol. 210, pp. 393–408, 2018.

[26] N. Komendantova, D. Kroos, D. Schweitzer, C. Leroy, E. Andreini, B. Baltasar, T. Boston, M. Keršnik, K. Botbaev, J. Cohen, *et al.*, *Protecting Electricity Networks from Natural Hazards*. Organization for Security and Cooperation in Europe (OSCE), 2016.

[27] P. Svitek, "Gov. Greg Abbott orders texas bars to close again and restaurants to reduce to 50% occupancy as coronavirus spreads," *Texas Tribune, June 26*, pp. https://www.texastribune.org/2020/06/26/texas–bars–restaurants–coronavirus–greg–abbott, 2020.

[28] M. Nicola, Z. Alsafi, C. Sohrabi, A. Kerwan, A. Al-Jabir, C. Iosifidis, M. Agha, and R. Agha, "The socio-economic implications of the coronavirus pandemic (COVID-19): A review," *International journal of surgery (London, England)*, vol. 78, p. 185, 2020.

[29] H. J. Song, J. Yeon, and S. Lee, "Impact of the COVID-19 pandemic: Evidence from the us restaurant industry," *International Journal of Hospitality Management*, vol. 92, p. 102702, 2020.

[30] A. Kumar, S. Luthra, S. K. Mangla, and Y. Kazançoğlu, "Covid-19 impact on sustainable production and operations management," *Sustainable Operations and Computers*, vol. 1, pp. 1–7, 2020.

[31] W. C. Shih, "Global supply chains in a post-pandemic world," *Harvard Business Review*, vol. Sep. - Oct., pp. hbr.org/2020/09/global–supply–chains–in–a–post–pandemic–world, 2020.

[32] "COVID-19 and supply-chain recovery: Planning for the future," pp. mckinsey.com/business–functions/operations/our–insights/covid–19–and–supply–chain–recovery–planning–for–the–future, 2020.

[33] L. Yang, I. E. Grossmann, and J. Manno, "Optimization models for shale gas water management," *AIChE Journal*, vol. 60, no. 10, pp. 3490–3501, 2014.

[34] L. Yang, I. E. Grossmann, M. S. Mauter, and R. M. Dilmore, "Investment optimization model for freshwater acquisition and wastewater handling in shale gas production," *AIChE Journal*, vol. 61, no. 6, pp. 1770–1782, 2015.

[35] J. Gao and F. You, "Optimal design and operations of supply chain networks for water management in shale gas production: Milfp model and algorithms for the water-energy nexus," *AIChE Journal*, vol. 61, no. 4, pp. 1184–1208, 2015.

[36] L. F. Lira-Barragán, J. M. Ponce-Ortega, G. Guillén-Gosálbez, and M. M. El-Halwagi, "Optimal water management under uncertainty for shale gas production," *Industrial & Engineering Chemistry Research*, vol. 55, no. 5, pp. 1322–1335, 2016.

[37] T. V. Bartholomew and M. S. Mauter, "Multiobjective optimization model for minimizing cost and environmental impact in shale gas water and wastewater management," *ACS Sustainable Chemistry & Engineering*, vol. 4, no. 7, pp. 3728–3735, 2016.

[38] L. F. Lira-Barragán, J. M. Ponce-Ortega, M. Serna-González, and M. M. El-Halwagi, "Optimal reuse of flowback wastewater in hydraulic fracturing including seasonal and environmental constraints," *AIChE Journal*, vol. 62, no. 5, pp. 1634–1645, 2016.

[39] O. J. Guerra, A. J. Calderón, L. G. Papageorgiou, J. J. Siirola, and G. V. Reklaitis, "An optimization framework for the integration of water management and shale gas supply chain design," *Computers & Chemical Engineering*, vol. 92, pp. 230–255, 2016.

[40] M. G. Drouven and I. E. Grossmann, "Optimization models for impaired water management in active shale gas development areas," *Journal of Petroleum Science and Engineering*, vol. 156, pp. 983–995, 2017.

[41] A. R. Bartman, P. D. Christofides, and Y. Cohen, "Nonlinear model-based control of an experimental reverse-osmosis water desalination system," *Industrial & Engineering Chemistry Research*, vol. 48, no. 13, pp. 6126–6136, 2009.

[42] A. Zhu, P. D. Christofides, and Y. Cohen, "Energy consumption optimization of reverse osmosis membrane water desalination subject to feed salinity fluctuation," *Industrial & Engineering Chemistry Research*, vol. 48, no. 21, pp. 9581–9589, 2009.

[43] A. Ghobeity and A. Mitsos, "Optimal time-dependent operation of seawater reverse osmosis," *Desalination*, vol. 263, no. 1-3, pp. 76–88, 2010.

[44] K. H. Mistry, A. Mitsos, and J. H. Lienhard, "Optimal operating conditions and configurations for humidification–dehumidification desalination cycles," *International Journal of Thermal Sciences*, vol. 50, no. 5, pp. 779–789, 2011.

[45] T. H. Dahdah and A. Mitsos, "Structural optimization of seawater desalination: I. a flexible superstructure and novel med–msf configurations," *Desalination*, vol. 344, pp. 252–265, 2014.

[46] T. H. Dahdah and A. Mitsos, "Structural optimization of seawater desalination: Ii novel med–msf–tvc configurations," *Desalination*, vol. 344, pp. 219–227, 2014.

[47] M. Li, "Analysis and optimization of pressure retarded osmosis for power generation," *AIChE Journal*, vol. 61, no. 4, pp. 1233–1241, 2015.

[48] J. Gong and F. You, "Global optimization for sustainable design and synthesis of algae processing network for co2 mitigation and biofuel production using life cycle optimization," *AIChE Journal*, vol. 60, no. 9, pp. 3195–3210, 2014.

[49] C. F. Murphy and D. T. Allen, "Energy-water nexus for mass cultivation of algae," *environmental science & technology*, vol. 45, no. 13, pp. 5861–5868, 2011.

[50] S. Adham, A. Hussain, J. M. Matar, R. Dores, and A. Janson, "Application of membrane distillation for desalting brines from thermal desalination plants," *Desalination*, vol. 314, pp. 101–108, 2013.

[51] E. Gençer and R. Agrawal, "Strategy to synthesize integrated solar energy coproduction processes with optimal process intensification. case study: Efficient solar thermal hydrogen production," *Computers & Chemical Engineering*, vol. 105, pp. 328–347, 2017.

[52] G. M. Zak, A. Ghobeity, M. H. Sharqawy, and A. Mitsos, "A review of hybrid desalination systems for co-production of power and water: analyses, methods, and considerations," *Desalination and Water Treatment*, vol. 51, no. 28-30, pp. 5381–5401, 2013.

[53] R. Mukherjee, R. González-Bravo, F. Nápoles-Rivera, P. Linke, J. M. Ponce-Ortega, and M. M. El-Halwagi, "Optimal design of water distribution networks with incorporation of uncertainties and energy nexus," *Process Integration and Optimization for Sustainability*, vol. 1, no. 4, pp. 275–292, 2017.

[54] B. Linnhoff and E. Hindmarsh, "The pinch design method for heat exchanger networks," *Chemical Engineering Science*, vol. 38, no. 5, pp. 745–763, 1983.

[55] M. M. El-Halwagi and V. Manousiouthakis, "Synthesis of mass exchange networks," *AIChE Journal*, vol. 35, no. 8, pp. 1233–1244, 1989.

[56] M. M. El-Halwagi, F. Gabriel, and D. Harell, "Rigorous graphical targeting for resource conservation via material recycle/reuse networks," *Industrial & Engineering Chemistry Research*, vol. 42, no. 19, pp. 4319–4328, 2003.

[57] D. C. Y. Foo, "State-of-the-art review of pinch analysis techniques for water network synthesis," *Industrial & Engineering Chemistry Research*, vol. 48, no. 11, pp. 5125–5159, 2009.

[58] S. A. Papoulias and I. E. Grossmann, "A structural optimization approach in process synthesis—ii: Heat recovery networks," *Computers & Chemical Engineering*, vol. 7, no. 6, pp. 707–721, 1983.

[59] Y. Chen, I. E. Grossmann, and D. C. Miller, "Computational strategies for large-scale milp transshipment models for heat exchanger network synthesis," *Computers & Chemical Engineering*, vol. 82, pp. 68–83, 2015.

[60] I. M. L. Chew, R. Tan, D. K. S. Ng, D. C. Y. Foo, T. Majozi, and J. Gouws, "Synthesis of direct and indirect interplant water network," *Industrial & engineering chemistry research*, vol. 47, no. 23, pp. 9485–9496, 2008.

[61] E. M. Lovelady and M. M. El-Halwagi, "Design and integration of eco-industrial parks for managing water resources," *Environmental Progress & Sustainable Energy: An Official Publication of the American Institute of Chemical Engineers*, vol. 28, no. 2, pp. 265–272, 2009.

[62] F. Nápoles-Rivera, M. Serna-González, M. M. El-Halwagi, and J. M. Ponce-Ortega, "Sustainable water management for macroscopic systems," *Journal of cleaner production*, vol. 47, pp. 102–117, 2013.

[63] S. K. Bishnu, P. Linke, S. Y. Alnouri, and M. El-Halwagi, "Multiperiod planning of optimal industrial city direct water reuse networks," *Industrial & Engineering Chemistry Research*, vol. 53, no. 21, pp. 8844–8865, 2014.

[64] S. Y. Alnouri, P. Linke, and M. El-Halwagi, "A synthesis approach for industrial city water reuse networks considering central and distributed treatment systems," *Journal of Cleaner Production*, vol. 89, pp. 231–250, 2015.

[65] S. Y. Alnouri, P. Linke, and M. M. El-Halwagi, "Accounting for central and distributed zero liquid discharge options in interplant water network design," *Journal of cleaner production*, vol. 171, pp. 644–661, 2018.

[66] R. C. Baliban, J. A. Elia, and C. A. Floudas, "Simultaneous process synthesis, heat, power, and water integration of thermochemical hybrid biomass, coal, and natural gas facilities," *Computers & Chemical Engineering*, vol. 37, pp. 297–327, 2012.

[67] K. J. Gabriel, P. Linke, A. Jiménez-Gutiérrez, D. Y. Martínez, M. Noureldin, and M. M. El-Halwagi, "Targeting of the water-energy nexus in gas-to-liquid processes: A comparison of syngas technologies," *Industrial & Engineering Chemistry Research*, vol. 53, no. 17, pp. 7087–7102, 2014.

[68] J. Tovar-Facio, L. F. Lira-Barragán, F. Nápoles-Rivera, H. S. Bamufleh, J. M. Ponce-Ortega, and M. M. El-Halwagi, "Optimal synthesis of refinery property-based water networks with electrocoagulation treatment systems," *ACS Sustainable Chemistry & Engineering*, vol. 4, no. 1, pp. 147–158, 2015.

[69] J. M. Núñez-López, E. Rubio-Castro, M. M. El-Halwagi, and J. M. Ponce-Ortega, "Optimal design of total integrated residential complexes involving water-energy-waste nexus," *Clean Technologies and Environmental Policy*, vol. 20, no. 5, pp. 1061–1085, 2018.

[70] J. M. Núñez-López, E. Villicaña-García, B. Cansino-Loeza, E. Rubio-Castro, and J. M. Ponce-Ortega, "Involving acceptability in the optimal design of total integrated residential complexes involving the water-energy-waste nexus," *ACS Sustainable Chemistry & Engineering*, vol. 6, no. 6, pp. 7390–7402, 2018.

[71] R. Segurado, M. Costa, N. Duić, and M. G. Carvalho, "Integrated analysis of energy and water supply in islands. case study of s. vicente, cape verde," *Energy*, vol. 92, pp. 639–648, 2015.

[72] X. Zhang and V. V. Vesselinov, "Energy-water nexus: Balancing the tradeoffs between two-level decision makers," *Applied energy*, vol. 183, pp. 77–87, 2016.

[73] K. J. Gabriel, M. M. El-Halwagi, and P. Linke, "Optimization across the water–energy nexus for integrating heat, power, and water for industrial processes, coupled with hybrid thermal-membrane desalination," *Industrial & Engineering Chemistry Research*, vol. 55, no. 12, pp. 3442–3466, 2016.

[74] S. Chen and B. Chen, "Urban energy–water nexus: A network perspective," *Applied energy*, vol. 184, pp. 905–914, 2016.

[75] Y. Saif and A. Almansoori, "A capacity expansion planning model for integrated water desalination and power supply chain problem," *Energy conversion and management*, vol. 122, pp. 462–476, 2016.

[76] S. J. Pereira-Cardenal, B. Mo, A. Gjelsvik, N. D. Riegels, K. Arnbjerg-Nielsen, and P. Bauer-Gottwein, "Joint optimization of regional water-power systems," *Advances in water resources*, vol. 92, pp. 200–207, 2016.

[77] R. González-Bravo, F. Nápoles-Rivera, J. M. Ponce-Ortega, and M. M. El-Halwagi, "Multi-objective optimization of dual-purpose power plants and water distribution networks," *ACS Sustainable Chemistry & Engineering*, vol. 4, no. 12, pp. 6852–6866, 2016.

[78] Y.-C. Tsai, C.-P. Chiu, F.-K. Ko, T.-C. Chen, and J.-T. Yang, "Desalination plants and renewables combined to solve power and water issues," *Energy*, vol. 113, pp. 1018–1030, 2016.

[79] Y.-C. Tsai, Y.-K. Chan, F.-K. Ko, and J.-T. Yang, "Integrated operation of renewable energy sources and water resources," *Energy Conversion and Management*, vol. 160, pp. 439–454, 2018.

[80] P.-C. Chen, V. Alvarado, and S.-C. Hsu, "Water energy nexus in city and hinterlands: Multi-regional physical input-output analysis for hong kong and south china," *Applied energy*, vol. 225, pp. 986–997, 2018.

[81] R. Payet-Burin, F. Bertoni, C. Davidsen, and P. Bauer-Gottwein, "Optimization of regional water-power systems under cooling constraints and climate change," *Energy*, vol. 155, pp. 484–494, 2018.

[82] M. Y. L. P. Hang, E. Martinez-Hernandez, M. Leach, and A. Yang, "Designing integrated local production systems: a study on the food-energy-water nexus," *Journal of Cleaner Production*, vol. 135, pp. 1065–1084, 2016.

[83] X. Zhang and V. V. Vesselinov, "Integrated modeling approach for optimal management of water, energy and food security nexus," *Advances in Water Resources*, vol. 101, pp. 1–10, 2017.

[84] N. Bieber, J. H. Ker, X. Wang, C. Triantafyllidis, K. H. van Dam, R. H. Koppelaar, and N. Shah, "Sustainable planning of the energy-water-food nexus using decision making tools," *Energy Policy*, vol. 113, pp. 584–607, 2018.

[85] J. Gao, X. Xu, G. Cao, Y. Ermoliev, T. Ermolieva, and E. Rovenskaya, "Optimizing regional food and energy production under limited water availability through integrated modeling," *Sustainability*, vol. 10, no. 6, p. 1689, 2018.

[86] A. M. Mroue, R. H. Mohtar, E. N. Pistikopoulos, and M. T. Holtzapple, "Energy portfolio assessment tool (epat): Sustainable energy planning using the wef nexus approach–texas case," *Science of the Total Environment*, vol. 648, pp. 1649–1664, 2019.

[87] Y. Nie, S. Avraamidou, J. Li, X. Xiao, and E. N. Pistikopoulos, "Land use modeling and optimization based on food-energy-water nexus: a case study on crop-livestock systems," in *Computer Aided Chemical Engineering*, vol. 44, pp. 1939–1944, Elsevier, 2018.

[88] Y. Nie, S. Avraamidou, X. Xiao, E. N. Pistikopoulos, J. Li, Y. Zeng, F. Song, J. Yu, and M. Zhu, "A food-energy-water nexus approach for land use optimization," *Science of The Total Environment*, vol. 659, pp. 7–19, 2019.

[89] M. Bruneau, S. E. Chang, R. T. Eguchi, G. C. Lee, T. D. O'Rourke, A. M. Reinhorn, M. Shinozuka, K. Tierney, W. A. Wallace, and D. Von Winterfeldt, "A framework to quantitatively

assess and enhance the seismic resilience of communities," *Earthquake spectra*, vol. 19, no. 4, pp. 733–752, 2003.

[90] M. M. El-Halwagi, D. Sengupta, E. N. Pistikopoulos, J. Sammons, F. Eljack, and M.-K. Kazi, "Disaster-resilient design of manufacturing facilities through process integration: Principal strategies, perspectives, and research challenges," *Frontiers in Sustainability*, vol. 1, p. 8, 2020.

[91] W. Hynes, B. Trump, P. Love, and I. Linkov, "Bouncing forward: a resilience approach to dealing with COVID-19 and future systemic shocks," *Environment Systems and Decisions*, pp. 1–11, 2020.

[92] M. S. Golan, L. H. Jernegan, and I. Linkov, "Trends and applications of resilience analytics in supply chain modeling: systematic literature review in the context of the covid-19 pandemic," *Environment Systems & Decisions*, p. 1, 2020.

[93] D. Ivanov and A. Das, "Coronavirus (COVID-19/SARS-CoV-2) and supply chain resilience: A research note," *International Journal of Integrated Supply Management*, vol. 13, no. 1, pp. 90–102, 2020.

[94] M. G. Richards, D. Hastings, D. Rhodes, and A. Weigel, "Defining survivability for engineering systems," in *5th Conference on Systems Engineering Research, Hoboken, NJ*, Citeseer, 2007.

[95] D. B. Atkinson, P. Blatt, L. Mahood, and D. W. Voyls, "Design of fighter aircraft for combat survivability," *Sae Transactions*, pp. 2338–2353, 1969.

[96] R. Ball and D. Atkinson, "A history of the survivability design of military aircraft," in *36th Structures, Structural Dynamics and Materials Conference*, p. 1421, 1995.

[97] V. Venkatasubramanian, S. Katare, P. R. Patkar, and F.-p. Mu, "Spontaneous emergence of complex optimal networks through evolutionary adaptation," *Computers & chemical engineering*, vol. 28, no. 9, pp. 1789–1798, 2004.

[98] H. Thadakamaila, U. N. Raghavan, S. Kumara, and R. Albert, "Survivability of multiagent-based supply networks: a topological perspect," *IEEE Intelligent Systems*, vol. 19, no. 5, pp. 24–31, 2004.

[99] D. Ivanov and A. Dolgui, "Viability of intertwined supply networks: extending the supply chain resilience angles towards survivability. a position paper motivated by COVID-19 outbreak," *International Journal of Production Research*, vol. 58, no. 10, pp. 2904–2915, 2020.

[100] M. Sharma, S. Luthra, S. Joshi, and A. Kumar, "Developing a framework for enhancing survivability of sustainable supply chains during and post-COVID-19 pandemic," *International Journal of Logistics Research and Applications*, pp. 1–21, 2020.

[101] D. J. Watts and S. H. Strogatz, "Collective dynamics of 'small-world'networks," *nature*, vol. 393, no. 6684, p. 440, 1998.

[102] V. Latora and M. Marchiori, "Efficient behavior of small-world networks," *Physical review letters*, vol. 87, no. 19, p. 198701, 2001.

[103] A. E. Motter and Y.-C. Lai, "Cascade-based attacks on complex networks," *Physical Review E*, vol. 66, no. 6, p. 065102, 2002.

[104] R. Albert, I. Albert, and G. L. Nakarado, "Structural vulnerability of the north american power grid," *Physical review E*, vol. 69, no. 2, p. 025103, 2004.

[105] R. Kinney, P. Crucitti, R. Albert, and V. Latora, "Modeling cascading failures in the north american power grid," *The European Physical Journal B-Condensed Matter and Complex Systems*, vol. 46, no. 1, pp. 101–107, 2005.

[106] D. Centola, V. M. Eguíluz, and M. W. Macy, "Cascade dynamics of complex propagation," *Physica A: Statistical Mechanics and its Applications*, vol. 374, no. 1, pp. 449–456, 2007.

[107] S. Pahwa, A. Hodges, C. Scoglio, and S. Wood, "Topological analysis of the power grid and mitigation strategies against cascading failures," in *2010 IEEE International Systems Conference*, pp. 272–276, IEEE, 2010.

[108] A. Yazdani and P. Jeffrey, "Applying network theory to quantify the redundancy and structural robustness of water distribution systems," *Journal of Water Resources Planning and Management*, vol. 138, no. 2, pp. 153–161, 2011.

[109] A. Yazdani and P. Jeffrey, "Complex network analysis of water distribution systems," *Chaos: An Interdisciplinary Journal of Nonlinear Science*, vol. 21, no. 1, p. 016111, 2011.

[110] A. Yazdani, R. A. Otoo, and P. Jeffrey, "Resilience enhancing expansion strategies for water distribution systems: A network theory approach," *Environmental Modelling & Software*, vol. 26, no. 12, pp. 1574–1582, 2011.

[111] A. Yazdani and P. Jeffrey, "Water distribution system vulnerability analysis using weighted and directed network models," *Water Resources Research*, vol. 48, no. 6, 2012.

[112] F. Meng, G. Fu, R. Farmani, C. Sweetapple, and D. Butler, "Topological attributes of network resilience: A study in water distribution systems," *Water research*, vol. 143, pp. 376–386, 2018.

[113] N. Ade, G. Liu, A. F. Al-Douri, M. M. El-Halwagi, and M. S. Mannan, "Investigating the effect of inherent safety principles on system reliability in process design," *Process Safety and Environmental Protection*, vol. 117, pp. 100–110, 2018.

[114] P. Jain, H. J. Pasman, S. Waldram, E. Pistikopoulos, and M. S. Mannan, "Process resilience analysis framework (praf): A systems approach for improved risk and safety management," *Journal of Loss Prevention in the Process Industries*, vol. 53, pp. 61–73, 2018.

[115] Y. Ye, I. E. Grossmann, and J. M. Pinto, "Mixed-integer nonlinear programming models for optimal design of reliable chemical plants," *Computers & Chemical Engineering*, vol. 116, pp. 3–16, 2018.

[116] K. Moreno-Sader, P. Jain, L. C. B. Tenorio, M. S. Mannan, and M. M. El-Halwagi, "Integrated approach of safety, sustainability, reliability, and resilience analysis via a return on investment metric," *ACS Sustainable Chemistry & Engineering*, vol. 7, no. 24, pp. 19522–19536, 2019.

[117] A. Al-Douri, V. Kazantzi, F. T. Eljack, M. S. Mannan, and M. M. El-Halwagi, "Mitigation of operational failures via an economic framework of reliability, availability, and maintainability (ram) during conceptual design," *Journal of Loss Prevention in the Process Industries*, vol. 67, p. 104261, 2020.

[118] J. Mula, R. Poler, J. P. García-Sabater, and F. C. Lario, "Models for production planning under uncertainty: A review," *International journal of production economics*, vol. 103, no. 1, pp. 271–285, 2006.

[119] D. Peidro, J. Mula, R. Poler, and F.-C. Lario, "Quantitative models for supply chain planning under uncertainty: a review," *The International Journal of Advanced Manufacturing Technology*, vol. 43, no. 3-4, pp. 400–420, 2009.

[120] K. Govindan, M. Fattahi, and E. Keyvanshokooh, "Supply chain network design under uncertainty: A comprehensive review and future research directions," *European Journal of Operational Research*, vol. 263, no. 1, pp. 108–141, 2017.

[121] F. You, J. M. Wassick, and I. E. Grossmann, "Risk management for a global supply chain planning under uncertainty: models and algorithms," *AIChE Journal*, vol. 55, no. 4, pp. 931–946, 2009.

[122] G. Guillén-Gosálbez and I. E. Grossmann, "Optimal design and planning of sustainable chemical supply chains under uncertainty," *AIChE Journal*, vol. 55, no. 1, pp. 99–121, 2009.

[123] D. J. Garcia and F. You, "Supply chain design and optimization: Challenges and opportunities," *Computers & Chemical Engineering*, vol. 81, pp. 153–170, 2015.

[124] N. V. Sahinidis, "Optimization under uncertainty: state-of-the-art and opportunities," *Computers & Chemical Engineering*, vol. 28, no. 6-7, pp. 971–983, 2004.

[125] M. Fisher, J. Hammond, W. Obermeyer, and A. Raman, "Configuring a supply chain to reduce the cost of demand uncertainty," *Production and operations management*, vol. 6, no. 3, pp. 211–225, 1997.

[126] P. Tsiakis, N. Shah, and C. C. Pantelides, "Design of multi-echelon supply chain networks under demand uncertainty," *Industrial & Engineering Chemistry Research*, vol. 40, no. 16, pp. 3585–3604, 2001.

[127] A. Gupta and C. D. Maranas, "Managing demand uncertainty in supply chain planning," *Computers & chemical engineering*, vol. 27, no. 8-9, pp. 1219–1227, 2003.

[128] J. Y. Jung, G. Blau, J. F. Pekny, G. V. Reklaitis, and D. Eversdyk, "A simulation based optimization approach to supply chain management under demand uncertainty," *Computers & chemical engineering*, vol. 28, no. 10, pp. 2087–2106, 2004.

[129] C.-L. Chen and W.-C. Lee, "Multi-objective optimization of multi-echelon supply chain networks with uncertain product demands and prices," *Computers & Chemical Engineering*, vol. 28, no. 6-7, pp. 1131–1144, 2004.

[130] F. You and I. E. Grossmann, "Design of responsive supply chains under demand uncertainty," *Computers & Chemical Engineering*, vol. 32, no. 12, pp. 3090–3111, 2008.

[131] Y. He and X. Zhao, "Coordination in multi-echelon supply chain under supply and demand uncertainty," *International Journal of Production Economics*, vol. 139, no. 1, pp. 106–115, 2012.

[132] L. J. Zeballos, C. A. Méndez, A. P. Barbosa-Povoa, and A. Q. Novais, "Multi-period design and planning of closed-loop supply chains with uncertain supply and demand," *Computers & Chemical Engineering*, vol. 66, pp. 151–164, 2014.

[133] L. V. Snyder, M. P. Scaparra, M. S. Daskin, and R. L. Church, "Planning for disruptions in supply chain networks," in *Models, methods, and applications for innovative decision making*, pp. 234–257, INFORMS, 2006.

[134] B. Tomlin, "On the value of mitigation and contingency strategies for managing supply chain disruption risks," *Management science*, vol. 52, no. 5, pp. 639–657, 2006.

[135] T. Wu, J. Blackhurst, and P. O'grady, "Methodology for supply chain disruption analysis," *International journal of production research*, vol. 45, no. 7, pp. 1665–1682, 2007.

[136] R. G. Richey, J. B. Skipper, and J. B. Hanna, "Minimizing supply chain disruption risk through enhanced flexibility," *International Journal of Physical Distribution & Logistics Management*, 2009.

[137] S. K. Paul and P. Chowdhury, "A production recovery plan in manufacturing supply chains for a high-demand item during COVID-19," *International Journal of Physical Distribution & Logistics Management*, 2020.

[138] K. Nikolopoulos, S. Punia, A. Schäfers, C. Tsinopoulos, and C. Vasilakis, "Forecasting and planning during a pandemic: COVID-19 growth rates, supply chain disruptions, and governmental decisions," *European journal of operational research*, vol. 290, no. 1, pp. 99–115, 2020.

[139] S. Terrazas-Moreno, I. E. Grossmann, J. M. Wassick, and S. J. Bury, "Optimal design of reliable integrated chemical production sites," *Computers & Chemical Engineering*, vol. 34, no. 12, pp. 1919–1936, 2010.

[140] M. Turnquist and E. Vugrin, "Design for resilience in infrastructure distribution networks," *Environment Systems & Decisions*, vol. 33, no. 1, pp. 104–120, 2013.

[141] G. Zhang, F. Zhang, X. Zhang, Q. Wu, and K. Meng, "A multi-disaster-scenario distributionally robust planning model for enhancing the resilience of distribution systems," *International Journal of Electrical Power & Energy Systems*, vol. 122, p. 106161, 2020.

[142] N. Xu, S. D. Guikema, R. A. Davidson, L. K. Nozick, Z. Çağnan, and K. Vaziri, "Optimizing scheduling of post-earthquake electric power restoration tasks," *Earthquake engineering & structural dynamics*, vol. 36, no. 2, pp. 265–284, 2007.

[143] D. Ivanov, A. Pavlov, A. Dolgui, D. Pavlov, and B. Sokolov, "Disruption-driven supply chain (re)-planning and performance impact assessment with consideration of pro-active and recovery policies," *Transportation Research Part E: Logistics and Transportation Review*, vol. 90, pp. 7–24, 2016.

[144] D. Ivanov, B. Sokolov, I. Solovyeva, A. Dolgui, and F. Jie, "Dynamic recovery policies for time-critical supply chains under conditions of ripple effect," *International Journal of Production Research*, vol. 54, no. 23, pp. 7245–7258, 2016.

[145] J. Gong and F. You, "Resilient design and operations of process systems: Nonlinear adaptive robust optimization model and algorithm for resilience analysis and enhancement," *Computers & Chemical Engineering*, vol. 116, pp. 231–252, 2018.

[146] S. Zhao and F. You, "Resilient supply chain design and operations with decision-dependent uncertainty using a data-driven robust optimization approach," *AIChE Journal*, vol. 65, no. 3, pp. 1006–1021, 2019.

[147] L. R. Matthews, C. E. Gounaris, and I. G. Kevrekidis, "Designing networks with resiliency to edge failures using two-stage robust optimization," *European Journal of Operational Research*, vol. 279, no. 3, pp. 704–720, 2019.

[148] J. Wu and P. Wang, "Post-disruption performance recovery to enhance resilience of interconnected network systems," *Sustainable and Resilient Infrastructure*, pp. 1–17, 2020.

[149] N. Ahmadian, G. J. Lim, J. Cho, and S. Bora, "A quantitative approach for assessment and improvement of network resilience," *Reliability Engineering & System Safety*, p. 106977, 2020.

[150] J.-Z. Yu and H. Baroud, "Modeling uncertain and dynamic interdependencies of infrastructure systems using stochastic block models," *ASCE-ASME J Risk and Uncert in Engrg Sys Part B Mech Engrg*, vol. 6, no. 2, 2020.

[151] G. Behzadi, M. J. O'Sullivan, and T. L. Olsen, "On metrics for supply chain resilience," *European Journal of Operational Research*, 2020.

[152] I. Bachmann, J. Bustos-Jiménez, and B. Bustos, "A survey on frameworks used for robustness analysis on interdependent networks," *Complexity*, vol. 2020, 2020.

[153] U.S. Energy Information Administration (EIA), "Electicity data browser." `https://www.eia.gov/electricity/data/browser/`. Accessed: May 2021.

[154] Texas Water Development Board (TWDB), "Historical water use estimates." https://www.twdb.texas.gov/waterplanning/waterusesurvey/estimates/index.asp. Accessed: May 2021.

[155] Energy Institute, The University of Texas at Austin, "The full cost of electricity." https://energy.utexas.edu/policy/fce. Accessed: May 2021.

APPENDIX A

SUPPLEMENTARY DATA FOR CHAPTER 2 RESULTS

Table A.1: Energy data and calculated water requirements used in the case study of Spain [5].

Energy Source		**Energy Source**	**Water for Fuel**	**Electricity Generated**	**Water for Electricity**	**Total Water**
Units		GWh	million m3	GWhe	million m3	million m3
Coal	OL	48,394	42	18,599	2,844	2,886
	CL	59,148	52	22,733	653	705
Oil	OL	12,932	9	6,193	939	947
	CL	15,806	11	7,570	56	67
NG	OL	60,211	27	25,891	3,924	3,951
	CL	73,592	33	31,645	236	269
Nuclear	OL	77,367	98	25,527	5,798	5,896
	CL	94,559	120	31,199	657	777
Biomass	OL	8,253	-	2,916	552	552
	CL	10,087	-	3,564	14	14
Hydro		-	-	41,052	2,797	2,797
Solar PV		-	-	8,327	7	7
Solar Thermal		-	-	4,770	9	9
Wind		-	-	55,646	-	-
Total		**460,350**	**391**	**285,632**	**18,486**	**18,877**

OL: Open-loop cooling
CL: Closed-loop cooling
NG: Natural Gas

Table A.2: Water data used in the Case Study on Spain [6, 7].

Water Source		**Water Withdrawn**	**Electricity Required**
Units		Mm^3	GWh_e
Surface water		29,870	11,047
Groundwater		6,884	3,273
Seawater Desalination			
Reverse Osmosis	88%	1,188	10,109
ED	8%	108	183
MED	3%	41	385
MSF	1%	14	338
Total		**38,105**	**25,335**

ED: Electrodialysis
MED: Multiple-Effect Distillation
MSF: Multi-Stage Flash

APPENDIX B

NOMENCLATURE FOR CHAPTER 4

Sets and Indices

$i \in I$	Set of available energy resources
$j \in J$	Set of available water resources
$k \in K$	Set of potential energy sources/water sinks
$l \in L$	Set of potential Water sources/energy sinks
$p \in P$	Set of final energy consumers
$q \in Q$	Set of final water consumers
$s \in S$	Set of potential connectivity-disruption scenarios
$m_1 \in M^{in}$	Set of energy resource types
$m_2 \in M^{out}$	Set of energy product types
$n_1 \in N^{in}$	Set of water resource types
$n_2 \in N^{out}$	Set of water product types
$i \in I_{m_1}$	Set of energy resources i with resource type m_1, $I_m \subseteq I$
$k \in K_{m_1}, K_{m_2}$	Set of energy sources k with energy type m_1, m_2, $K_{m_1}, K_{m_2} \subseteq K$
$p \in P_{m_2}$	Set of energy consumers p with product type m_2, $P_{m_2} \subseteq P$
$j \in J_{n_1}$	Set of water resources j with resource type n_1, $J_{n_1} \subseteq J$
$l \in L_{n_1}, L_{n_2}$	Set of water sources l with water type n_1, n_2, $L_{n_1}, L_{n_2} \subseteq L$
$q \in Q_{n_2}$	Set of water resources q of water type n_2, $Q_{n_2} \subseteq Q$
$O^{eres}_{i,k,s}$	Mapping set of i, k connection to disruption scenarios s
$O^{esws}_{k,l,s}$	Mapping set of k, l connection to disruption scenarios s
$O^{esec}_{k,p,s}$	Mapping set of k, p connection to disruption scenarios s
$O^{wrws}_{j,l,s}$	Mapping set of j, l connection to disruption scenarios s

$O^{wses}_{l,k,s}$	Mapping set of l, k connection to disruption scenarios s
$O^{wswc}_{l,q,s}$	Mapping set of l, q connection to disruption scenarios s
Parameters	
era_i	Energy resource i availability
$ersc_i$	Energy resource i supply cost
wra_j	Water resource j availability
$wrsc_j$	Water resource j supply cost
ecd_p	Energy final consumer p demand
wcd_q	Water final consumer q demand
CAP^{es}_k	Upper bound of generating capacity for energy source k
β^{es}_k	Conversion factor for energy source k
ϕ^{es}_k	Water withdrawal intensity factor for energy source k
cf^{es}_k	Capacity factor for energy source k
τ^{es}_y	Operational time (in time units of energy generating capacity) within a year
EFC_k	Fixed cost coefficient for energy source k
EVC_k	Capital cost coefficient for energy source k
EOC_k	Variable operating cost coefficient for energy source k
CAP^{ws}_l	Upper bound of generating capacity for water source l
β^{ws}_k	Conversion factor for water source l
ϕ^{ws}_l	Energy consumption intensity factor for water source l
cf^{ws}_l	Capacity factor for water source l
τ^{ws}_y	Operational time (in time units of water generating capacity) within a year
WFC_l	Fixed cost coefficient for water source l
WVC_l	Capital cost coefficient for water source l
WOC_l	Variable operating cost coefficient for water source l
$EFTC$	Fixed cost of energy transmission coefficient
$EVTC$	Capital cost of energy transmission coefficient

$EOTC$	Variable cost of energy transmission coefficient
$WFTC$	Fixed cost of water transportation coefficient
$WVTC$	Capital cost of water transportation coefficient
$WOTC$	Variable cost of water transportation coefficient
λ	Unit penalty cost per product for unsatisfied demands of energy and water

Continuous variables

cap_k^{es}	Generating capacity of energy source k in MW
cap_l^{ws}	Generating capacity of water source l in mgd
$es_{k,s}$	Energy source k generation in scenario s in MWh
$ws_{l,s}$	Water source l generation in scenario s in MGal
$cap_{i,k}^{eres}$	Energy stream from energy resource i to energy source k
$cap_{k,l}^{esws}$	Energy stream from energy source k to water source l
$cap_{k,p}^{esec}$	Energy stream from energy source k to final consumer p
$cap_{j,l}^{wrws}$	Water stream from water resource j to water source l
$cap_{l,k}^{wses}$	Water stream from water source l to energy source k
$cap_{l,q}^{wswc}$	Water stream from energy source k to water source l
$e_{i,k,s}$	Energy stream from energy resource i to energy source k in scenario s
$e_{k,l,s}$	Energy stream from energy source k to water source l in scenario s
$e_{k,p,s}$	Energy stream from energy source k to final consumer p in scenario s
$w_{j,l,s}$	Water stream from water resource j to water source l in scenario s
$w_{k,l,s}$	Water stream from water source l to energy source k in scenario s
$w_{l,k,s}$	Water stream from energy source k to water source l in scenario s
$w_{l,q,s}$	Water stream from water source l to water consumer q in scenario s

$\theta^{e}_{p,s}$	Fraction of demands for energy consumer p satisfied in scenario s
$\theta^{w}_{q,s}$	Fraction of demands for water consumer q satisfied in scenario s

Binary variables

z^{es}_{k}	Selection of energy source k (1 if k is selected, 0 otherwise)
z^{ws}_{l}	Selection of water source l (1 if l is selected, 0 otherwise)
$z_{i,k}$	Existence of energy stream from energy resource i to energy source k
$z_{k,l}$	Existence of energy stream from energy source k to water source l
$z_{k,p}$	Existence of energy stream from energy source k to final consumer source p
$z_{j,l}$	Existence of water stream from water resource j to water source l
$z_{l,k}$	Existence of water stream from water source l to energy source k
$z_{l,q}$	Existence of water stream from water source l to water consumer q